Greenland Lake Ice Break-up Detection from Sentinel-1 SAR

Christoph Posch and Jakob Abermann

christoph.posch@edu.uni-graz.at and jakob.abermann@uni-graz.at

Institute of Geography and Regional Science, University of Graz, Austria

Introduction

Lake ice is a parameter of the Essential Climate Variable (ECV) "lakes"[1] and plays an important role in the biological, chemical, and physical processes of cold region freshwater[2]. The timing of lake ice freeze-up and break-up are relevant climate indicators and can be useful for climate monitoring[1]. Synthetic aperture radar (SAR) is unaffected by cloud cover and exhibits backscatter differences between water and ice due to dielectric properties of the materials. Several studies investigated the evolution and characteristics of freshwater ice such as river ice[3][4] and lake ice[5][6]. In this study, we explore the potential of utilizing Sentinel-1 SAR data for identifying temporal and spatial variations of lake ice break-up across Greenland between 2017 and 2021 and assess its latitudinal and vertical gradients. We apply a dynamic numerical threshold to identify the annual timing of break-up from SAR backscatter decline within three consecutive days. The term "lake ice break-up" used in this study describes the timing when most of the lake surface is liquid water and is therefore an approximation to the timing of "water clear of ice" (WCI)[1] given the nature and limitations of the applied methods.

Data and Methods

The satellites of the Sentinel-1 mission acquires data with a center frequency of 5.407 GHz[7]. Single polarized horizontal transmit/horizontal receive (HH) Level-1 ground range detected (GRD) data in both ascending and descending orbit is used in this study. The data is acquired in Interferometric Wide (IW) swath mode with a swath width of 250 km, which results in a revisiting time of a few days and a GRD resolution of 10 x 10 m[7]. SAR data acquisition and processing is done using the Google Earth Engine Data Catalogue[8] and Google Earth Engine Code Editor[9], while the statistical analysis is performed using Python[10].

The lake inventory[11] includes peripheral lakes in Greenland ranging from 1.6 * 10^{-3} km^2 to 138 km^2 (n = 155870). We retrieve SAR backscatter data of lakes with a surface area ≥ 0.1 km^2 (n = 14336) to exclude potential inaccuracies due to the lake size. Lakes with a temporal acquisition resolution larger than ~ 3 days are excluded from the analysis. Backscatter data which lacks a pronounced annual evolution and exhibits strong uniformal characteristics is also excluded. This means that only lakes with a difference in mean backscatter of ≥ 8 dB between January/February (most certainly ice covered) and August (most certainly ice free) are considered (Fig. 1 ①). After this pre-selection ~ 16 % (n = 2281) of the initial number of lakes with a surface area ≥ 0.1 km^2 are suitable to perform the data analysis.

The backscatter signal for ice break-up detection is averaged for the central 20 % of the lake area to mitigate edge effects of the lake and surrounding terrain (Fig. 2 ②). This results in an area of ~ 0.02 km^2 for the smallest lake, which corresponds to at least 200 pixels considered for averaging. We apply a locally weighted scatterplot smoothing (LOWESS) filter to reduce the temporal variability to ensure a more robust and confident ice break-up detection (Fig. 1 ③). Several trials proofed that using 1 % of the data for LOWESS filtering is robust for the analysis. For each lake, a dynamic numerical threshold is applied in each year to identify the timing of ice break-up. This yearly threshold amounts to 25 % of the backscatter difference between the 98th and 2nd quantile and must be at least 2.5 dB. The day of year (DOY) of lake ice break-up is detected when the absolute value of backscatter decrease exceeds the threshold value within three consecutive acquisitions (Fig. 1 ④). The detection algorithm is applied between May 1 and August 1 to exclude misdetections (Fig. 1⑤).

The study area is divided into six regions (N, NE, SE, S, SW, NW) to explore spatio-temporal statistics. We choose a 0.95 significance level to assess differences and trends. In the statistics we include only lakes with detected break-up DOYs in at least 3 out of the 5 years (2017-2021) to get robust detection statistics and to mitigate random detections. Daily mean temperature data at 2 m is retrieved from the automated weather stations (AWS) KAN_L (67.09 °N, 49.97 °W, 631 m a.s.l), NUK_L (64.48 °N, 49.55 °W, 500 m a.s.l) and AWS QAS_M (61.11 °N, 46.81 °W, 678 m a.s.l) operated by the Geological Survey of Denmark and Greenland[12] (Fig. 5). We calculate daily cumulative positive degree days (PDD) to explore correlations with the timing of ice break-up for lakes within ± 0.5 °N and ± 200 m (KAN_L: n = 24, NUK_L: n = 6, QAS_M: n = 21). The break-up detection is assessed and validated by utilizing daily time-lapse images of three lakes in SW Greenland between 2017 and 2020[13].

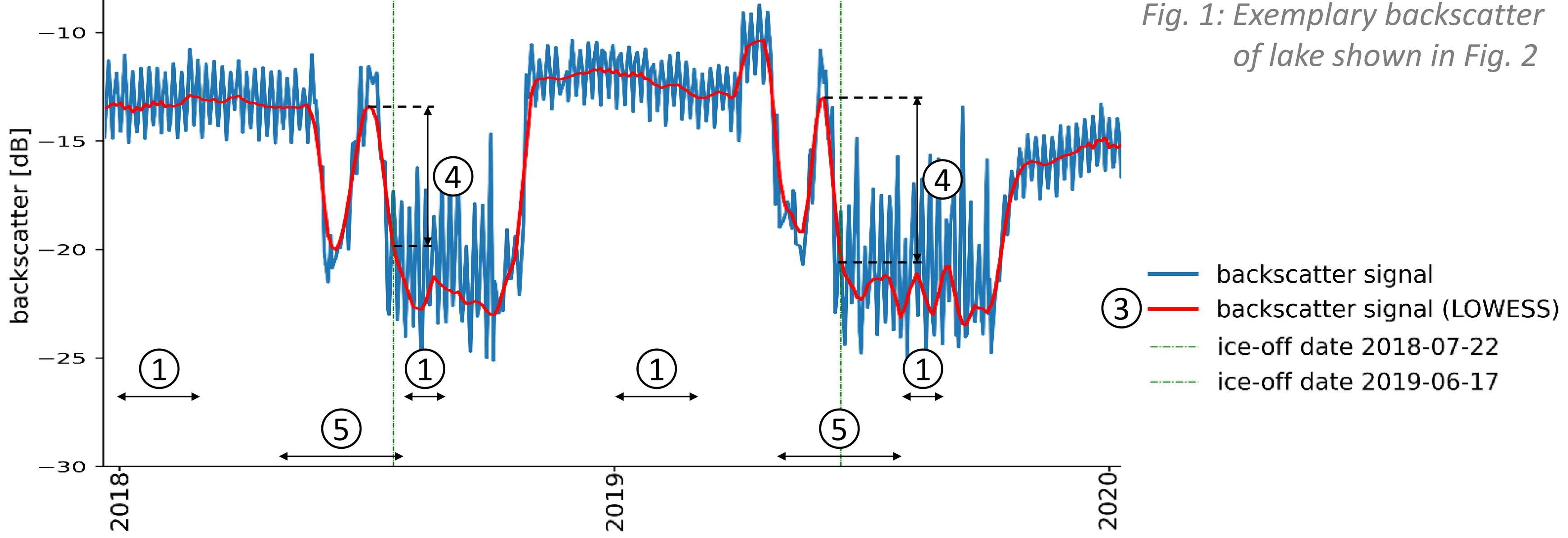

Fig. 1: Exemplary backscatter of lake shown in Fig. 2

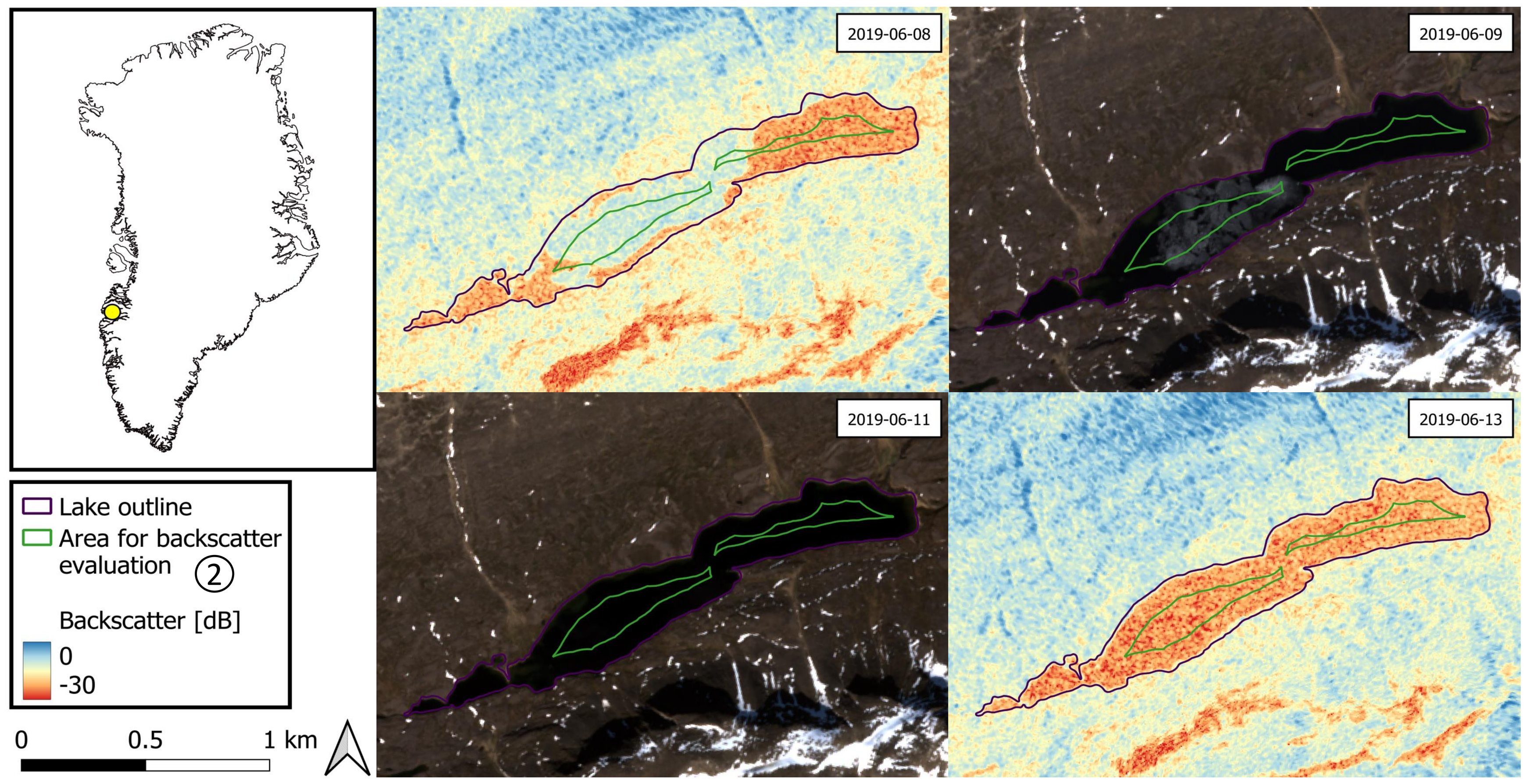

Fig. 2: Sentinel-1 and Sentinel-2 images of an exemplary lake

Results

The detection of the timing from SAR data proves to be conservative (i.e., later) compared to validation based on time-lapse camera data and allows characterizing break-up timing with a mean error of ~ 7 days. We find that only data from lakes in SE, S, SW, and NW exhibits characteristics for break-up detection (14 %, 17 %, 17 % and 19 % suitable) while coverage for lakes in N and NE lacks necessary radiometric and temporal characteristics (1 % and 0 % suitable).

Our results indicate that no significant trend of break-up timing between 2017 and 2021 can be identified. Annual median DOYs range between 179-205 (SE), 163-198 (S), 164-189 (SW) and 156-191 (NW) (Fig. 3). Annual ice break-up DOYs in SE are significantly later compared to S, SW and NW, except showing no difference to S in 2017, 2020 and 2021. The annual break-up timings in NW are significantly earlier in 2018 & 2021 compared to S as well as in 2019 & 2021 compared to SW. We explore spatio-temporal characteristics regarding latitudinal and vertical gradients for the regions S, SW and NW. Annual median DOYs for the regions S, SW and NW combined range between 164 (2019) and 191 (2018). The lake-specific break-up timings as well as median break-up DOYs for 2017-2021 increase with elevation, while no confident latitudinal gradients could be identified. Subdivided into latitudinal bands of 1 ° between 60 °N and 71 °N, strong correlations (0.61 ≤ r ≤ 0.84) can be identified in several years which exhibit an increase of 3-5 DOY/100 m. The 2017-2021 median break-up DOY of lakes between 60-61 °N and 67-68 °N increase by 4 DOY/100 m (r = 0.81 and r = 0.63, respectively).

We find that cumulative PDD increase earliest and are highest in 2019 while increasing latest and being lowest in 2018 at every AWS, except being lowest in 2017 at QAS_M. NUK_L exhibits the fastest aggregation of cumulative PDDs and highest annual values, while QAS_M shows the slowest built-up and lowest values. For most of the years, the annual median DOY for lakes around QAS_M are latest, while being earliest for lakes around NUK_L. Median break-op DOYs for 2017-2021 exhibit a decrease by 1 DOY/12 °C cumulative PDD (r = 0.86) when comparing the three AWS locations (Fig. 6).

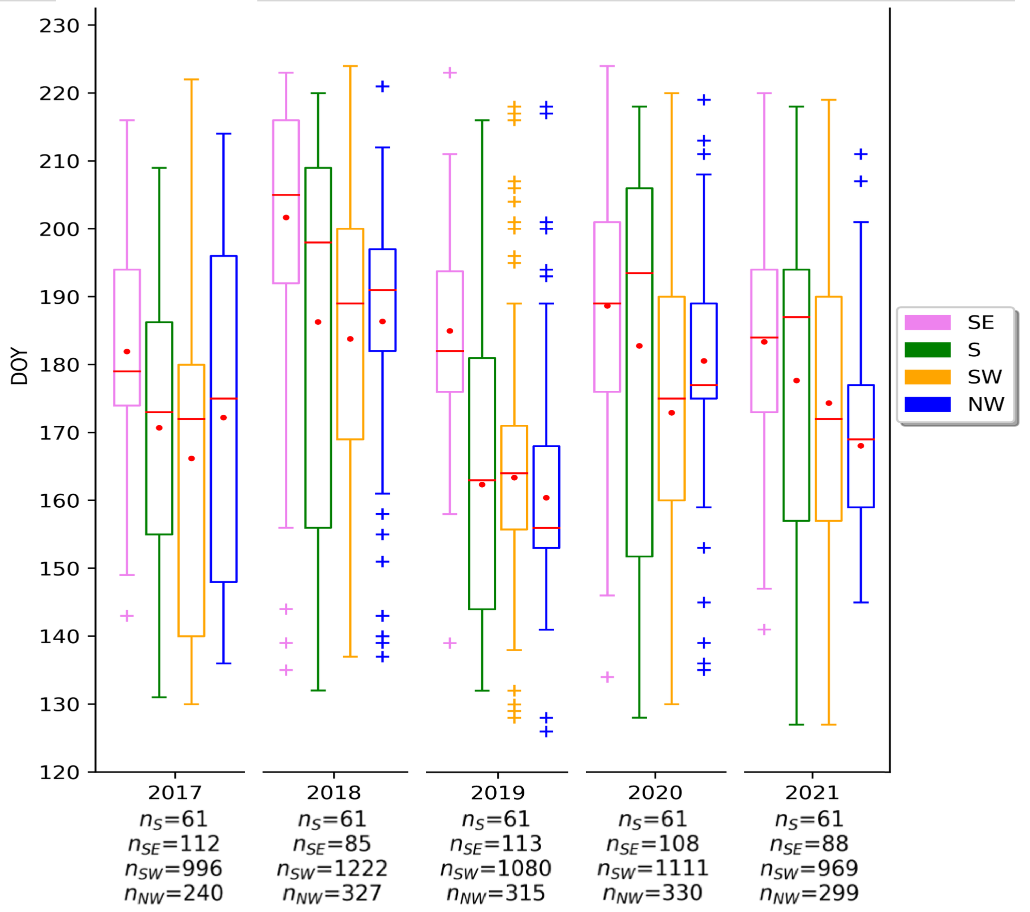

Fig. 3: Yearly break-up DOY for the regions SE, S, SW and NW

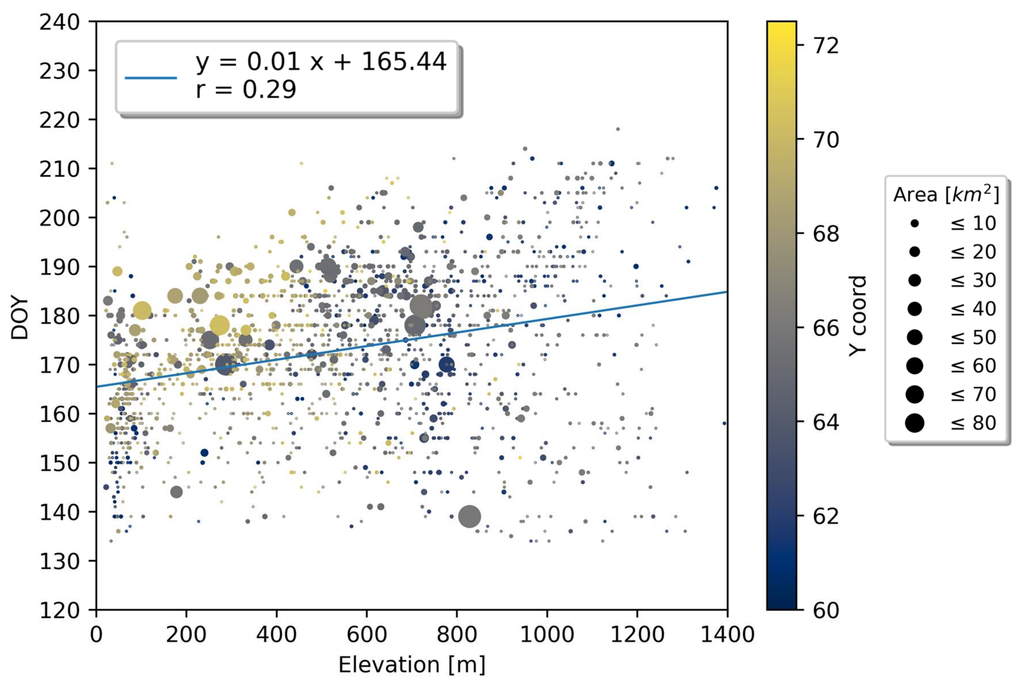

Fig. 4: DOY vs elevation of lakes in S, SW and NW Greenland

Discussion

We assess that elevation more strongly determines lake ice break-up timing than latitude does (Fig. 4). The significantly later timing of yearly median break-up DOYs in S compared to SW and NW can be explained by fewer lakes close to sea level (Fig. 5). Local topography such as elevation and extent of fjord systems might have a strong influence on the timing of break-up. Cumulative PDD at three AWS locations in S and SW are in line with median DOYs. The year 2019 with the lowest median DOY (164) for S, SW and NW combined exhibits the earliest increasing and highest cumulative PDD, while cumulative PDD are increasing latest and are lowest in the year 2018 with the highest median DOY (191). The presented vertical gradients of break-up timing in the magnitude of 3-5 DOY must be interpreted in regards with temporal limitation of the data and method. Very few higher elevated lakes exhibit early detection timings which must be questioned and explored in greater detail. However, the detection method proves to be conservative (i.e., later) and allows spatially characterizing lake ice break-up timing in Greenland.

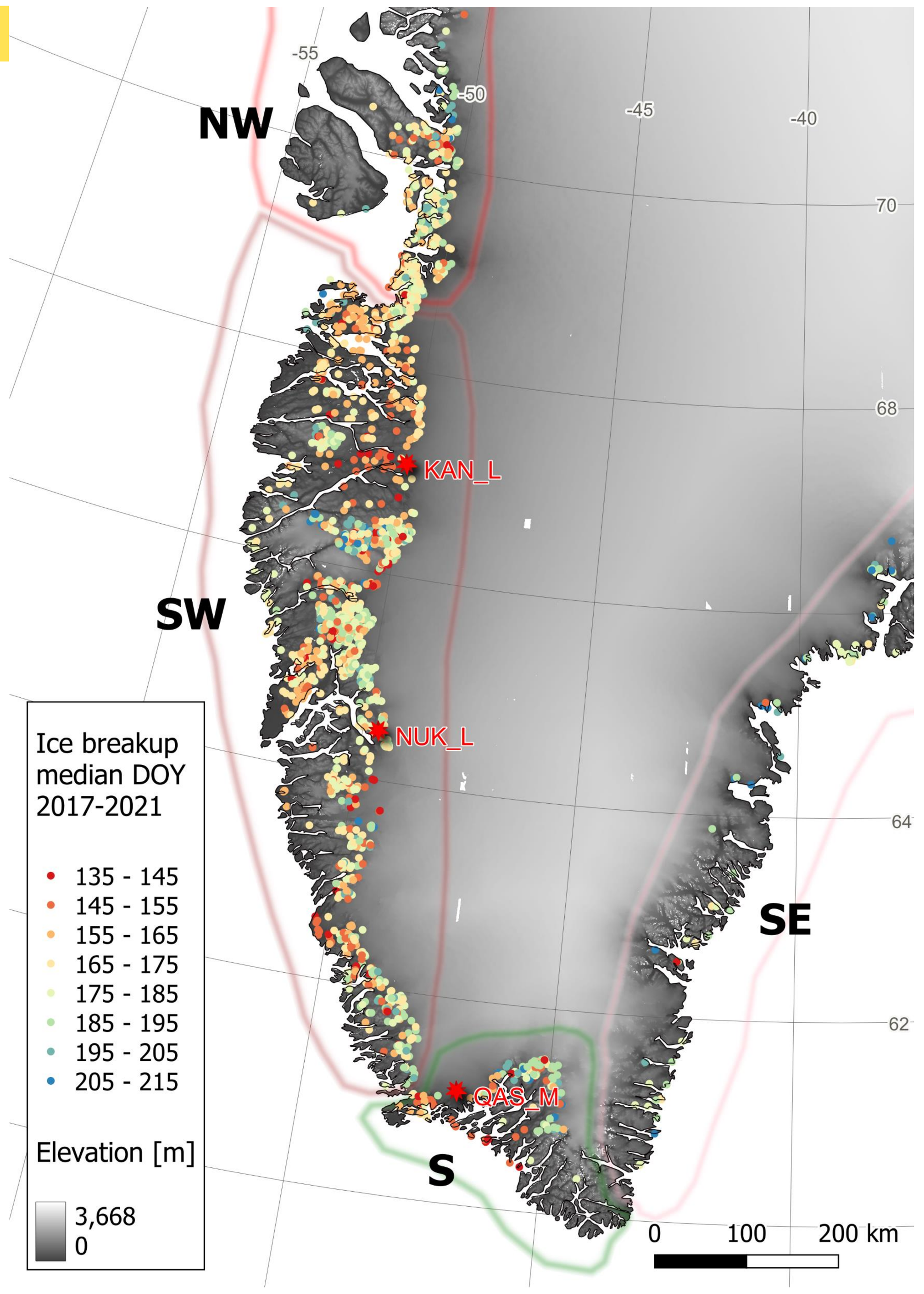

Fig. 5: Median break-up DOY (2017-2021) in SE, S, SW and NW

Conclusion

Sentinel-1 SAR data can be utilized to detect the timing of lake ice break-up in SE, S, SW and NW Greenland limited by radiometric and temporal characteristics. We show that there is no significant trend in break-up timing between 2017 and 2021, however, early median DOYs are in agreement with years exhibiting early increasing and high cumulative PDD. Vertical gradients of break-up DOY can be identified in several years while no strong correlations can be found regarding latitude. The annual temporal evolution of SAR backscatter allows detecting the timing of lake ice break-up by a dynamic numerical threshold, while the gradual backscatter increase during freeze-up does not allow a robust detection. Excluding data from days with high wind speeds or coupling the SAR-based detection with optical detections from Sentinel-2 might yield more robust results but might also additionally decrease the temporal resolution. Applying machine learning or deep learning algorithms as a next step might further improve the break-up detection and decrease the number of pre-filtered lakes. We aim to explore the relationship between break-up timing and climatological variables such as radiation and temperature across Greenland in greater detail and intend to apply this algorithm for an analysis of lake ice break-up timing on a global scale.

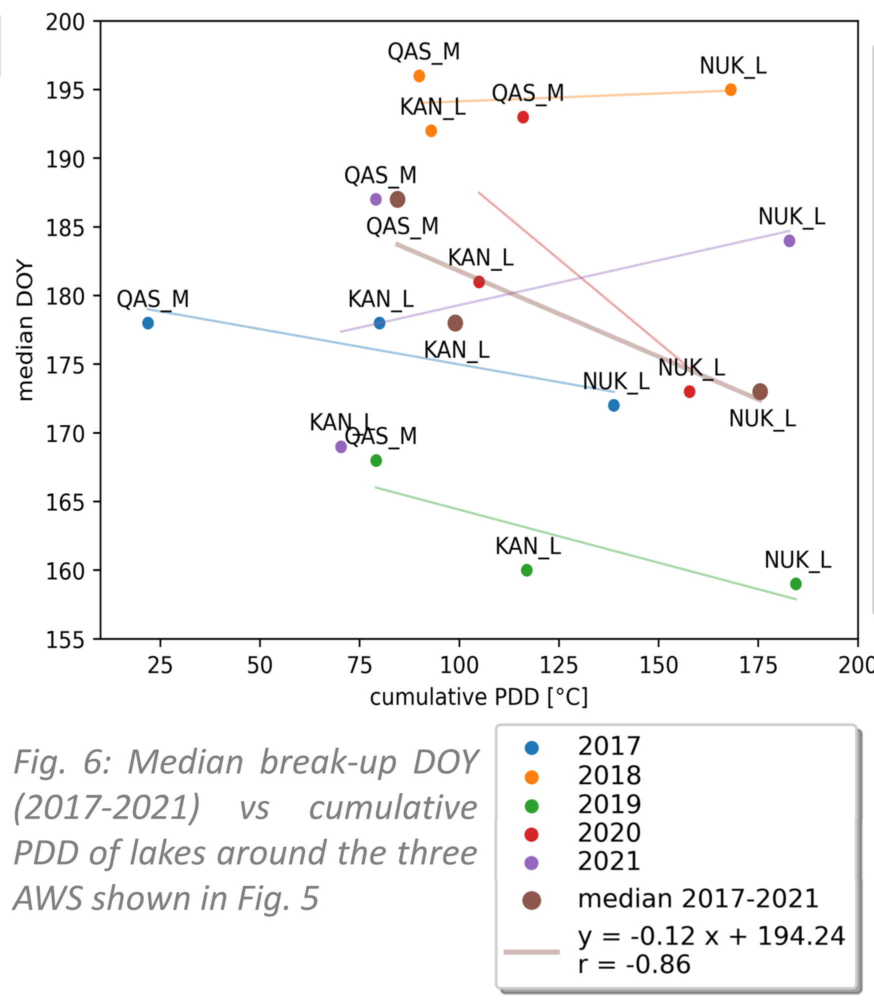

Fig. 6: Median break-up DOY (2017-2021) vs cumulative PDD of lakes around the three AWS shown in Fig. 5

[1] World Meteorological Organization, 2023. Global Climate Observing System (GCOS). Essential Climate Variables (ECV). https://gcos.wmo.int/en/essential-climate-variables, accessed: 2023-04-16
[2] Duguay, C.R., Bernier, M., Gauthier, Y., Kouraev, A., 2015. Remote sensing of lake and river ice. In: Tedesco, M. (ed.). Remote Sensing of the Cryosphere, 1st Edition. John Wiley & Sons, Hoboken, New Jersey
[3] Stonevicius, E., Uselis, G., Grendaite, D., 2022. Ice Detection with Sentinel-1 SAR Backscatter Threshold in Long Sections of Temperate Climate Rivers. Remote Sensing 2022, 14, 1627. https://doi.org/10.3390/rs14071627
[4] Lindenschmidt, K.-E., van der Sanden, J., Demski, A., Drouin, H., Geldsetzer, T., 2011. Characterising river ice along the Lower Red River using RADARSAT-2 imagery. CGU HS Committee on River Ice Processes and the Environment, 16th Workshop on River Ice. September 18 – 22, 2011, Winnipeg, Manitoba
[5] Tom, M., Aguilar, R., Imhof, P., Leinss, S., Baltsavias, E., Schindler, K., 2020. International Society for Photogrammetry and Remote Sensing, Commission III, WG III/9, pp 1-8
[6] Siles, G., Leconte, R., Peters D.L., 2022. Retrieval of Lake Ice Characteristics from SAR Imagery. Canadian Journal of Remote Sensing 2022, 48, 3, 379–399. https://doi.org/10.1080/07038992.2022.2042227
[7] European Space Agency, 2023. Sentinel-1. https://sentinel.esa.int/web/sentinel/missions/sentinel-1, accessed: 2023-04-16
[8] Google Inc., 2023a. Earth Engine Data Catalogue. https://developers.google.com/earth-engine/datasets, accessed: 2023-04-16
[9] Google Inc., 2023b.Earth Engine Code Editor. https://code.earthengine.google.com, accessed: 2023-04-16
[10] Python Software Foundation, 2023. Python. https://www.python.org, accessed: 2023-04-16
[11] Styrelsen for Dataforsyning og Infrastruktur, 2023. Åbent Land Grønland. https://dataforsyningen.dk/data/4771, accessed: 2023-04-16
[12] How, P., Mankoff, K.D., Wright, P.J., Vandecrux, B., Ahlstrøm A.P., Fausto, R.S., 2022. AWS one boom tripod Edition 4, GEUS Dataverse, V6. https://doi.org/10.22008/FK2/IW73UU
[13] Abermann, J., Eckerstorfer, M., Malnes, E., Hansen, B.U., 2019. A large wet snow avalanche cycle in West Greenland quantified using remote sensing and in situ observations. Natural Hazards 2019, 97, pp 517–534. https://doi.org/10.1007/s11069-019-03655-8

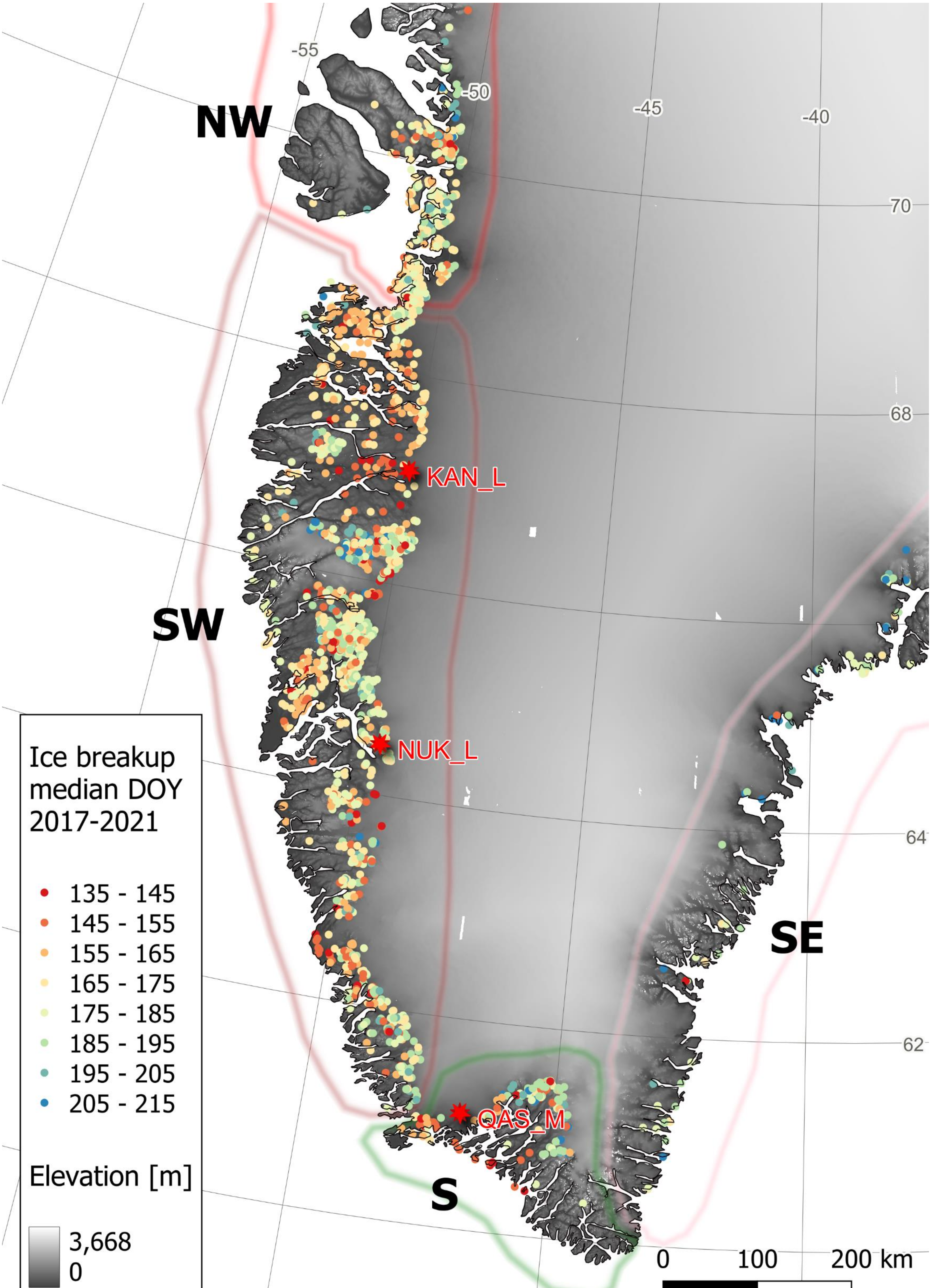

NW
SW
SE
S
KAN_L
NUK_L
QAS_M
-55
-50
-45
-40
70
68
64
62
Ice breakup median DOY 2017-2021
135 - 145
145 - 155
155 - 165
165 - 175
175 - 185
185 - 195
195 - 205
205 - 215
Elevation [m]
3,668
0
0
100
200 km

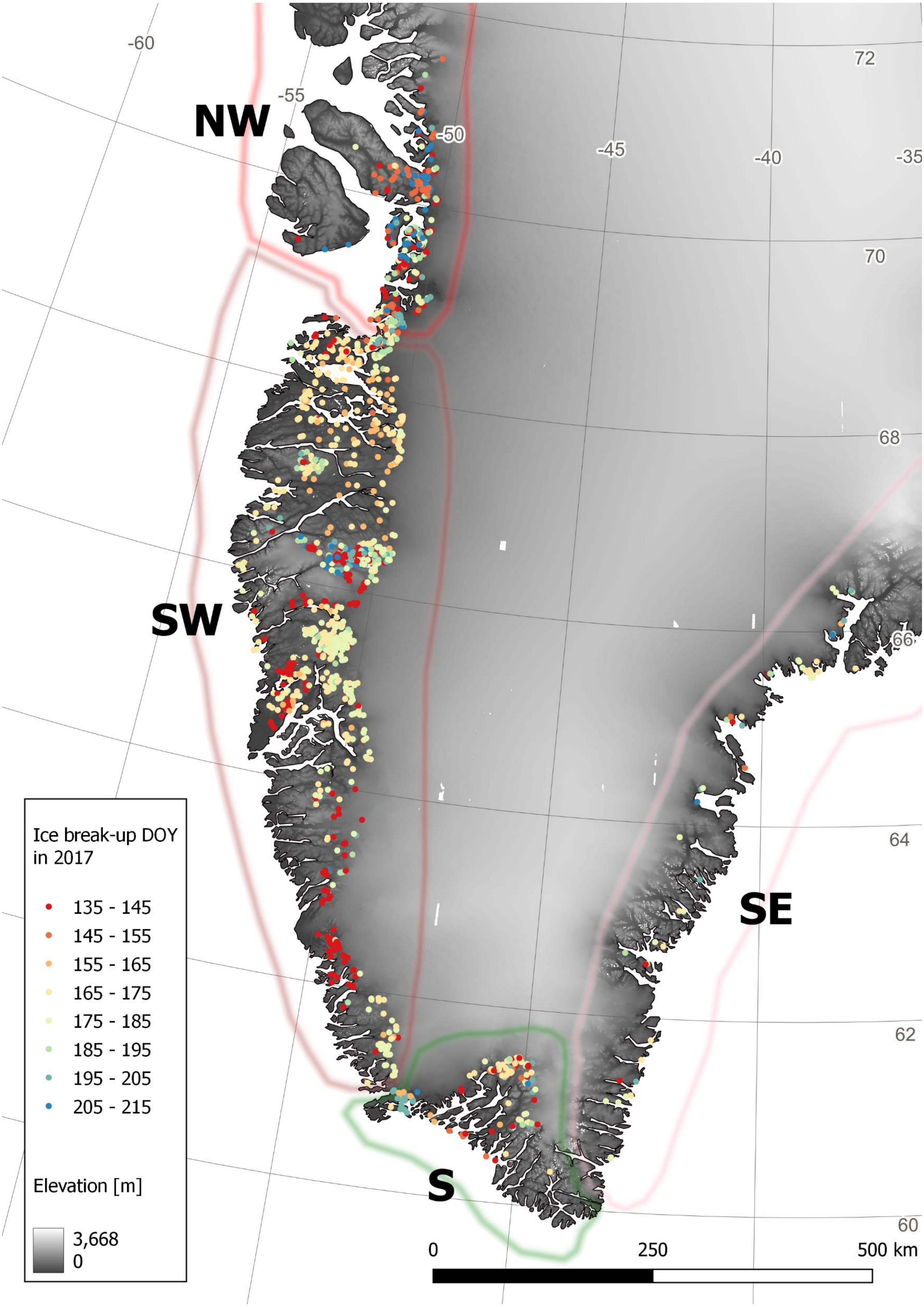

NW
SW
SE
S
-60
-55
-50
-45
-40
-35
72
70
68
66
64
62
60
Ice break-up DOY in 2017
135 - 145
145 - 155
155 - 165
165 - 175
175 - 185
185 - 195
195 - 205
205 - 215
Elevation [m]
3,668
0
0
250
500 km

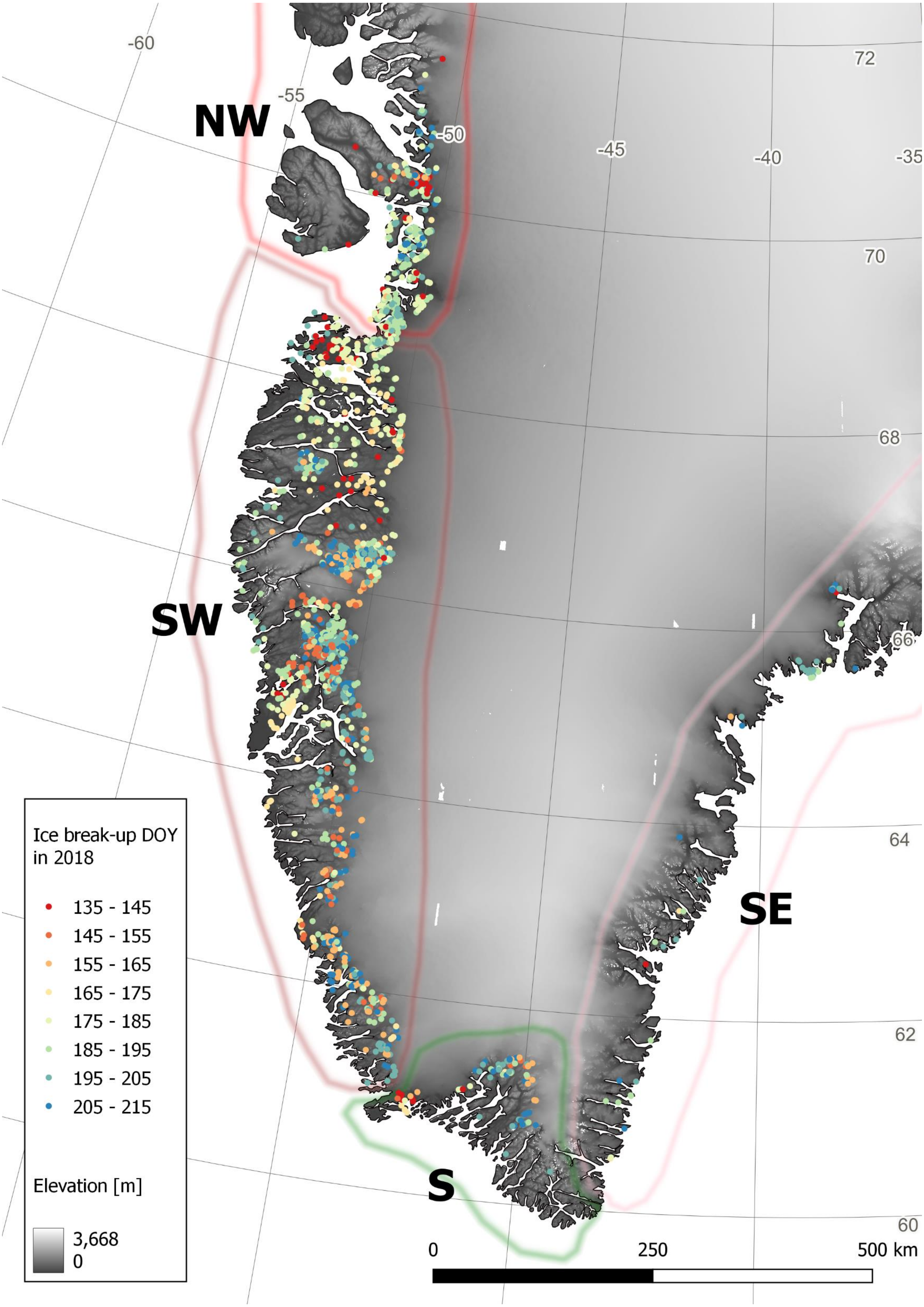

NW
SW
SE
S
-60
-55
-50
-45
-40
-35
72
70
68
66
64
62
60
Ice break-up DOY in 2018
135 - 145
145 - 155
155 - 165
165 - 175
175 - 185
185 - 195
195 - 205
205 - 215
Elevation [m]
3,668
0
0
250
500 km

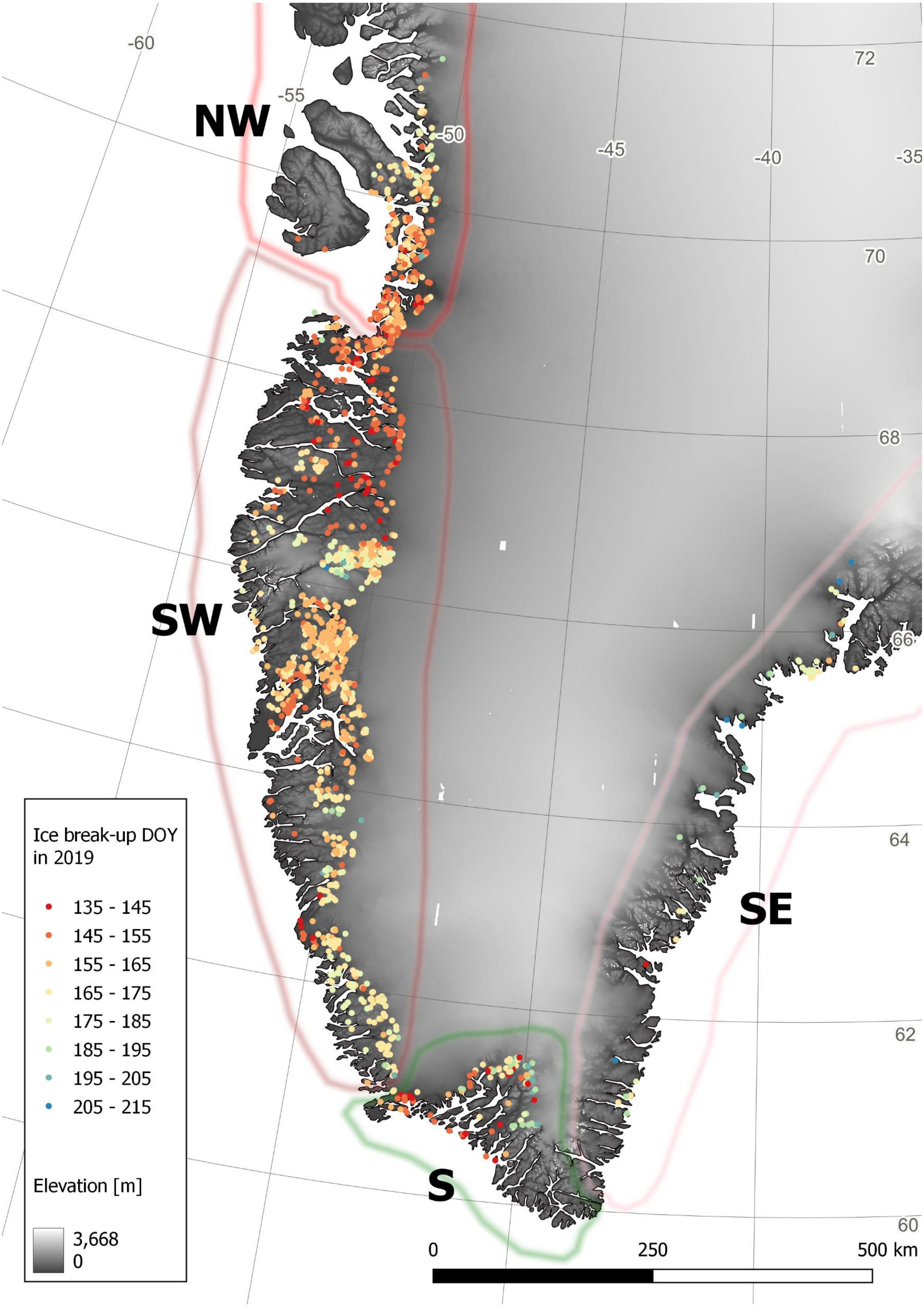
-60
-55
-50
-45
-40
-35
72
70
68
66
64
62
60
NW
SW
SE
S
Ice break-up DOY in 2019
135 - 145
145 - 155
155 - 165
165 - 175
175 - 185
185 - 195
195 - 205
205 - 215
Elevation [m]
3,668
0
0
250
500 km

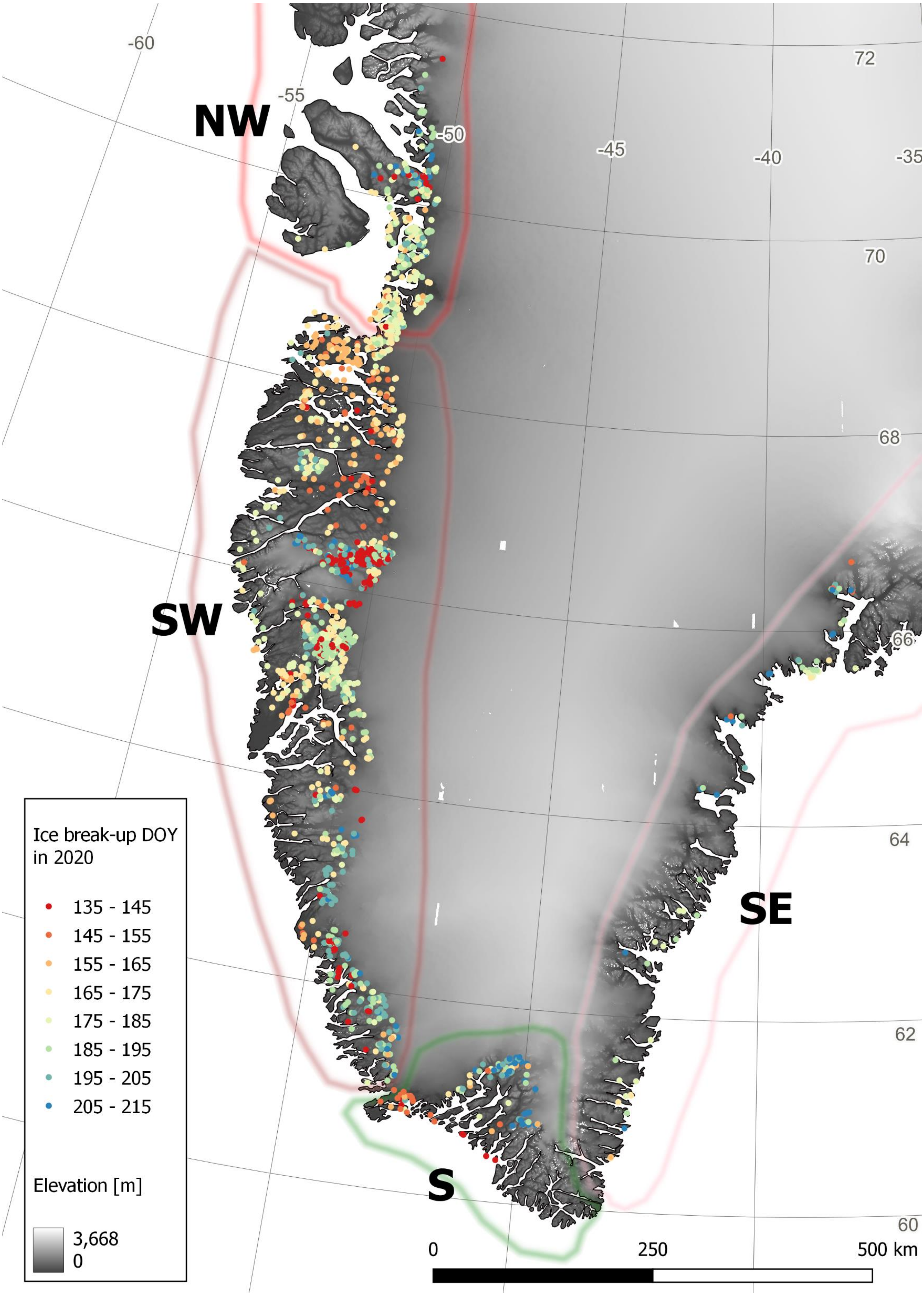

NW
SW
SE
S
-60
-55
-50
-45
-40
-35
72
70
68
66
64
62
60
Ice break-up DOY in 2020
135 - 145
145 - 155
155 - 165
165 - 175
175 - 185
185 - 195
195 - 205
205 - 215
Elevation [m]
3,668
0
0
250
500 km

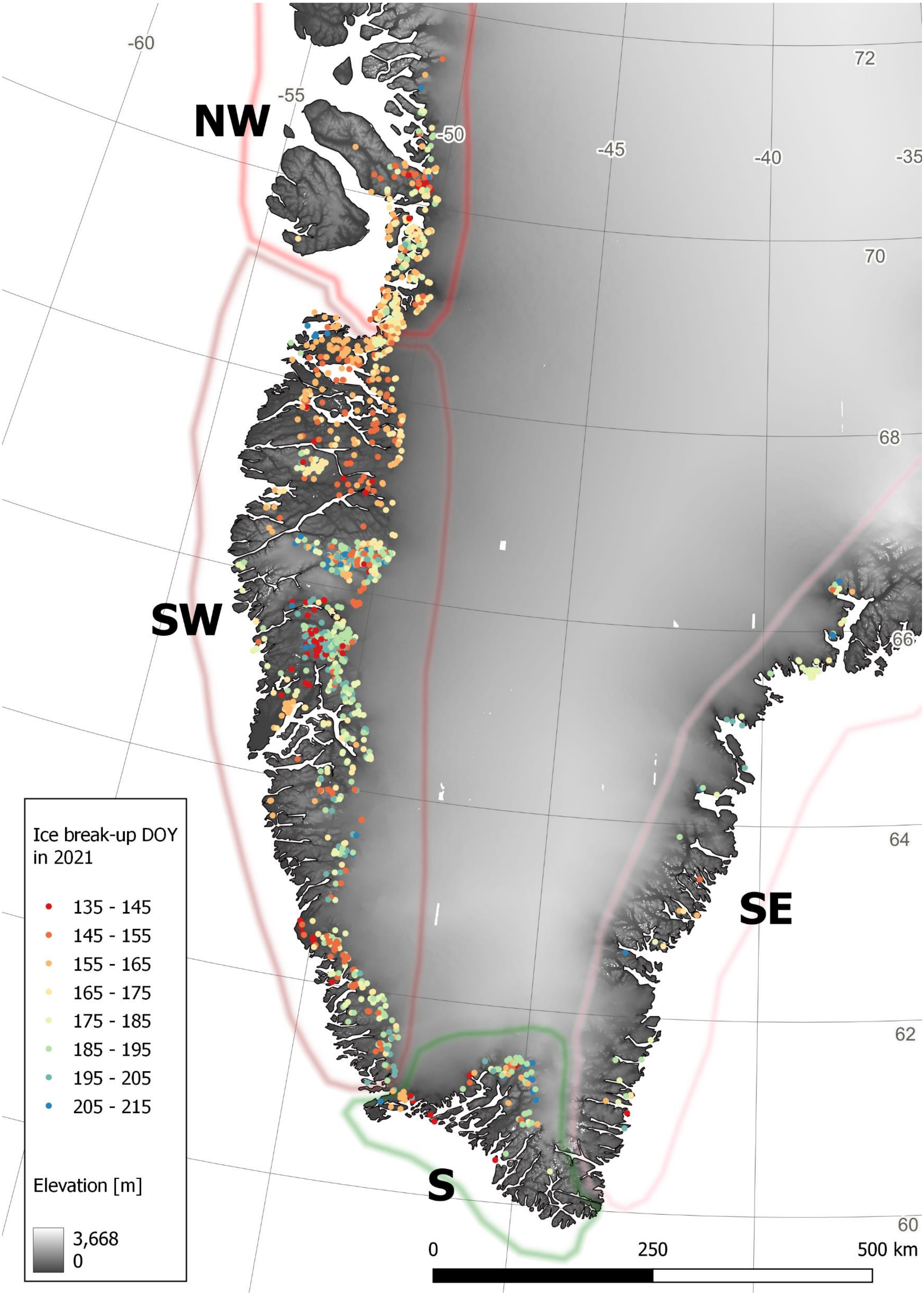

NW
SW
SE
S
-60
-55
-50
-45
-40
-35
72
70
68
66
64
62
60
Ice break-up DOY in 2021
135 - 145
145 - 155
155 - 165
165 - 175
175 - 185
185 - 195
195 - 205
205 - 215
Elevation [m]
3,668
0
0
250
500 km

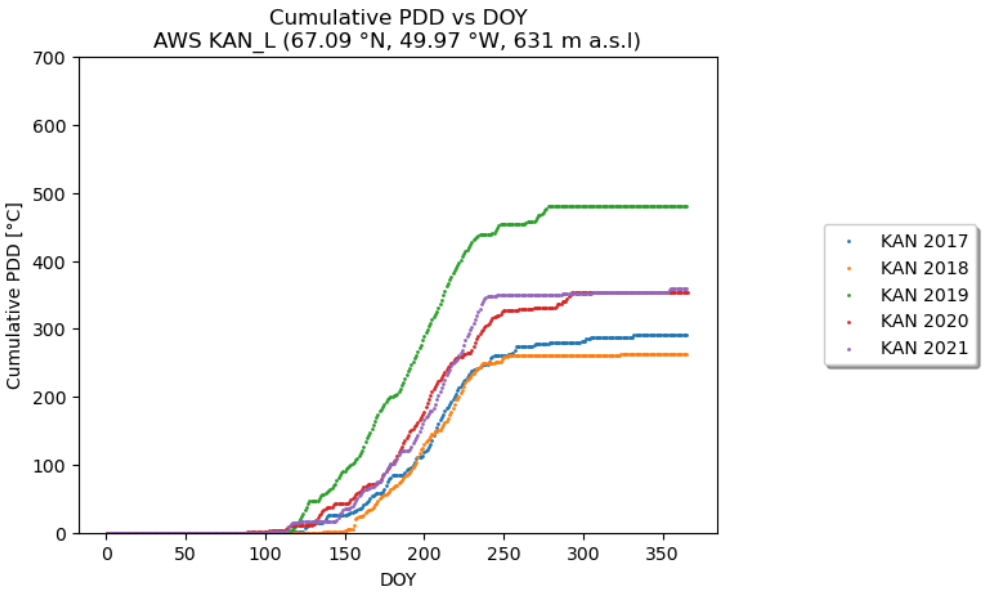
Cumulative PDD vs DOY
AWS KAN_L (67.09 °N, 49.97 °W, 631 m a.s.l)
Cumulative PDD [°C]
DOY
KAN 2017
KAN 2018
KAN 2019
KAN 2020
KAN 2021

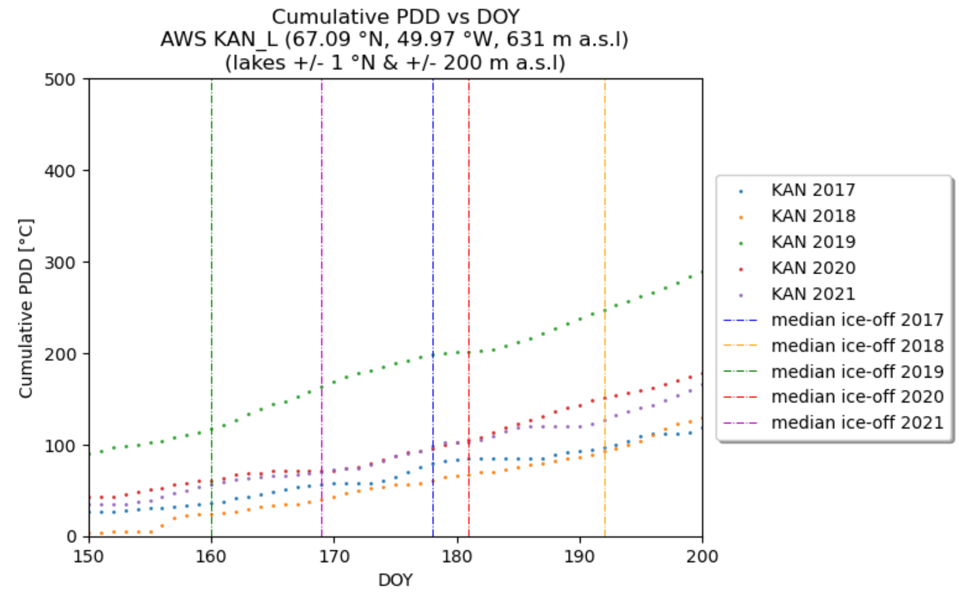
Cumulative PDD vs DOY
AWS KAN_L (67.09 °N, 49.97 °W, 631 m a.s.l)
(lakes +/- 1 °N & +/- 200 m a.s.l)
Cumulative PDD [°C]
DOY
KAN 2017
KAN 2018
KAN 2019
KAN 2020
KAN 2021
median ice-off 2017
median ice-off 2018
median ice-off 2019
median ice-off 2020
median ice-off 2021

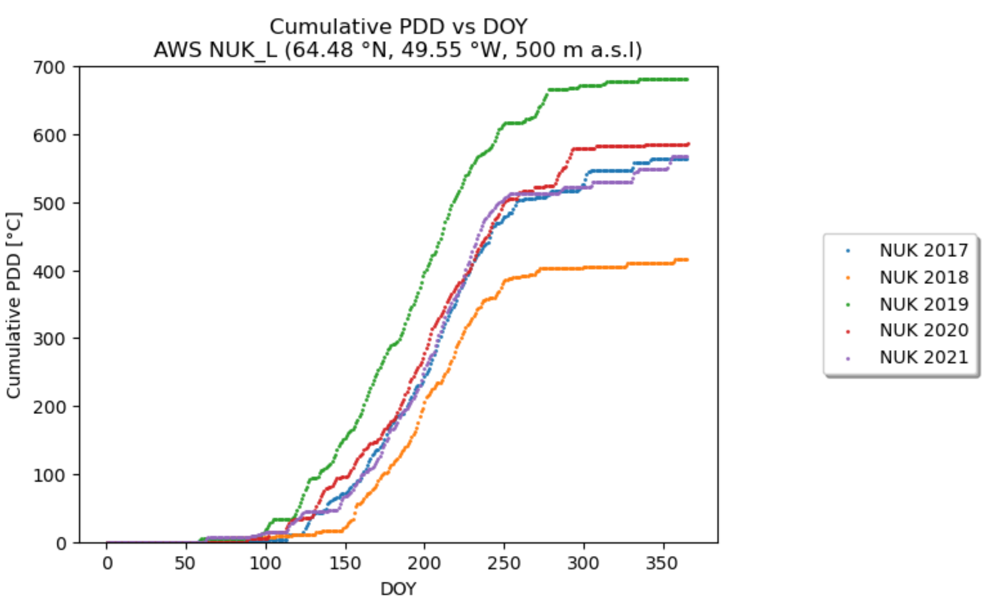
Cumulative PDD vs DOY
AWS NUK_L (64.48 °N, 49.55 °W, 500 m a.s.l)
Cumulative PDD [°C]
DOY
NUK 2017
NUK 2018
NUK 2019
NUK 2020
NUK 2021

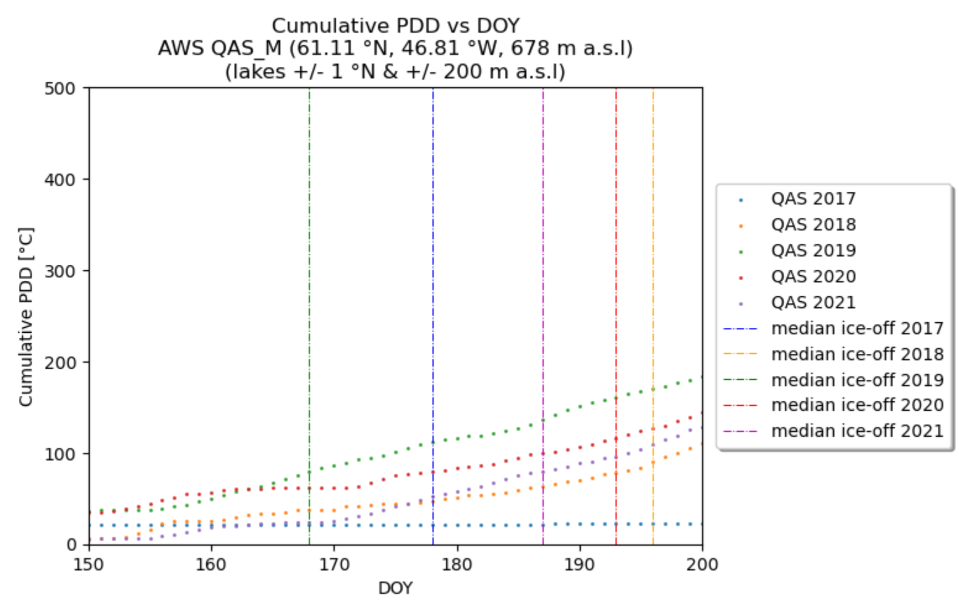
Cumulative PDD vs DOY
AWS QAS_M (61.11 °N, 46.81 °W, 678 m a.s.l)
(lakes +/- 1 °N & +/- 200 m a.s.l)
Cumulative PDD [°C]
DOY
QAS 2017
QAS 2018
QAS 2019
QAS 2020
QAS 2021
median ice-off 2017
median ice-off 2018
median ice-off 2019
median ice-off 2020
median ice-off 2021

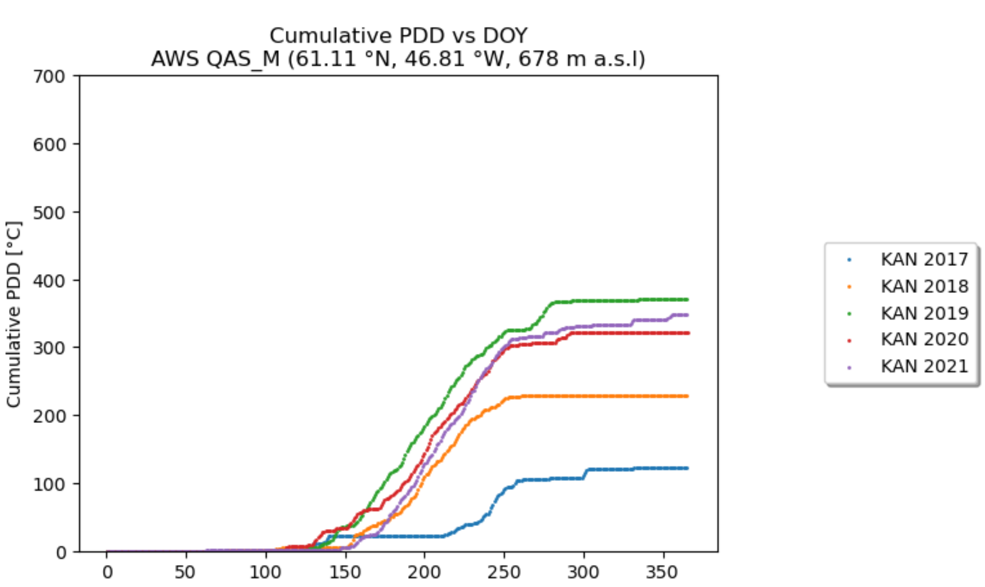
Cumulative PDD vs DOY
AWS QAS_M (61.11 °N, 46.81 °W, 678 m a.s.l)
Cumulative PDD [°C]
DOY
KAN 2017
KAN 2018
KAN 2019
KAN 2020
KAN 2021

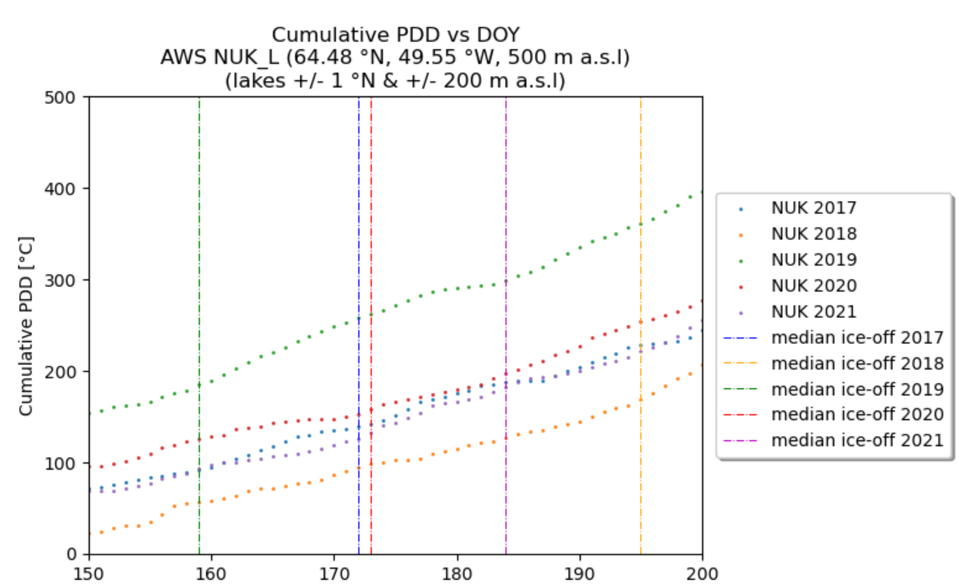
Cumulative PDD vs DOY
AWS NUK_L (64.48 °N, 49.55 °W, 500 m a.s.l)
(lakes +/- 1 °N & +/- 200 m a.s.l)
Cumulative PDD [°C]
DOY
NUK 2017
NUK 2018
NUK 2019
NUK 2020
NUK 2021
median ice-off 2017
median ice-off 2018
median ice-off 2019
median ice-off 2020
median ice-off 2021

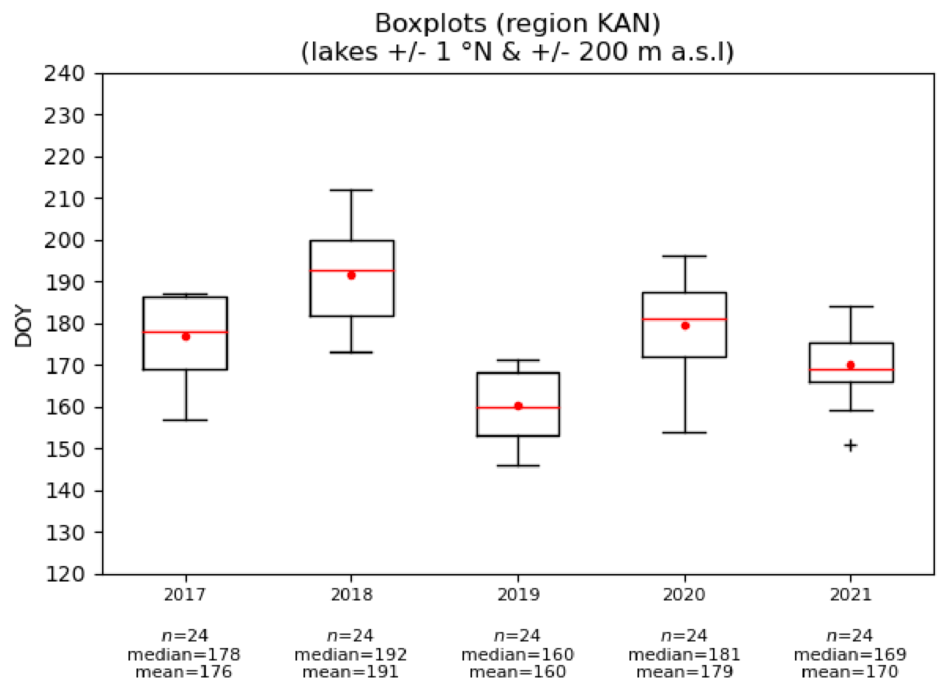
Boxplots (region KAN)
(lakes +/- 1 °N & +/- 200 m a.s.l)
DOY
240
230
220
210
200
190
180
170
160
150
140
130
120
2017
2018
2019
2020
2021
n=24
median=178
mean=176
n=24
median=192
mean=191
n=24
median=160
mean=160
n=24
median=181
mean=179
n=24
median=169
mean=170

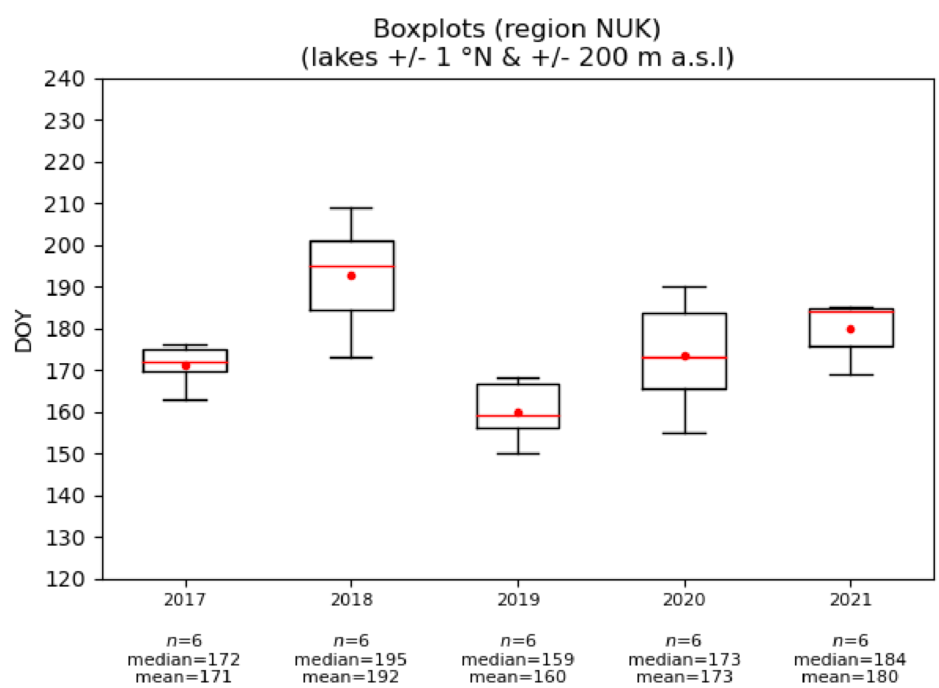
Boxplots (region NUK)
(lakes +/- 1 °N & +/- 200 m a.s.l)
DOY
240
230
220
210
200
190
180
170
160
150
140
130
120
2017
2018
2019
2020
2021
n=6
median=172
mean=171
n=6
median=195
mean=192
n=6
median=159
mean=160
n=6
median=173
mean=173
n=6
median=184
mean=180

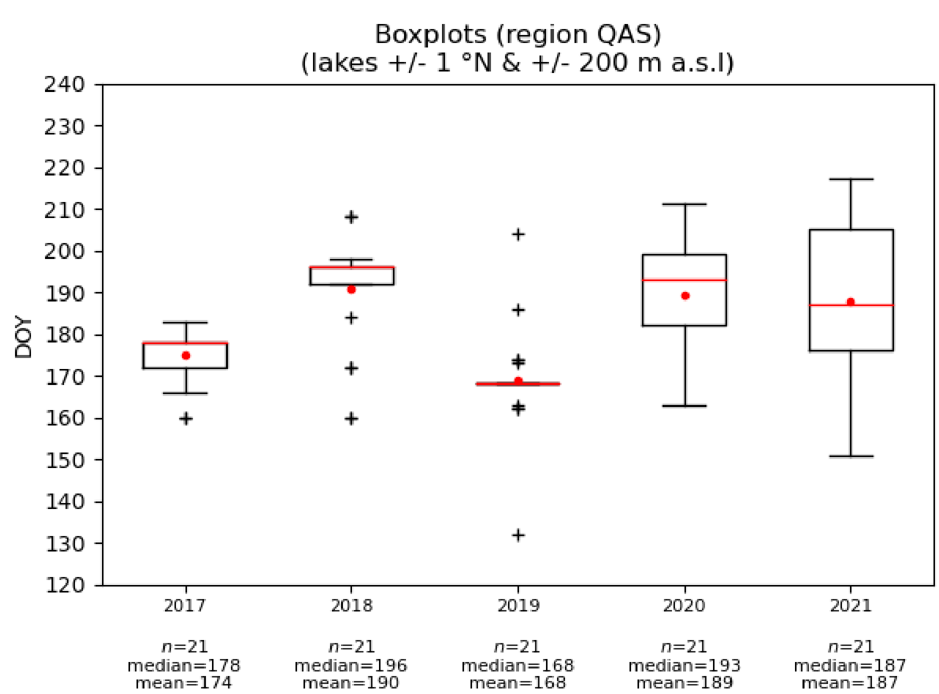
Boxplots (region QAS)
(lakes +/- 1 °N & +/- 200 m a.s.l)
DOY
240
230
220
210
200
190
180
170
160
150
140
130
120
2017
2018
2019
2020
2021
n=21
median=178
mean=174
n=21
median=196
mean=190
n=21
median=168
mean=168
n=21
median=193
mean=189
n=21
median=187
mean=187

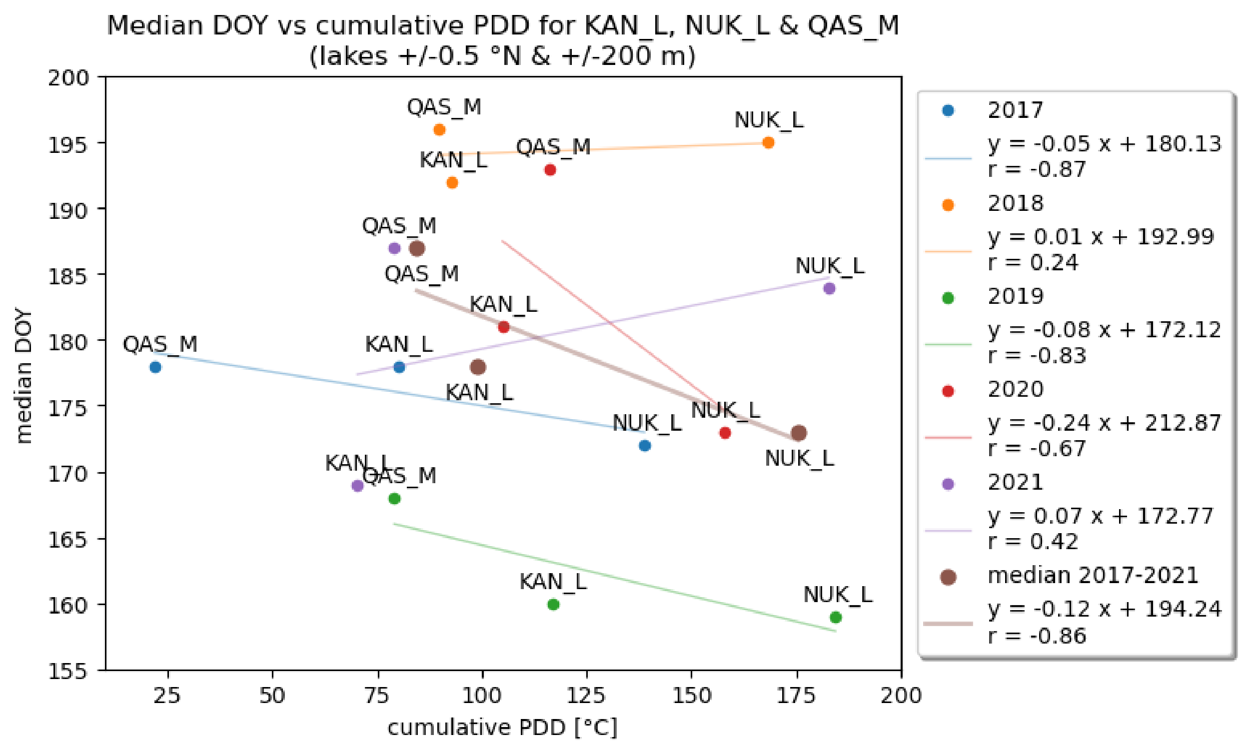
Median DOY vs cumulative PDD for KAN_L, NUK_L & QAS_M
(lakes +/-0.5 °N & +/-200 m)
median DOY
cumulative PDD [°C]
2017
y = -0.05 x + 180.13
r = -0.87
2018
y = 0.01 x + 192.99
r = 0.24
2019
y = -0.08 x + 172.12
r = -0.83
2020
y = -0.24 x + 212.87
r = -0.67
2021
y = 0.07 x + 172.77
r = 0.42
median 2017-2021
y = -0.12 x + 194.24
r = -0.86

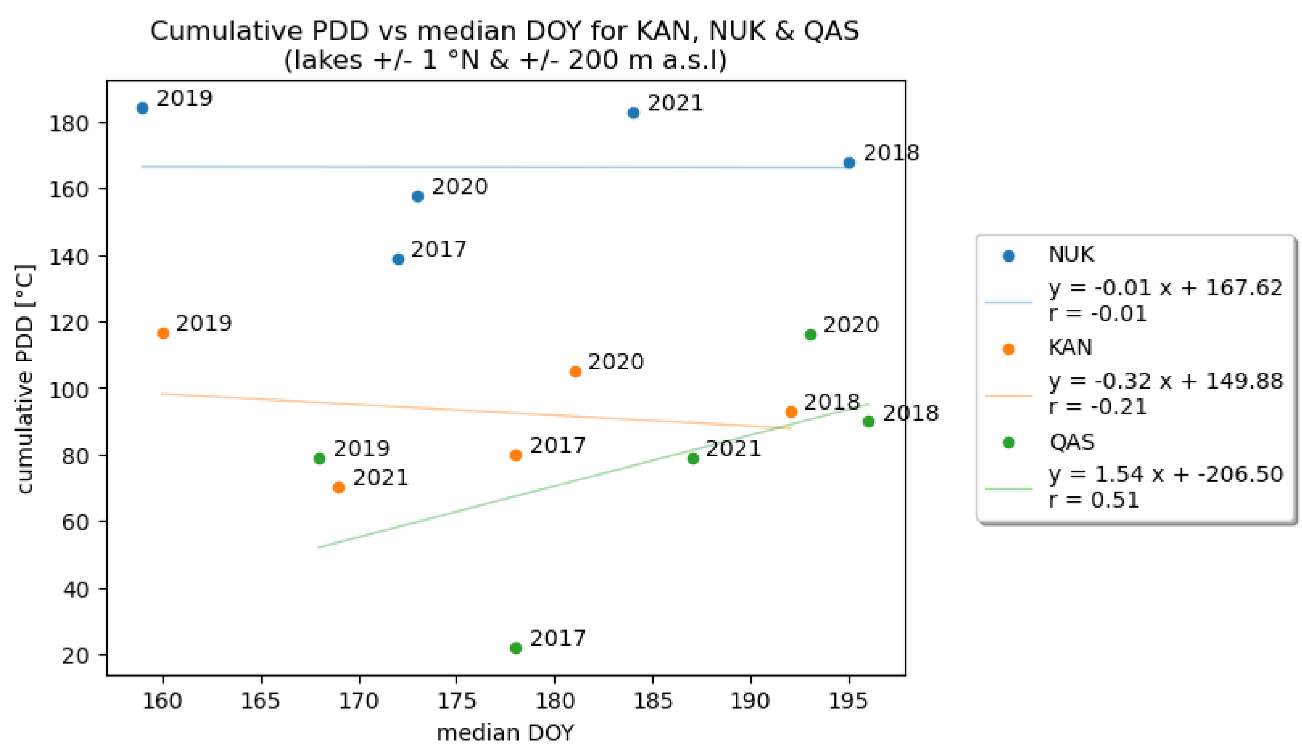
Cumulative PDD vs median DOY for KAN, NUK & QAS
(lakes +/- 1 °N & +/- 200 m a.s.l)
cumulative PDD [°C]
median DOY
NUK
y = -0.01 x + 167.62
r = -0.01
KAN
y = -0.32 x + 149.88
r = -0.21
QAS
y = 1.54 x + -206.50
r = 0.51

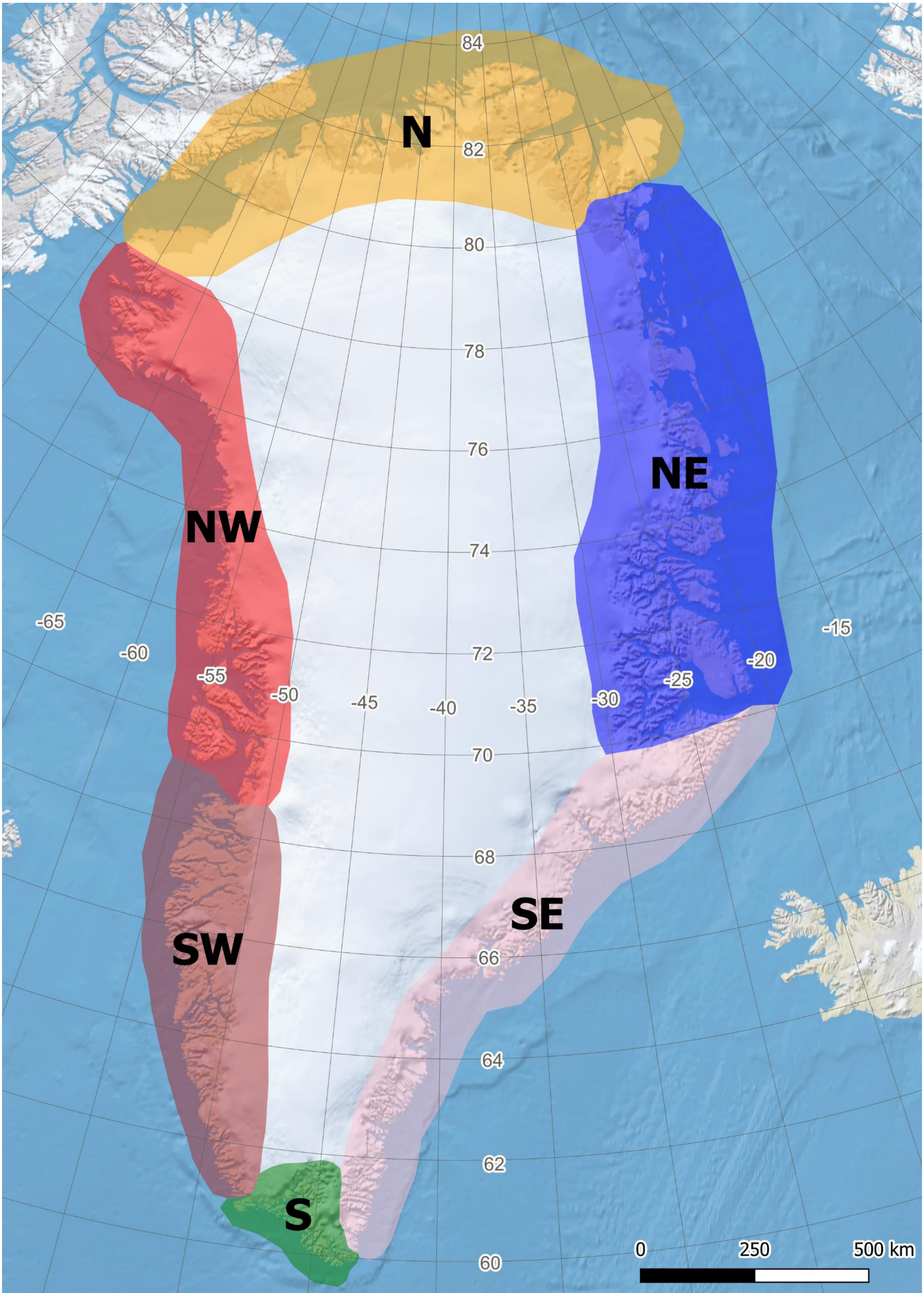

84
N
82
80
78
76
NE
NW
74
-65
-15
-60
72
-20
-55
-25
-50
-45
-40
-35
-30
70
68
SE
SW
66
64
62
S
0
250
500 km
60

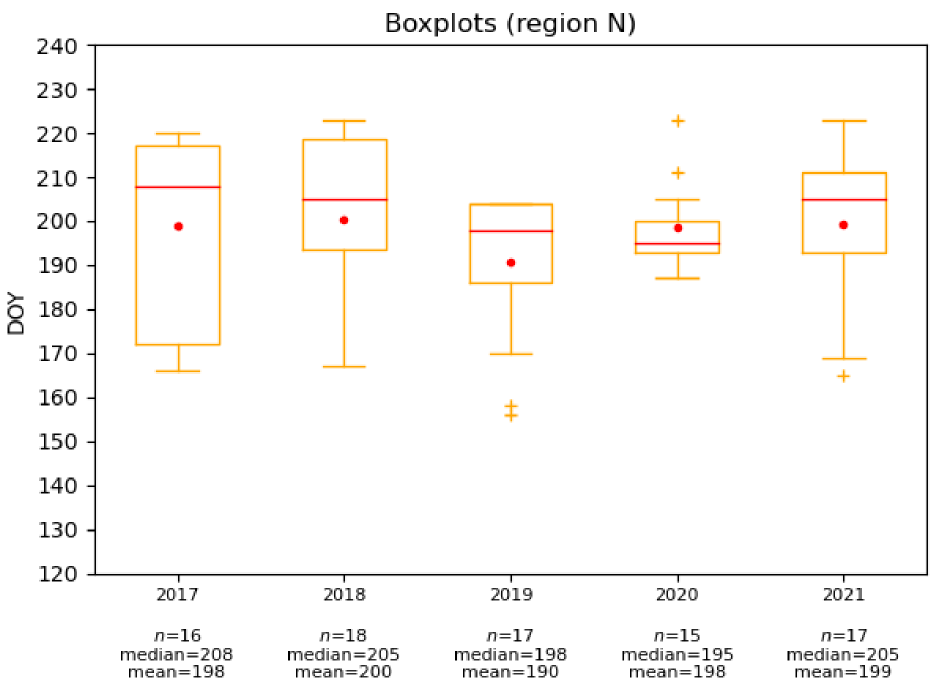
Boxplots (region N)
DOY
2017
n=16
median=208
mean=198
2018
n=18
median=205
mean=200
2019
n=17
median=198
mean=190
2020
n=15
median=195
mean=198
2021
n=17
median=205
mean=199

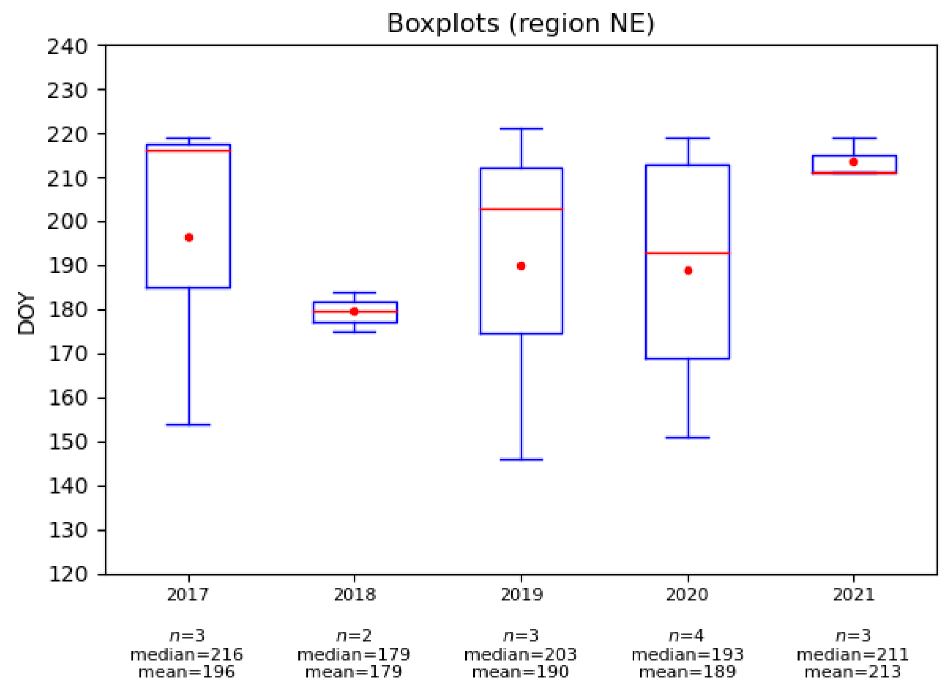
Boxplots (region NE)
DOY
2017
n=3
median=216
mean=196
2018
n=2
median=179
mean=179
2019
n=3
median=203
mean=190
2020
n=4
median=193
mean=189
2021
n=3
median=211
mean=213

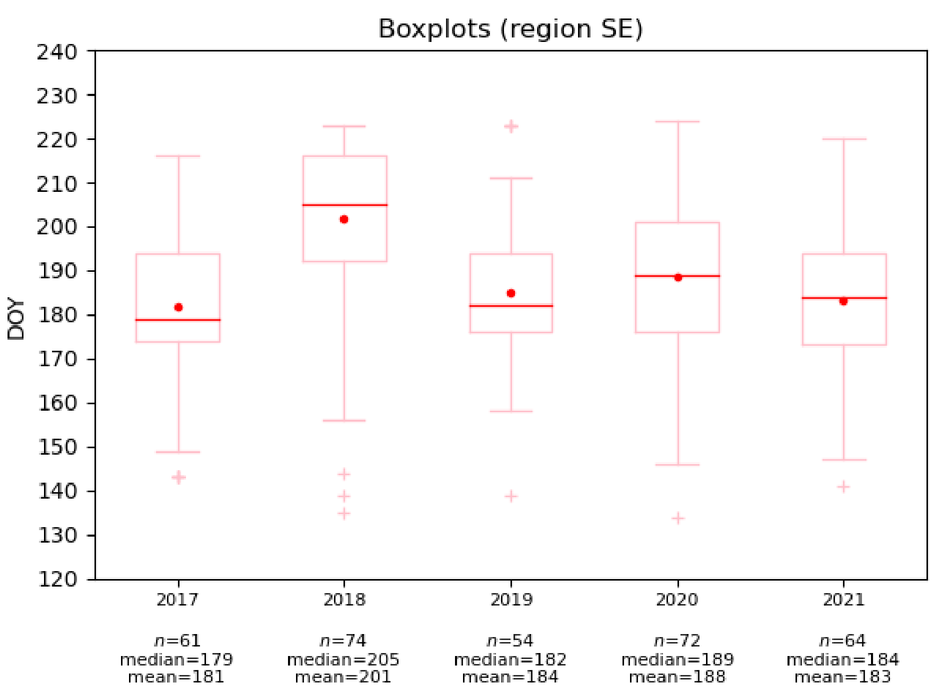
Boxplots (region SE)
DOY
2017
n=61
median=179
mean=181
2018
n=74
median=205
mean=201
2019
n=54
median=182
mean=184
2020
n=72
median=189
mean=188
2021
n=64
median=184
mean=183

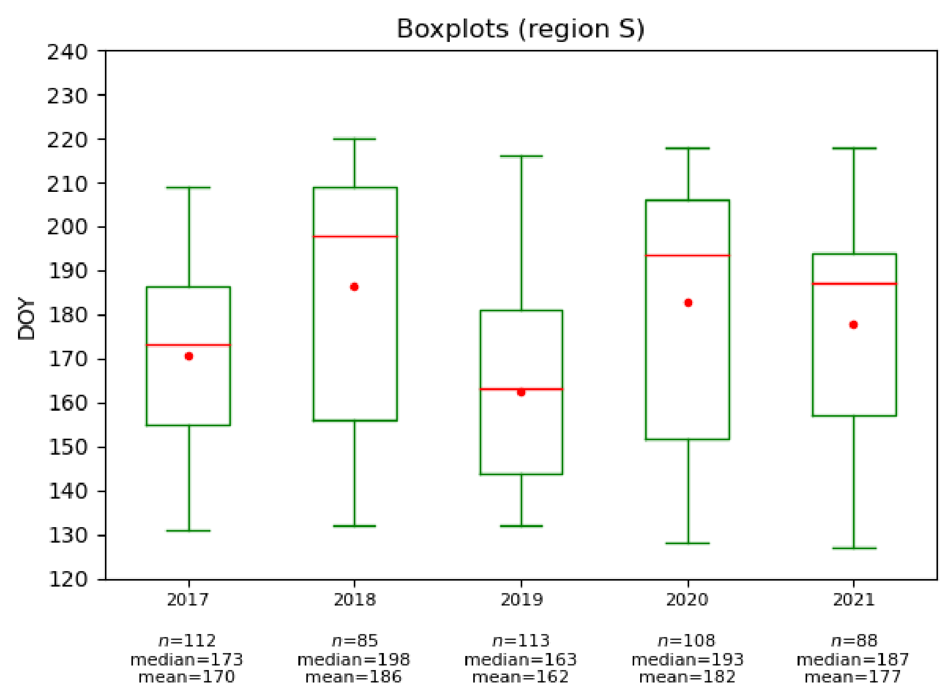
Boxplots (region S)
DOY
2017
n=112
median=173
mean=170
2018
n=85
median=198
mean=186
2019
n=113
median=163
mean=162
2020
n=108
median=193
mean=182
2021
n=88
median=187
mean=177

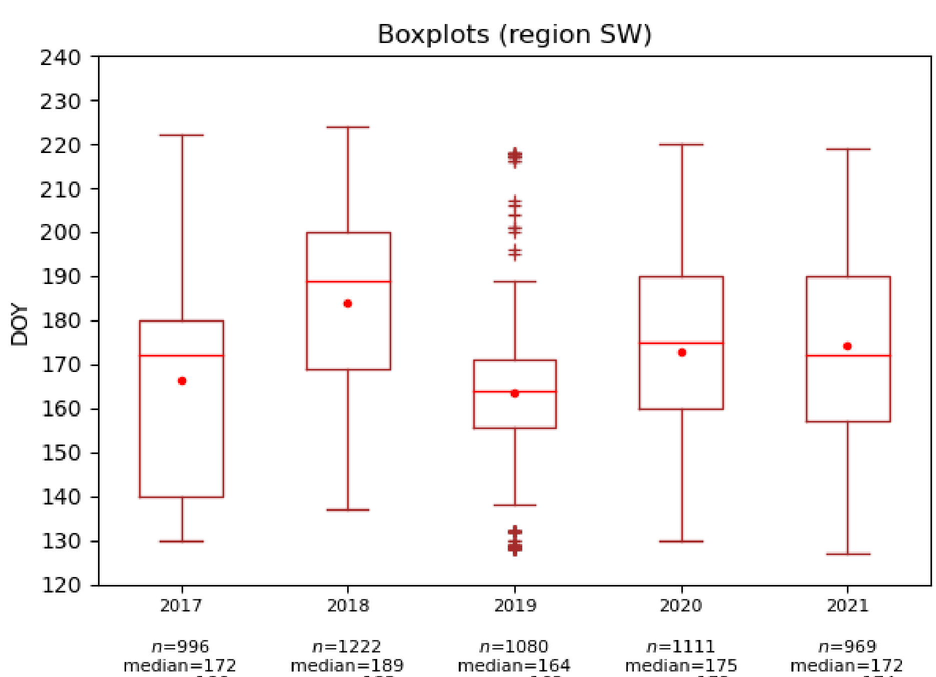
Boxplots (region SW)
DOY
2017
n=996
median=172
mean=166
2018
n=1222
median=189
mean=183
2019
n=1080
median=164
mean=163
2020
n=1111
median=175
mean=172
2021
n=969
median=172
mean=174

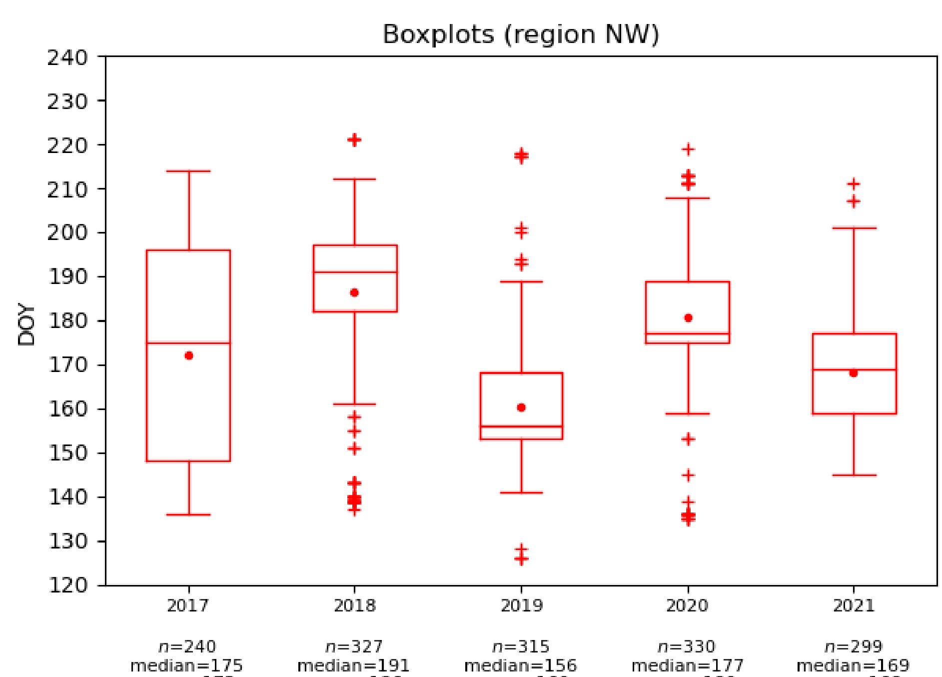
Boxplots (region NW)
DOY
2017
n=240
median=175
mean=172
2018
n=327
median=191
mean=186
2019
n=315
median=156
mean=160
2020
n=330
median=177
mean=180
2021
n=299
median=169
mean=168

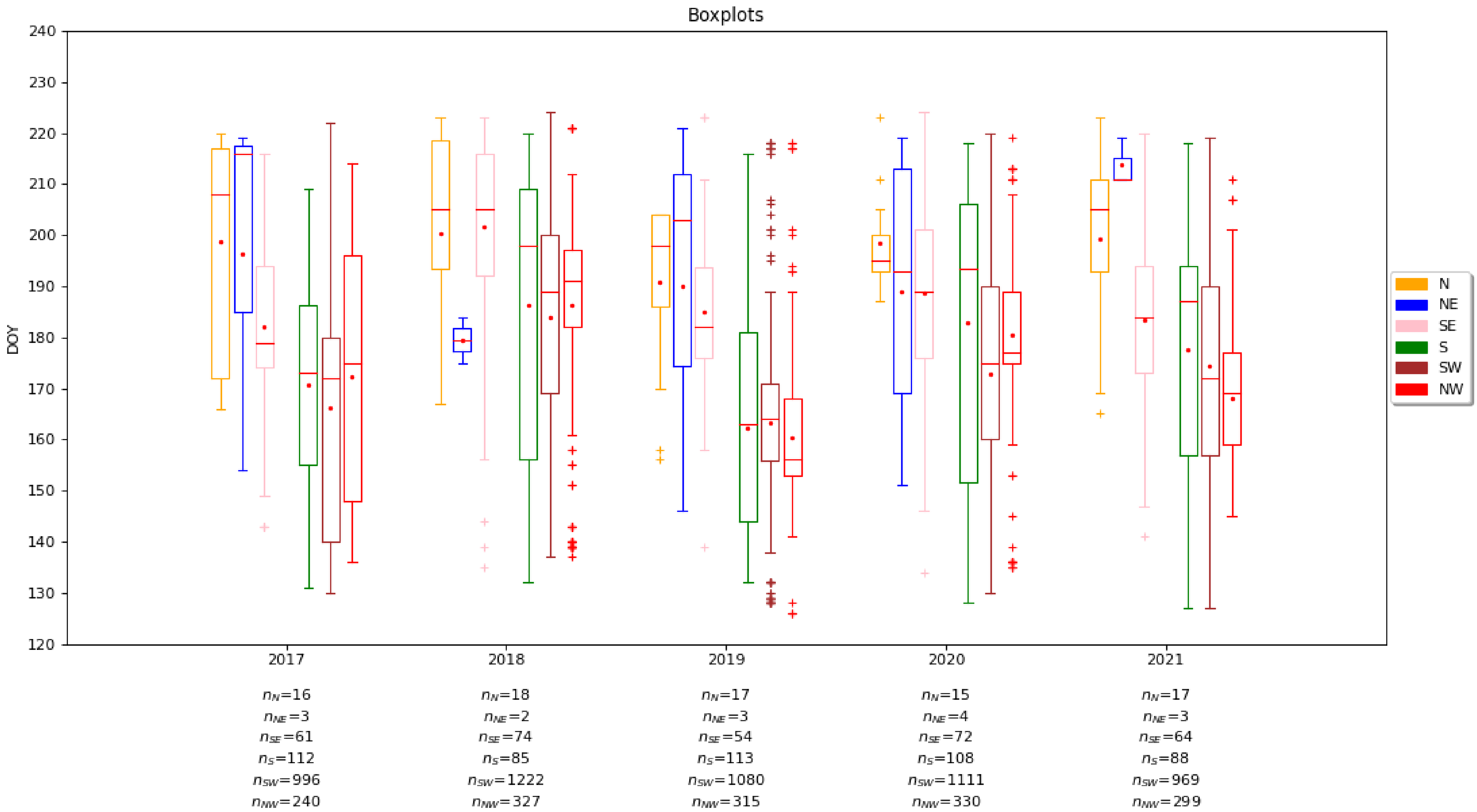
Boxplots
DOY
240
230
220
210
200
190
180
170
160
150
140
130
120
2017
2018
2019
2020
2021
N
NE
SE
S
SW
NW
n_{N}=16
n_{NE}=3
n_{SE}=61
n_{S}=112
n_{SW}=996
n_{NW}=240
n_{N}=18
n_{NE}=2
n_{SE}=74
n_{S}=85
n_{SW}=1222
n_{NW}=327
n_{N}=17
n_{NE}=3
n_{SE}=54
n_{S}=113
n_{SW}=1080
n_{NW}=315
n_{N}=15
n_{NE}=4
n_{SE}=72
n_{S}=108
n_{SW}=1111
n_{NW}=330
n_{N}=17
n_{NE}=3
n_{SE}=64
n_{S}=88
n_{SW}=969
n_{NW}=299

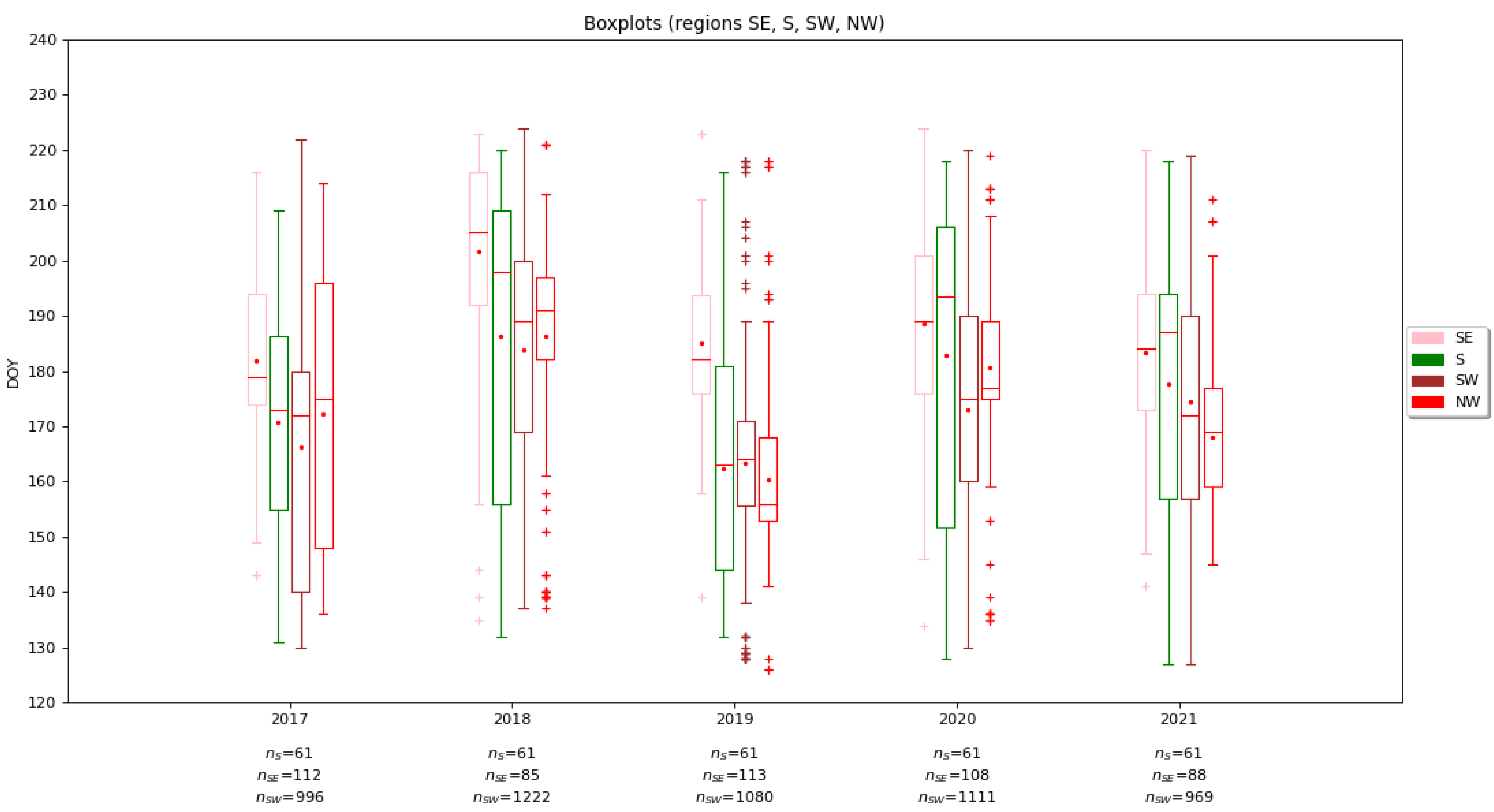
Boxplots (regions SE, S, SW, NW)
DOY
240
230
220
210
200
190
180
170
160
150
140
130
120
2017
2018
2019
2020
2021
SE
S
SW
NW
n_{S}=61
n_{SE}=112
n_{SW}=996
n_{NW}=240
n_{S}=61
n_{SE}=85
n_{SW}=1222
n_{NW}=327
n_{S}=61
n_{SE}=113
n_{SW}=1080
n_{NW}=315
n_{S}=61
n_{SE}=108
n_{SW}=1111
n_{NW}=330
n_{S}=61
n_{SE}=88
n_{SW}=969
n_{NW}=299

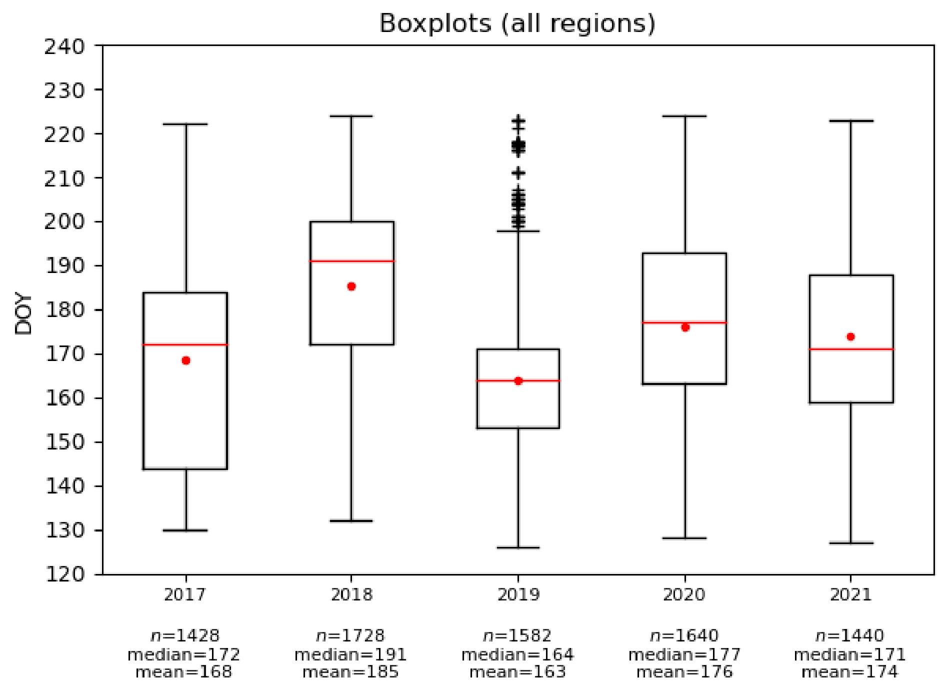
Boxplots (all regions)
DOY
2017
2018
2019
2020
2021
n=1428
median=172
mean=168
n=1728
median=191
mean=185
n=1582
median=164
mean=163
n=1640
median=177
mean=176
n=1440
median=171
mean=174

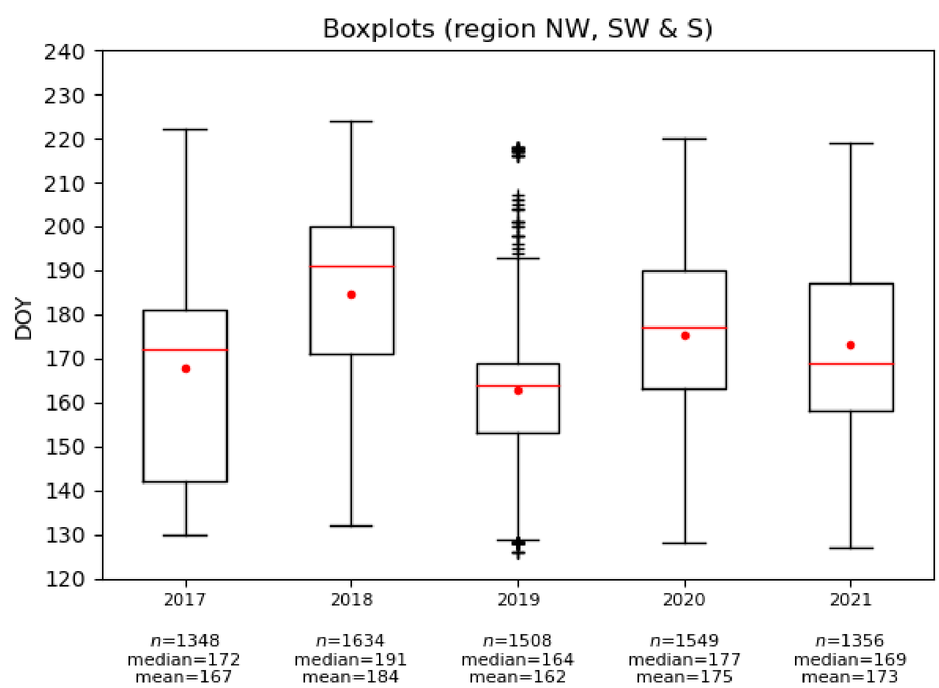
Boxplots (region NW, SW & S)
DOY
2017
2018
2019
2020
2021
n=1348
median=172
mean=167
n=1634
median=191
mean=184
n=1508
median=164
mean=162
n=1549
median=177
mean=175
n=1356
median=169
mean=173

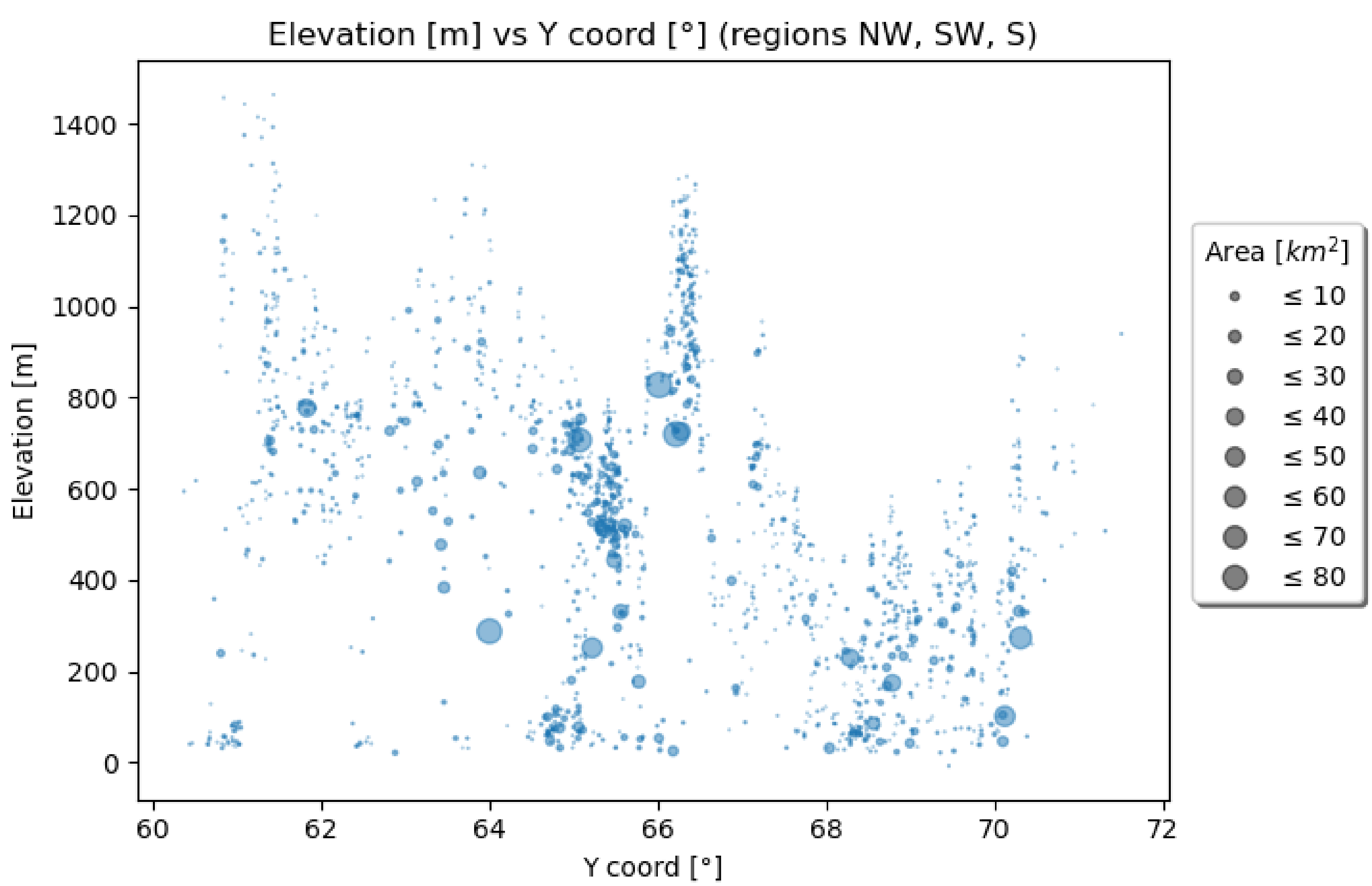
Elevation [m] vs Y coord [°] (regions NW, SW, S)
Elevation [m]
0
200
400
600
800
1000
1200
1400
Y coord [°]
60
62
64
66
68
70
72
Area [km^2]
≤ 10
≤ 20
≤ 30
≤ 40
≤ 50
≤ 60
≤ 70
≤ 80

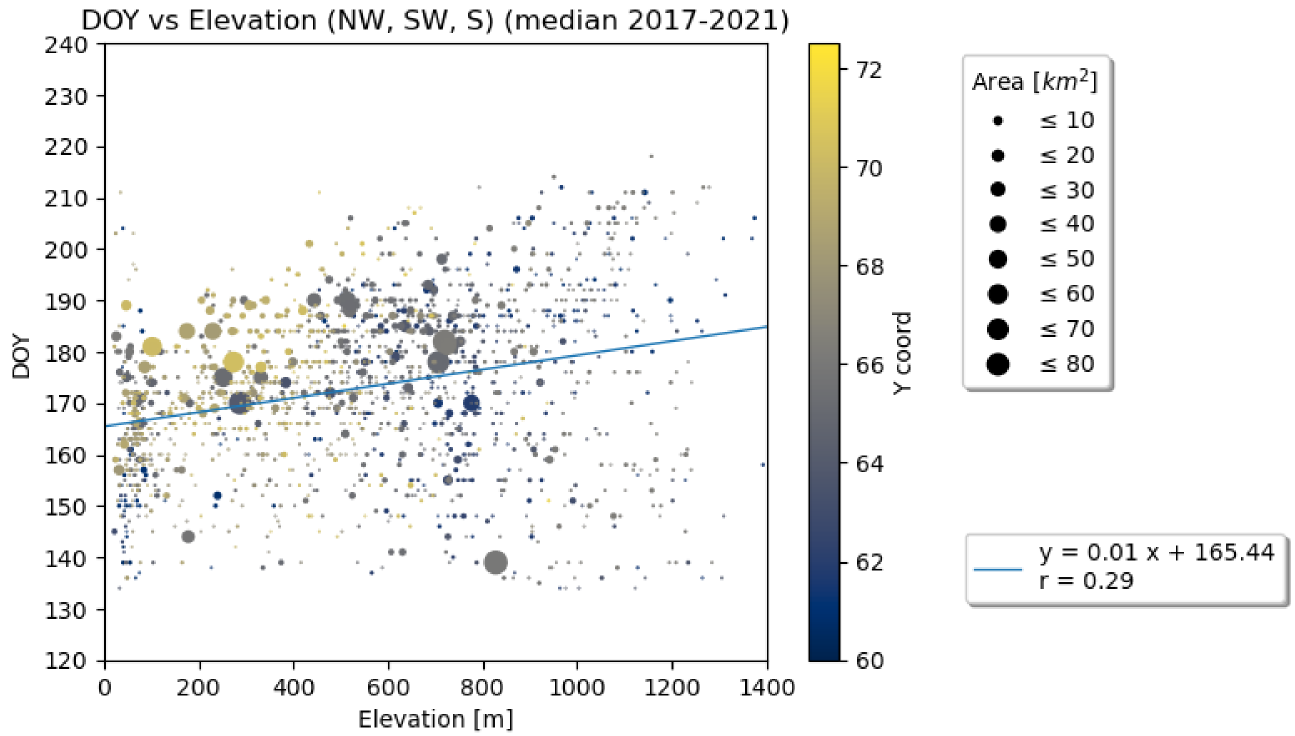
DOY vs Elevation (NW, SW, S) (median 2017-2021)
DOY
Elevation [m]
Y coord
Area [km^2]
≤ 10
≤ 20
≤ 30
≤ 40
≤ 50
≤ 60
≤ 70
≤ 80
y = 0.01 x + 165.44
r = 0.29

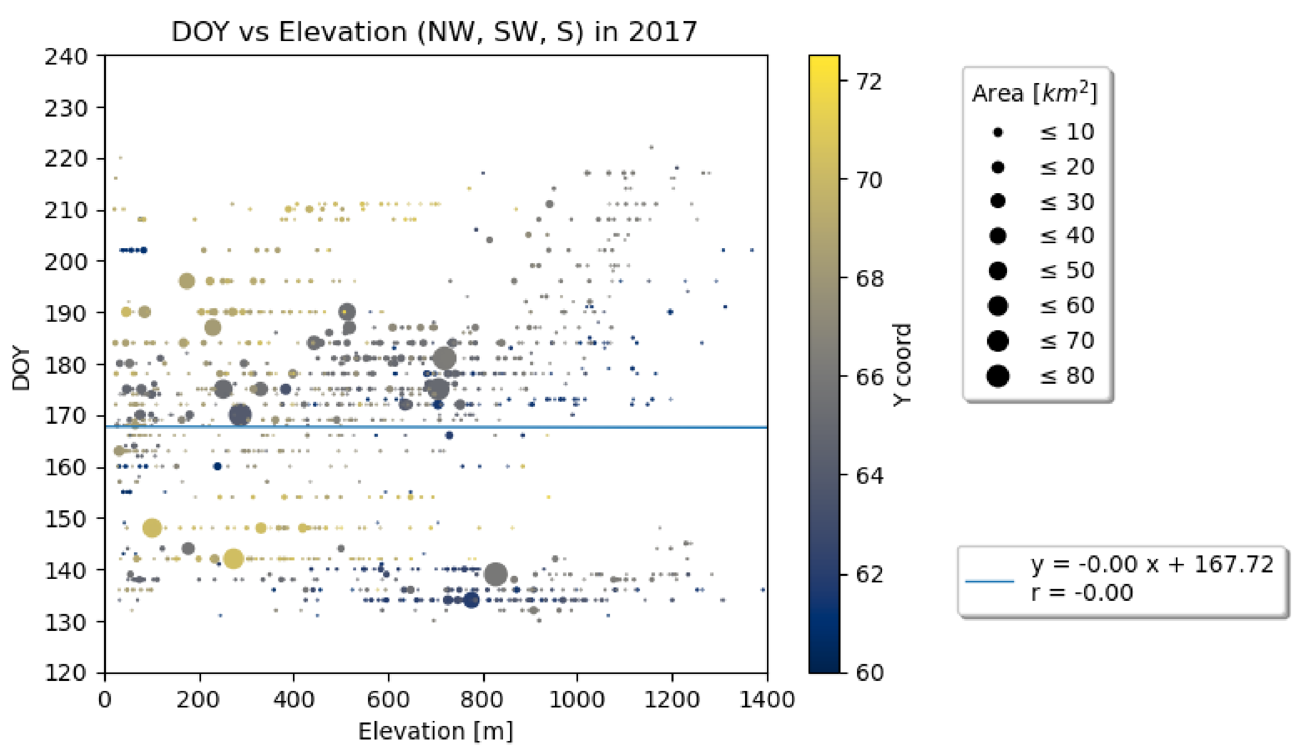
DOY vs Elevation (NW, SW, S) in 2017
DOY
Elevation [m]
Y coord
Area [km^2]
≤ 10
≤ 20
≤ 30
≤ 40
≤ 50
≤ 60
≤ 70
≤ 80
y = -0.00 x + 167.72
r = -0.00

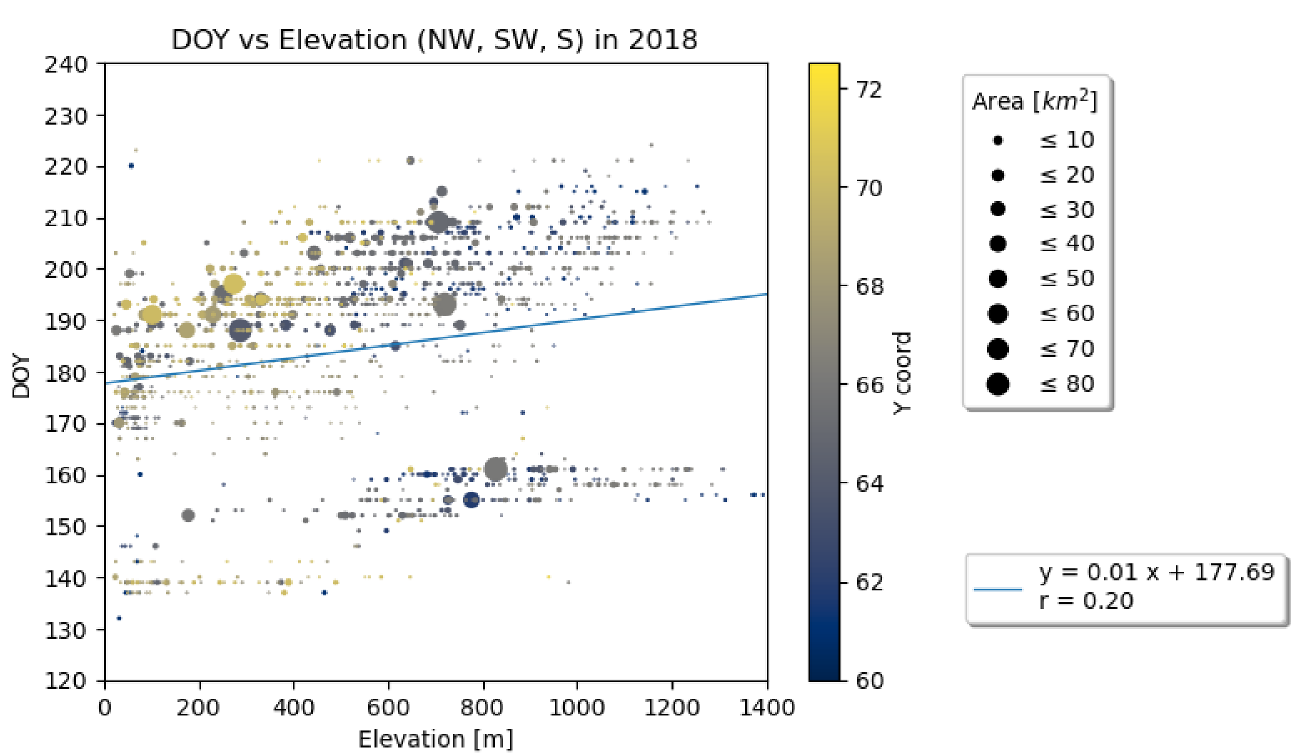
DOY vs Elevation (NW, SW, S) in 2018
DOY
Elevation [m]
Y coord
Area [km^2]
≤ 10
≤ 20
≤ 30
≤ 40
≤ 50
≤ 60
≤ 70
≤ 80
y = 0.01 x + 177.69
r = 0.20

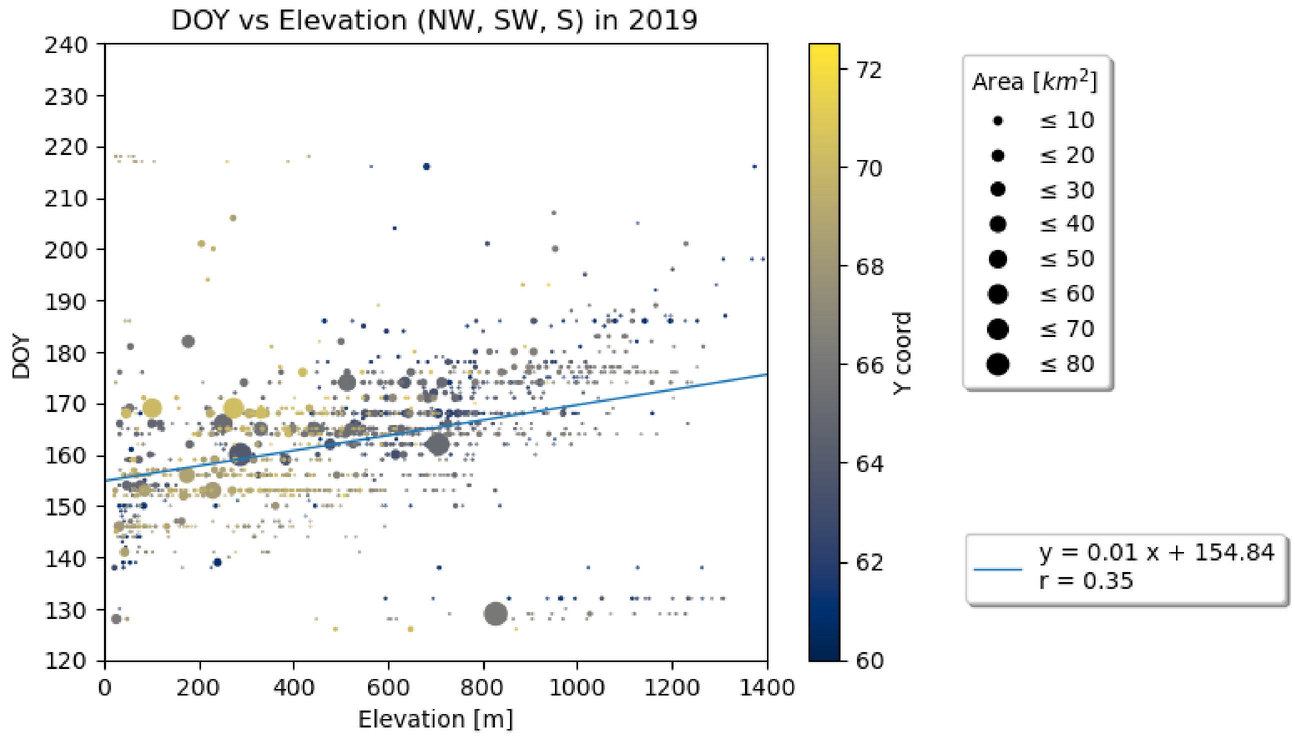
DOY vs Elevation (NW, SW, S) in 2019
DOY
Elevation [m]
Y coord
Area [km^2]
≤ 10
≤ 20
≤ 30
≤ 40
≤ 50
≤ 60
≤ 70
≤ 80
y = 0.01 x + 154.84
r = 0.35

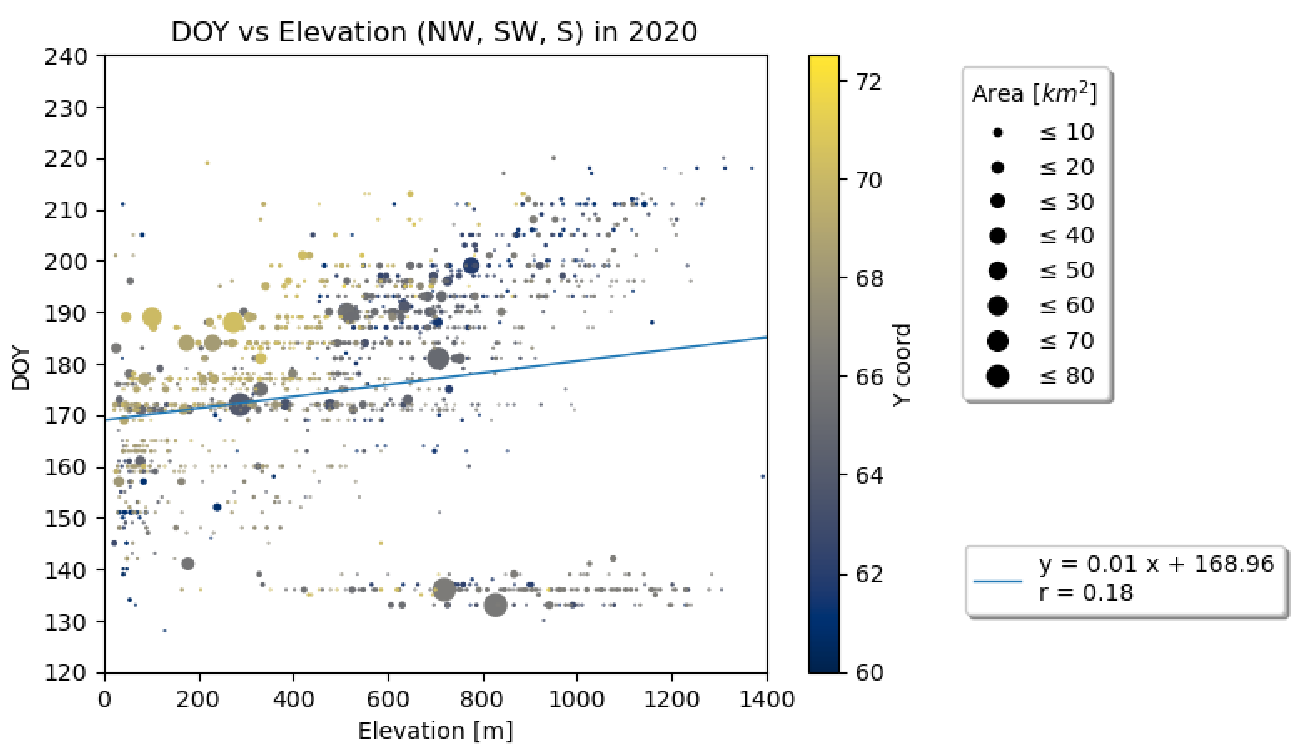
DOY vs Elevation (NW, SW, S) in 2020
DOY
Elevation [m]
Y coord
Area [km^2]
≤ 10
≤ 20
≤ 30
≤ 40
≤ 50
≤ 60
≤ 70
≤ 80
y = 0.01 x + 168.96
r = 0.18

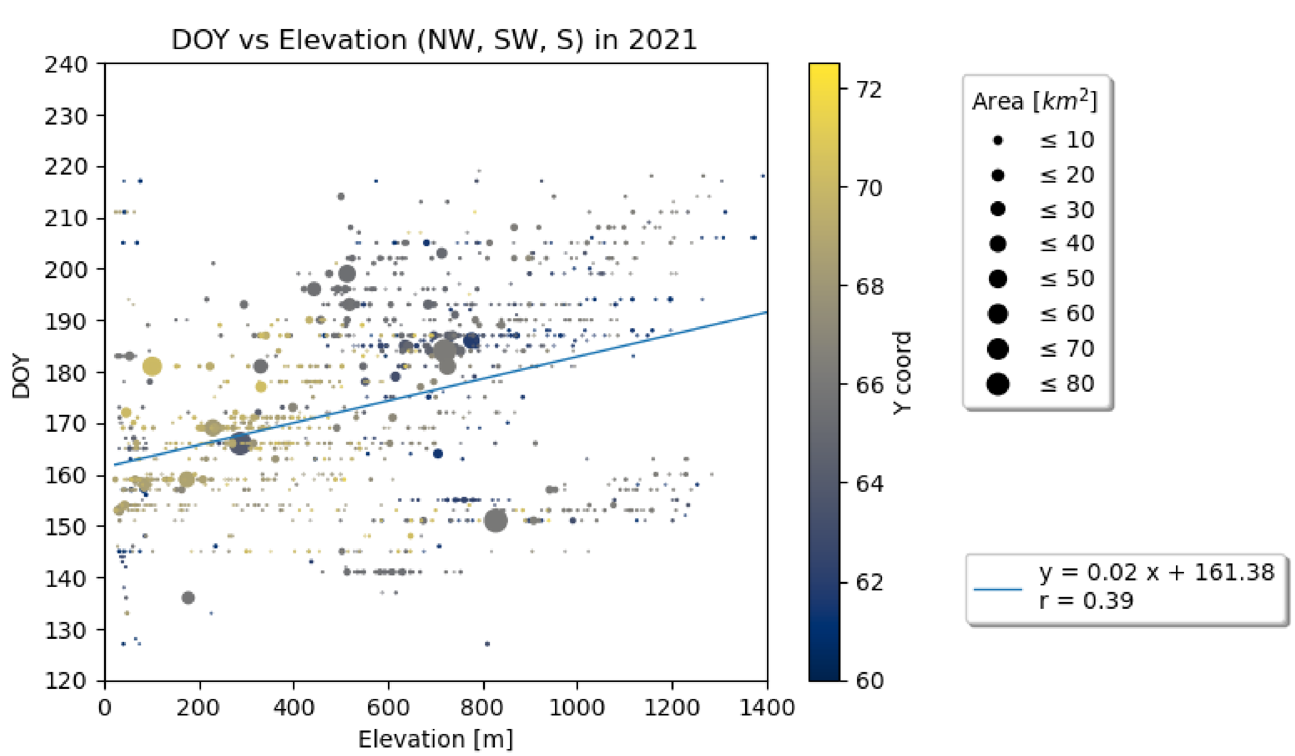
DOY vs Elevation (NW, SW, S) in 2021
DOY
Elevation [m]
Y coord
Area [km^2]
≤ 10
≤ 20
≤ 30
≤ 40
≤ 50
≤ 60
≤ 70
≤ 80
y = 0.02 x + 161.38
r = 0.39

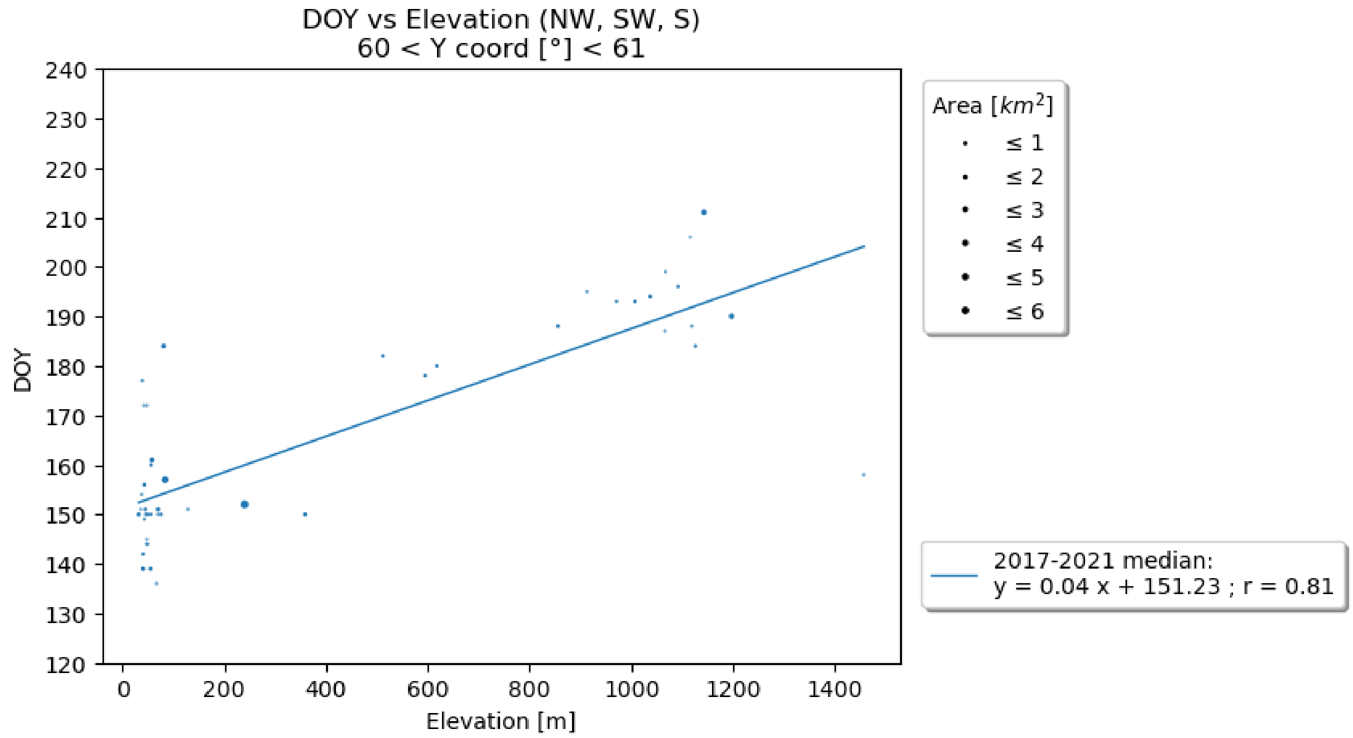

DOY vs Elevation (NW, SW, S)
60 < Y coord [°] < 61
DOY
Elevation [m]
Area [km^2]
≤ 1
≤ 2
≤ 3
≤ 4
≤ 5
≤ 6
2017-2021 median:
y = 0.04 x + 151.23 ; r = 0.81

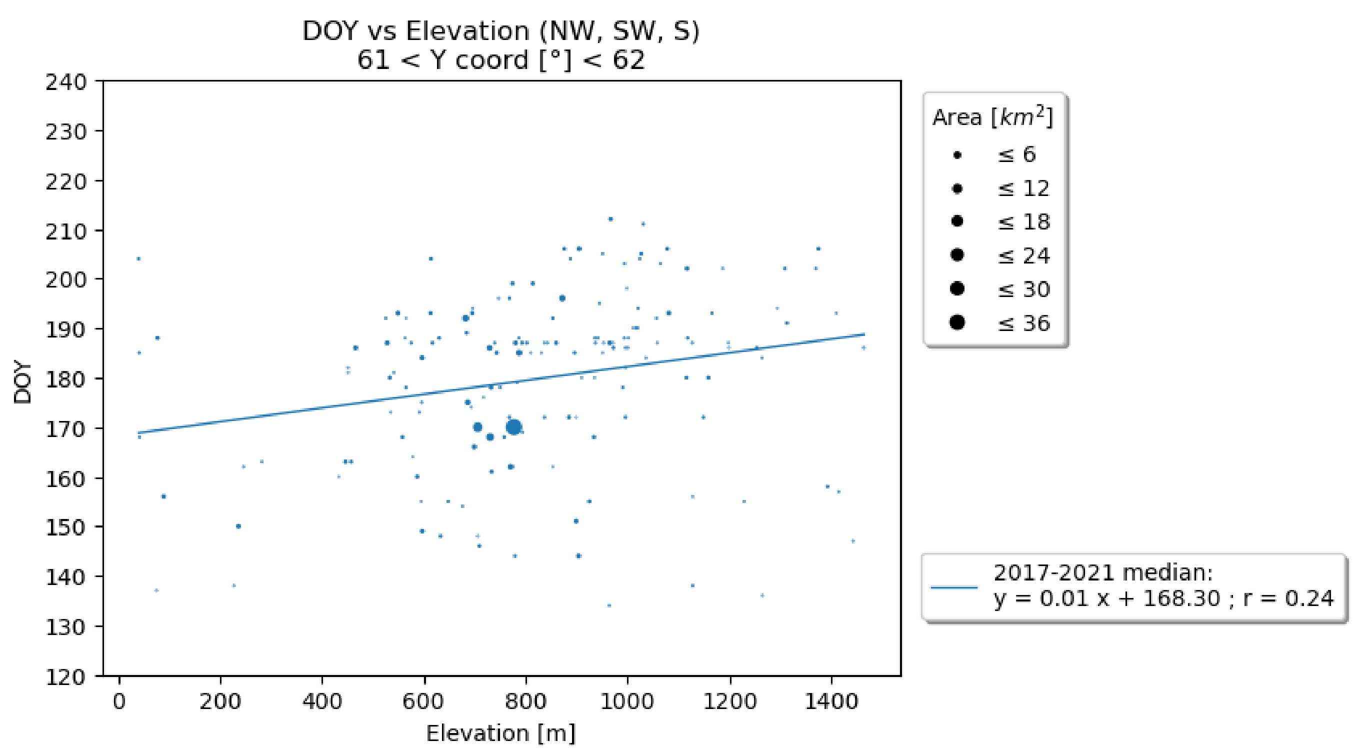

DOY vs Elevation (NW, SW, S)
61 < Y coord [°] < 62
DOY
Elevation [m]
Area [km^2]
≤ 6
≤ 12
≤ 18
≤ 24
≤ 30
≤ 36
2017-2021 median:
y = 0.01 x + 168.30 ; r = 0.24

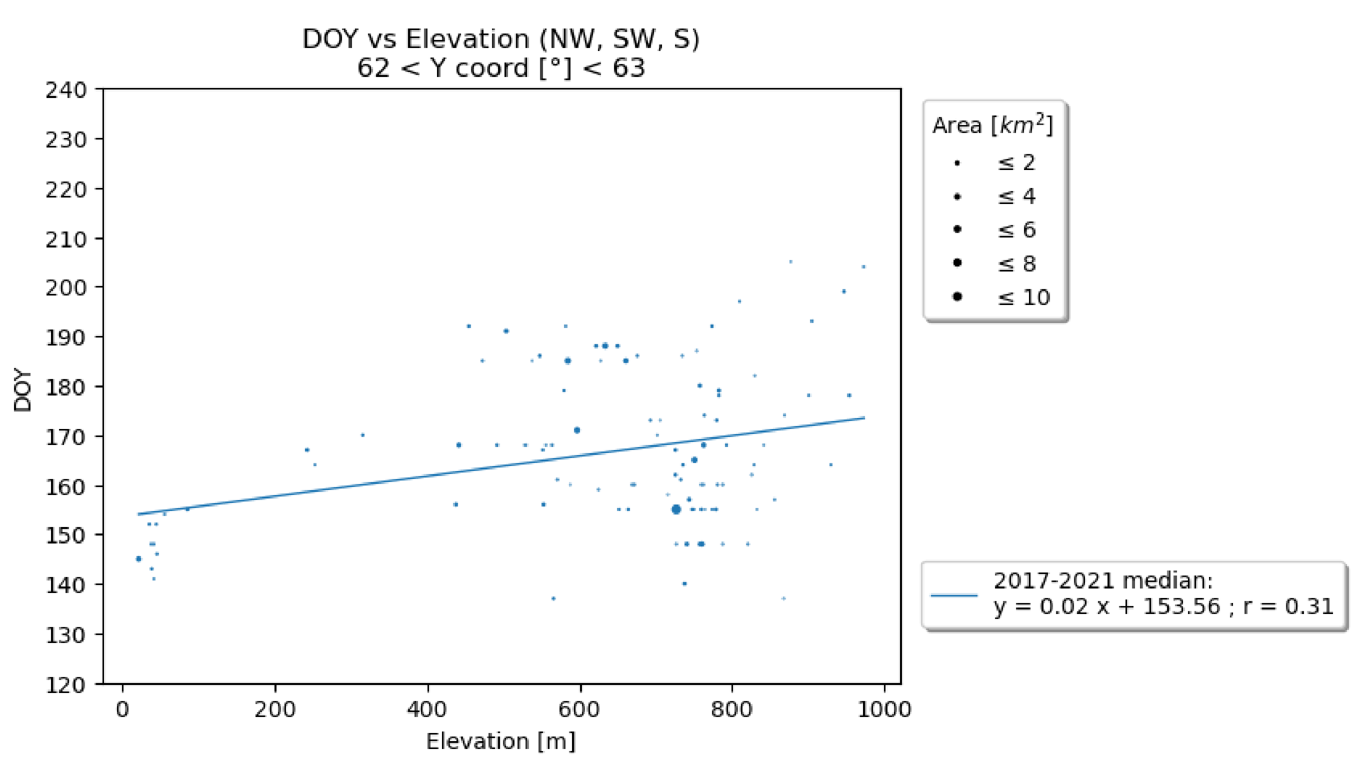

DOY vs Elevation (NW, SW, S)
62 < Y coord [°] < 63
DOY
Elevation [m]
Area [km^2]
≤ 2
≤ 4
≤ 6
≤ 8
≤ 10
2017-2021 median:
y = 0.02 x + 153.56 ; r = 0.31

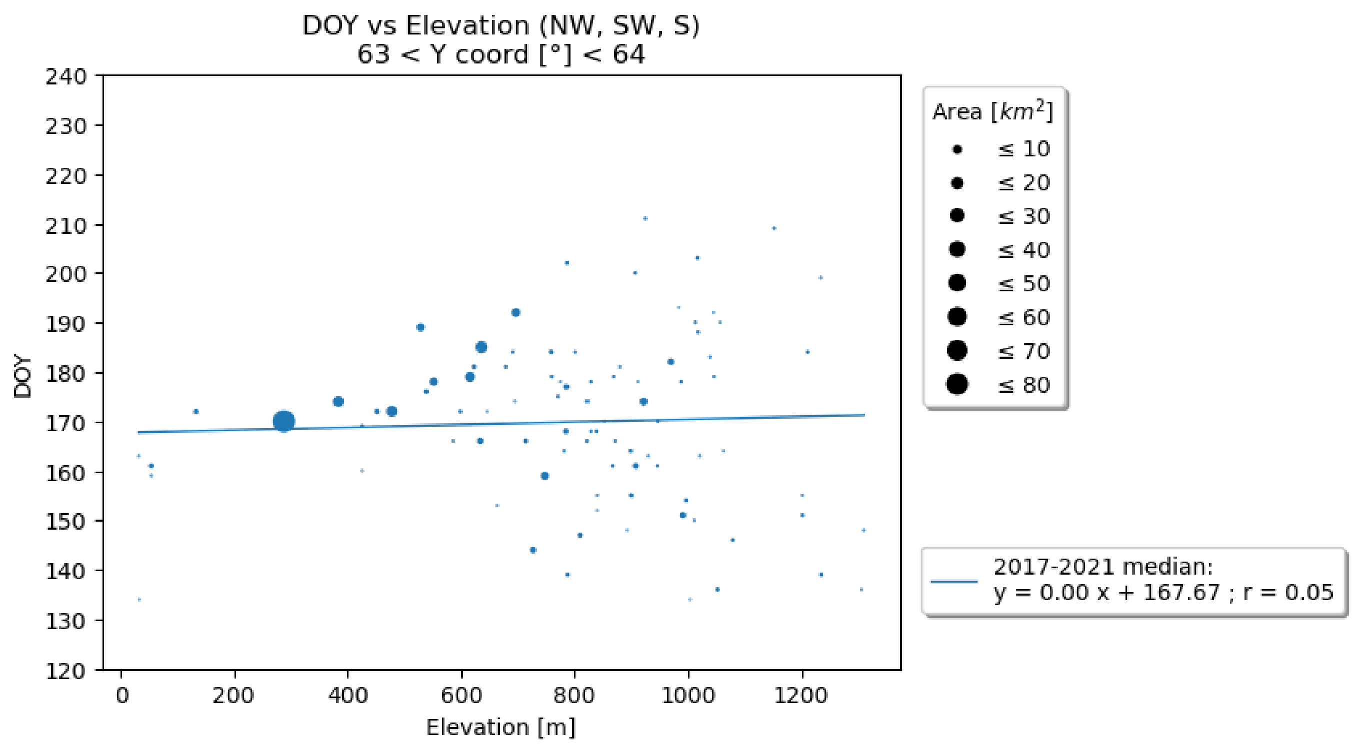
DOY vs Elevation (NW, SW, S)
63 < Y coord [°] < 64
DOY
Elevation [m]
Area [km^2]
≤ 10
≤ 20
≤ 30
≤ 40
≤ 50
≤ 60
≤ 70
≤ 80
2017-2021 median:
y = 0.00 x + 167.67 ; r = 0.05

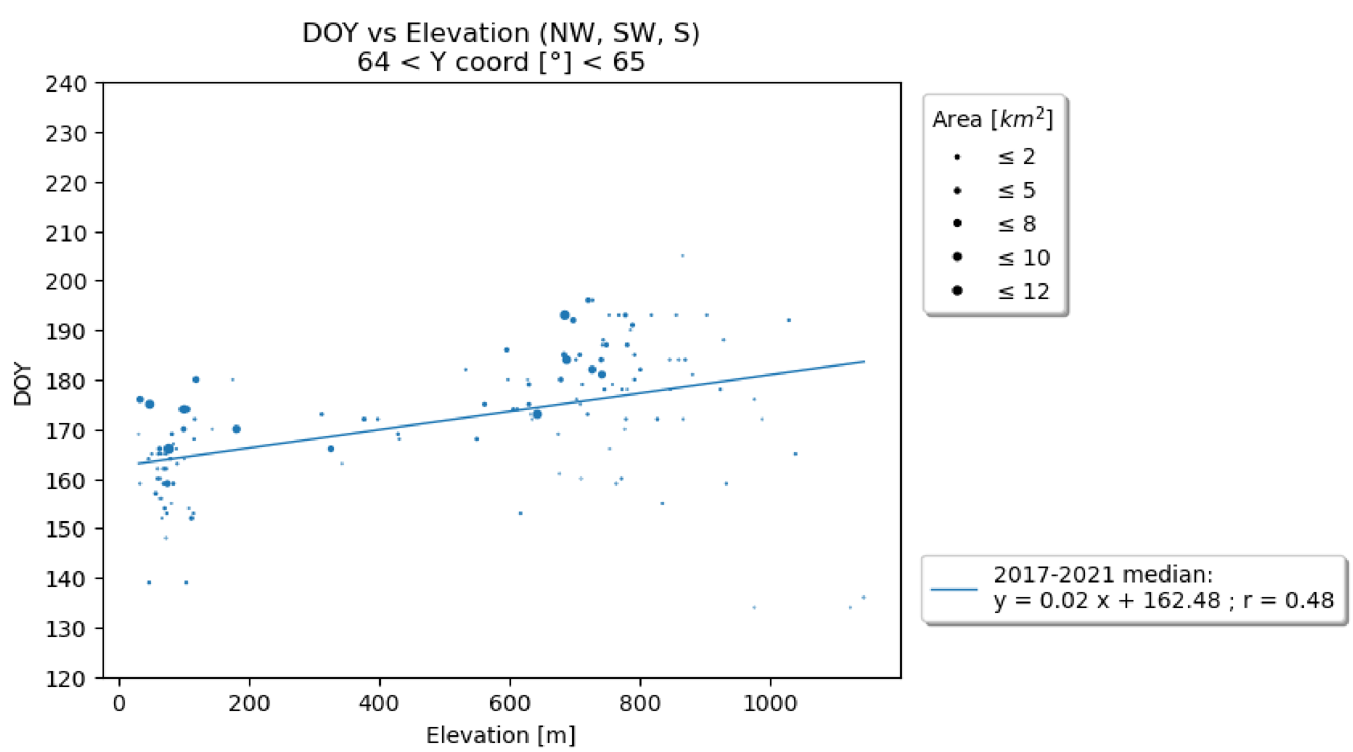
DOY vs Elevation (NW, SW, S)
64 < Y coord [°] < 65
DOY
Elevation [m]
Area [km^2]
≤ 2
≤ 5
≤ 8
≤ 10
≤ 12
2017-2021 median:
y = 0.02 x + 162.48 ; r = 0.48

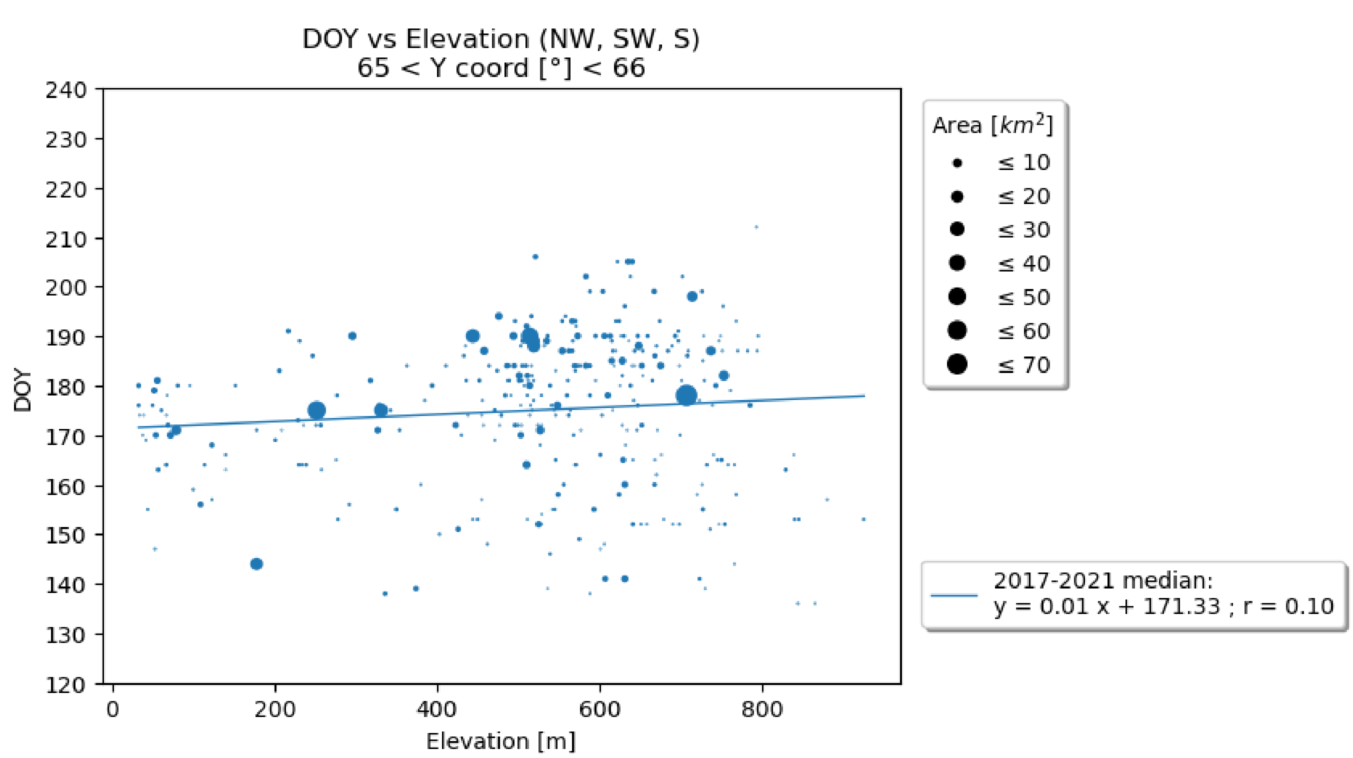
DOY vs Elevation (NW, SW, S)
65 < Y coord [°] < 66
DOY
Elevation [m]
Area [km^2]
≤ 10
≤ 20
≤ 30
≤ 40
≤ 50
≤ 60
≤ 70
2017-2021 median:
y = 0.01 x + 171.33 ; r = 0.10

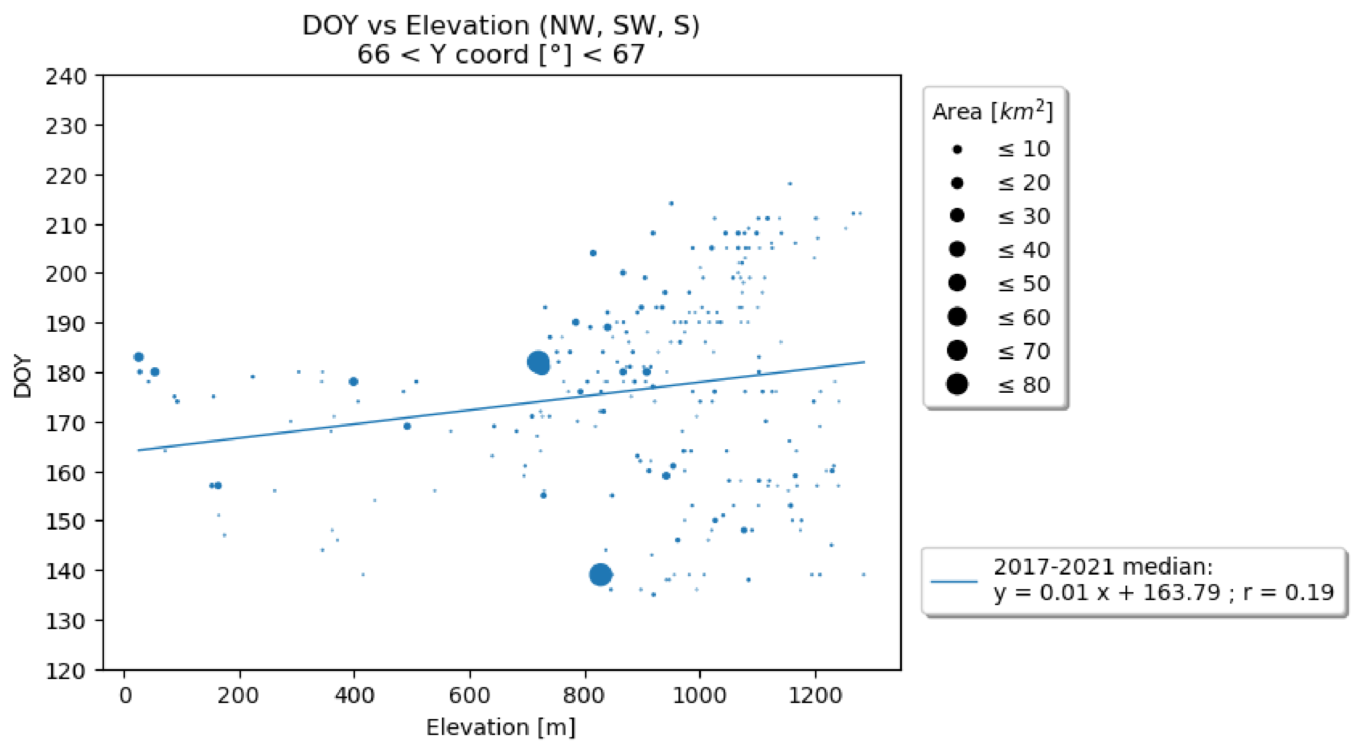
DOY vs Elevation (NW, SW, S)
66 < Y coord [°] < 67
DOY
Elevation [m]
Area [km^2]
≤ 10
≤ 20
≤ 30
≤ 40
≤ 50
≤ 60
≤ 70
≤ 80
2017-2021 median:
y = 0.01 x + 163.79 ; r = 0.19

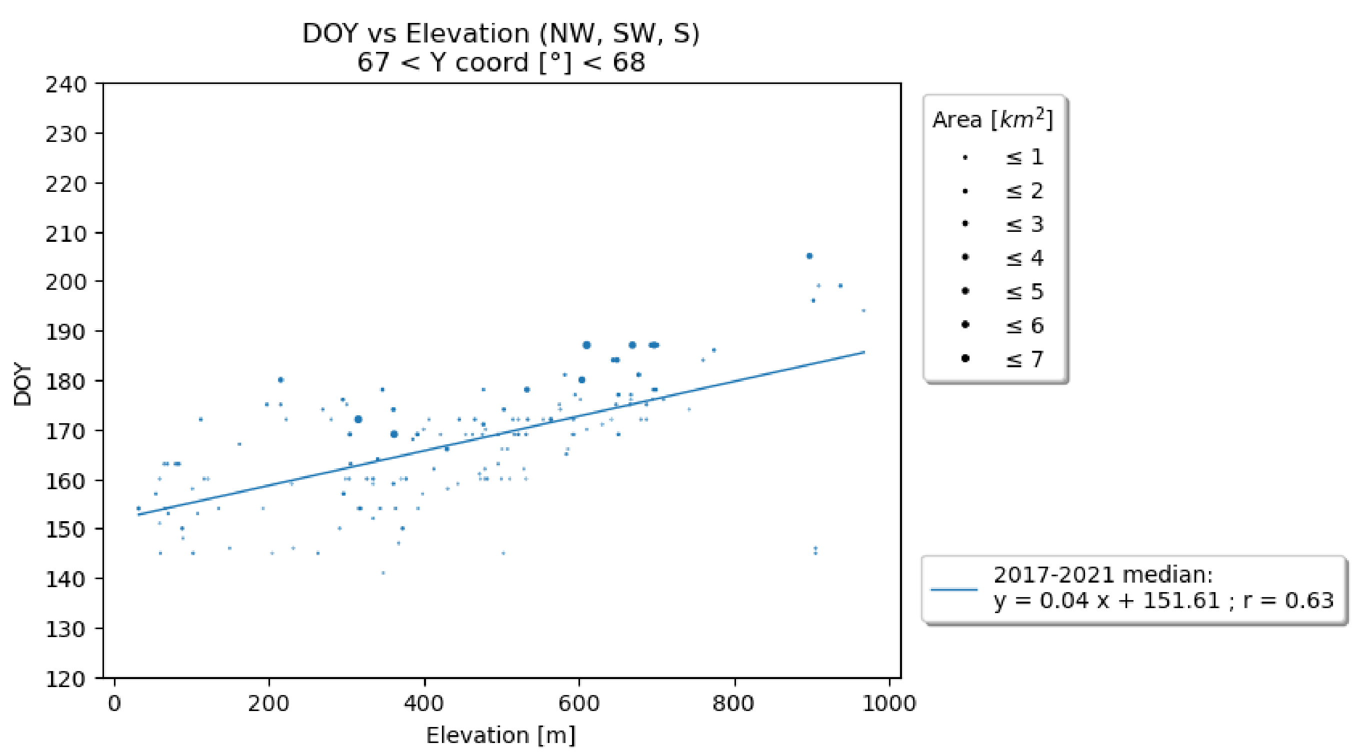
DOY vs Elevation (NW, SW, S)
67 < Y coord [°] < 68
DOY
Elevation [m]
Area [km^2]
≤ 1
≤ 2
≤ 3
≤ 4
≤ 5
≤ 6
≤ 7
2017-2021 median:
y = 0.04 x + 151.61 ; r = 0.63

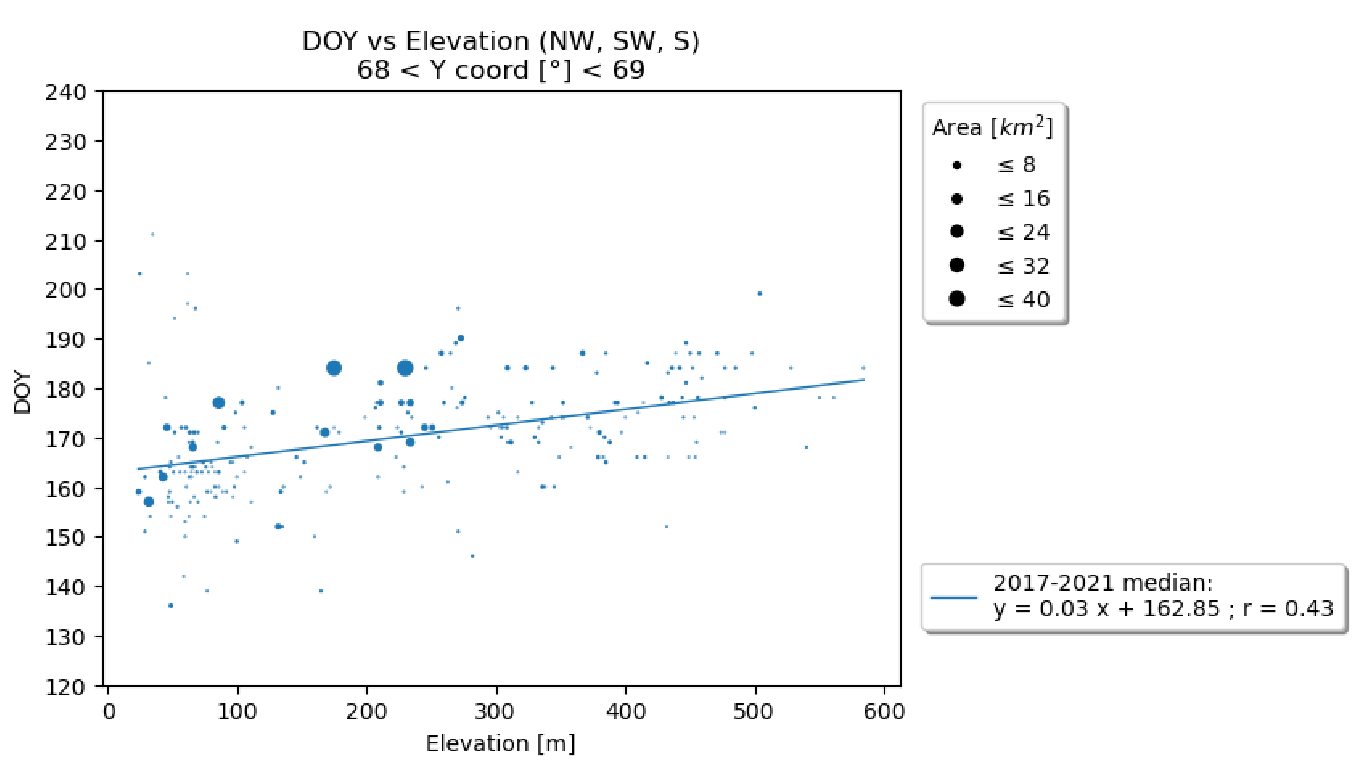
DOY vs Elevation (NW, SW, S)
68 < Y coord [°] < 69
DOY
Elevation [m]
Area [km^2]
≤ 8
≤ 16
≤ 24
≤ 32
≤ 40
2017-2021 median:
y = 0.03 x + 162.85 ; r = 0.43

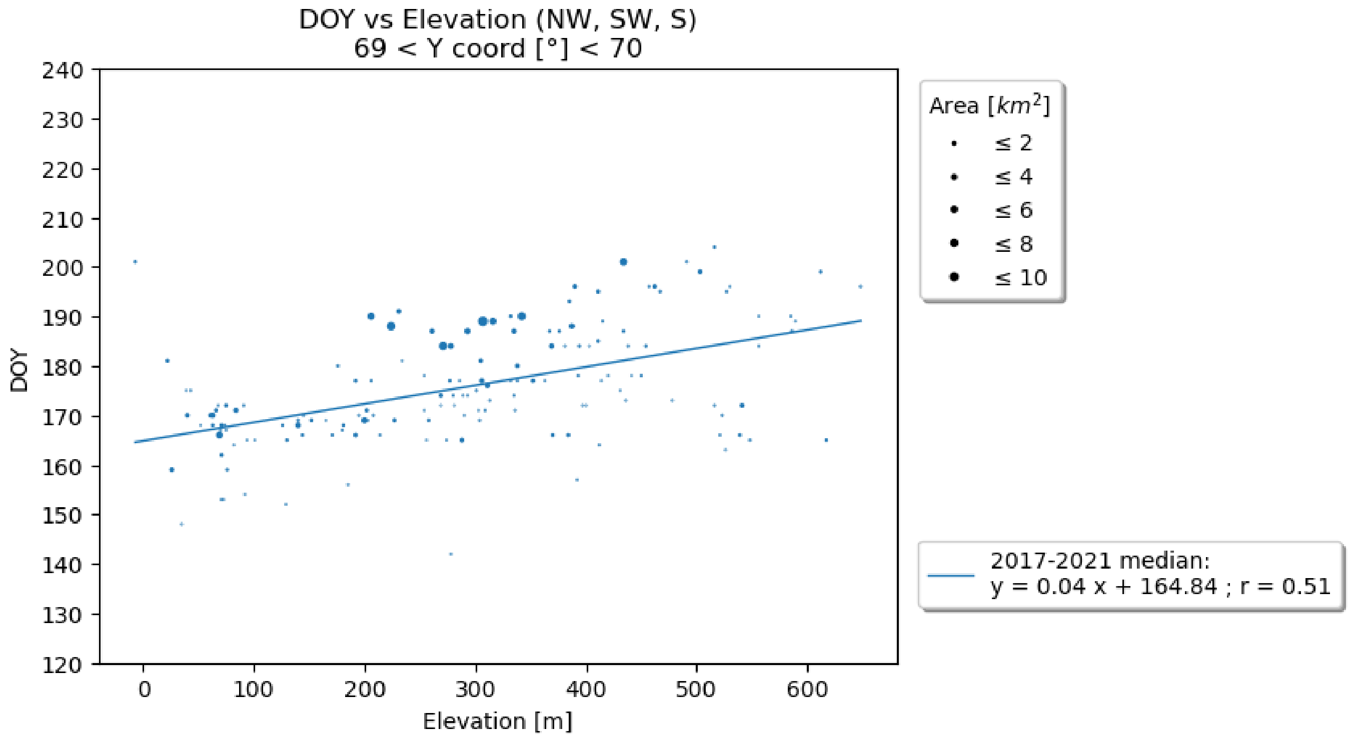
DOY vs Elevation (NW, SW, S)
69 < Y coord [°] < 70
DOY
Elevation [m]
Area [km^2]
≤ 2
≤ 4
≤ 6
≤ 8
≤ 10
2017-2021 median:
y = 0.04 x + 164.84 ; r = 0.51

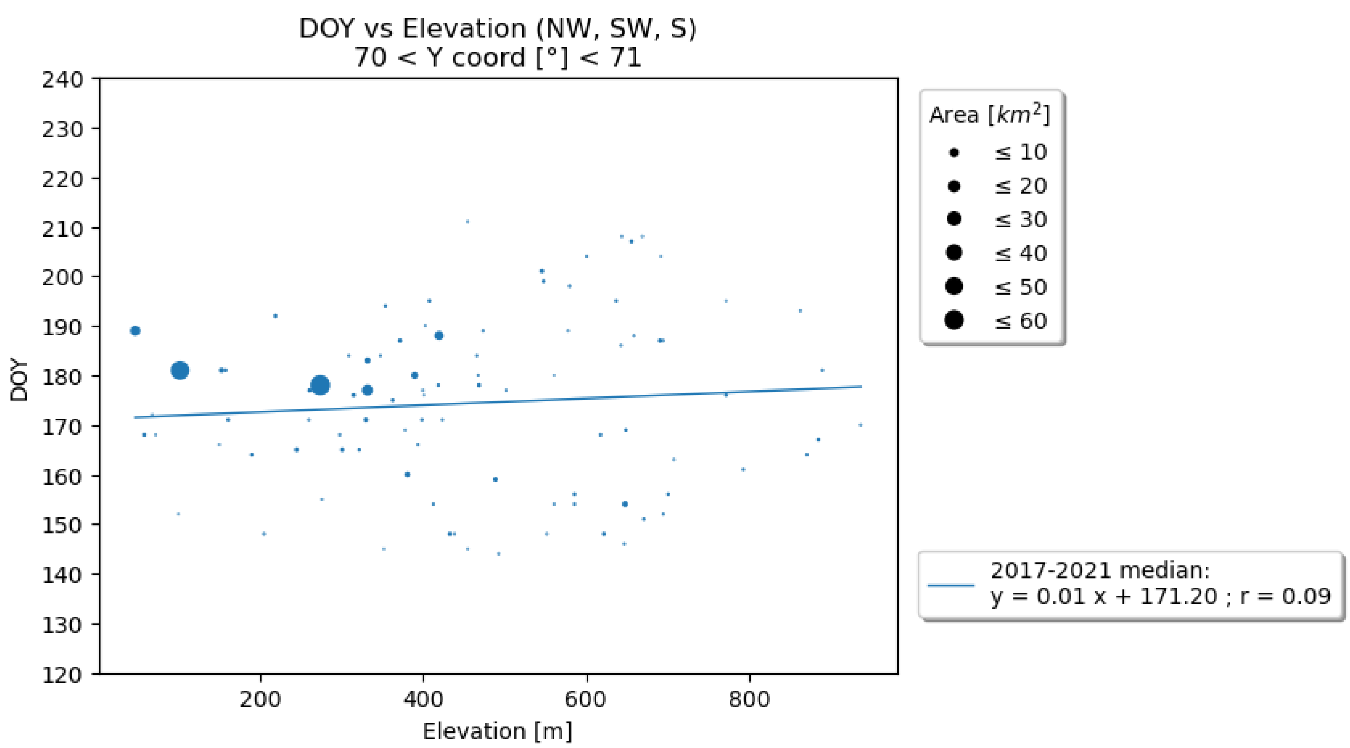
DOY vs Elevation (NW, SW, S)
70 < Y coord [°] < 71
DOY
Elevation [m]
Area [km^2]
≤ 10
≤ 20
≤ 30
≤ 40
≤ 50
≤ 60
2017-2021 median:
y = 0.01 x + 171.20 ; r = 0.09

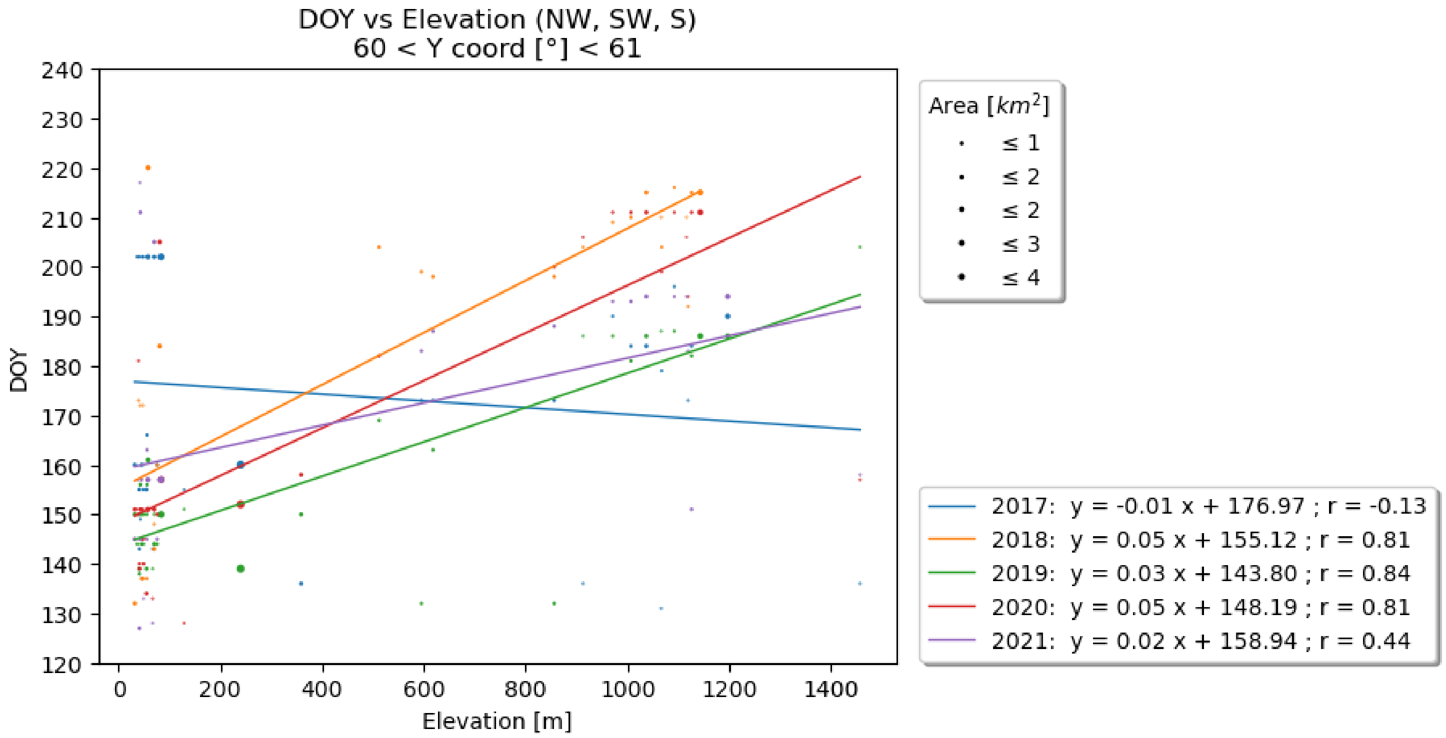
DOY vs Elevation (NW, SW, S)
60 < Y coord [°] < 61
DOY
Elevation [m]
Area [km^2]
≤ 1
≤ 2
≤ 2
≤ 3
≤ 4
2017: y = -0.01 x + 176.97 ; r = -0.13
2018: y = 0.05 x + 155.12 ; r = 0.81
2019: y = 0.03 x + 143.80 ; r = 0.84
2020: y = 0.05 x + 148.19 ; r = 0.81
2021: y = 0.02 x + 158.94 ; r = 0.44

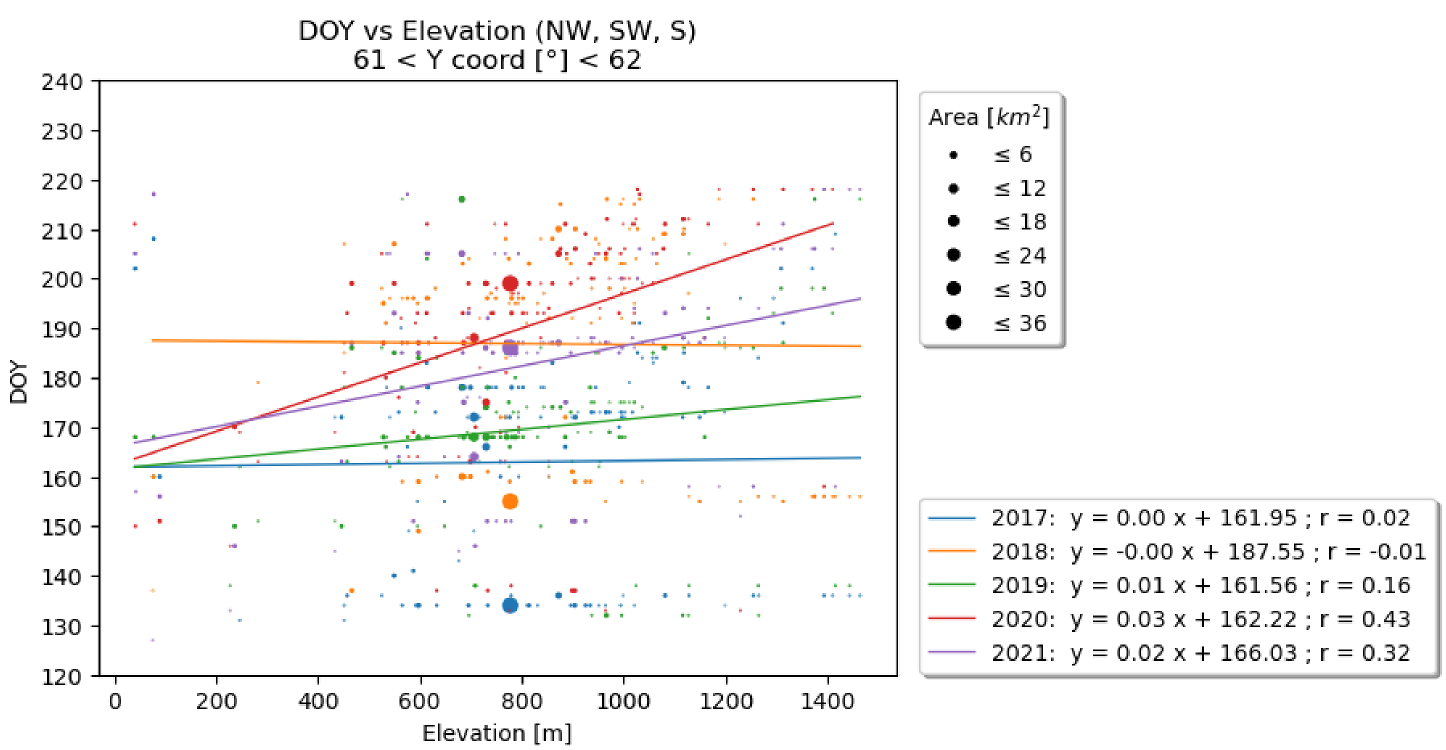
DOY vs Elevation (NW, SW, S)
61 < Y coord [°] < 62
DOY
Elevation [m]
Area [km^2]
≤ 6
≤ 12
≤ 18
≤ 24
≤ 30
≤ 36
2017: y = 0.00 x + 161.95 ; r = 0.02
2018: y = -0.00 x + 187.55 ; r = -0.01
2019: y = 0.01 x + 161.56 ; r = 0.16
2020: y = 0.03 x + 162.22 ; r = 0.43
2021: y = 0.02 x + 166.03 ; r = 0.32

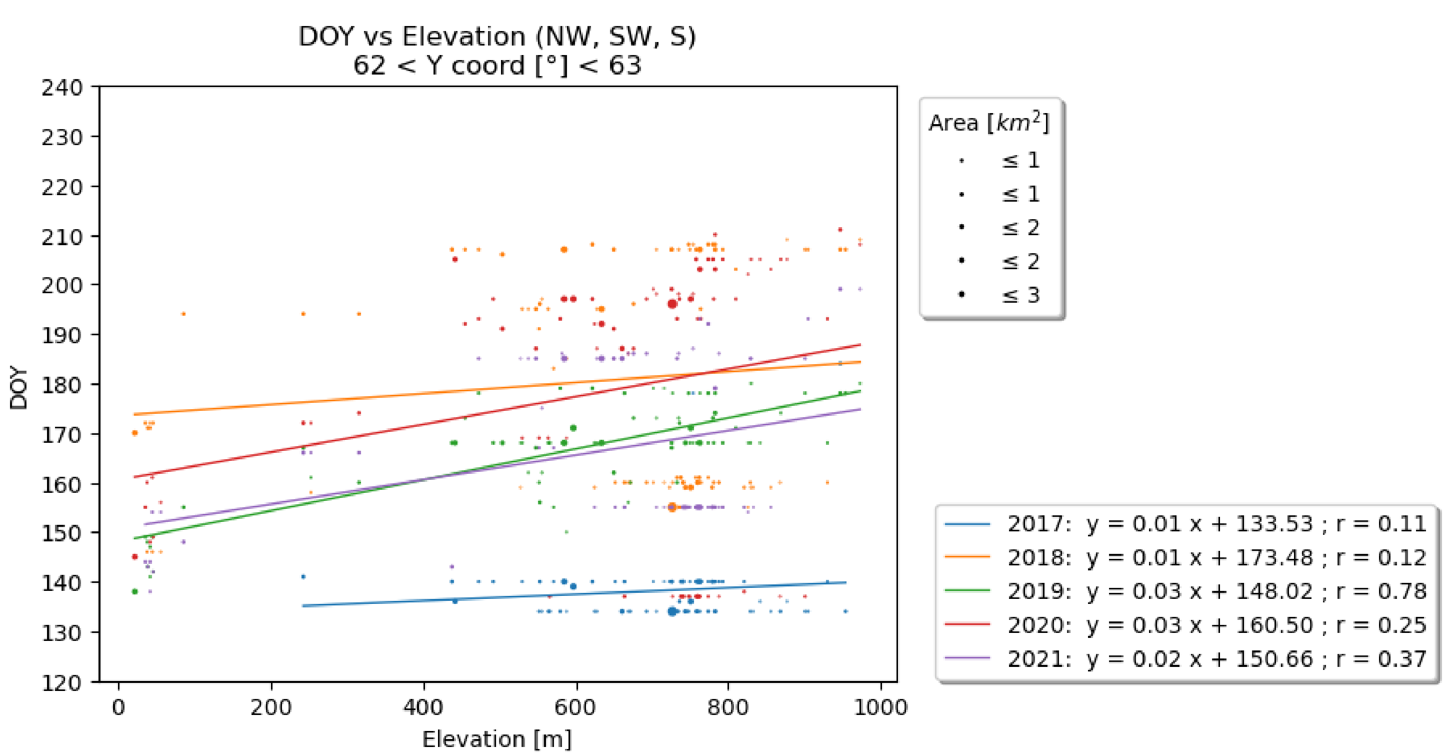
DOY vs Elevation (NW, SW, S)
62 < Y coord [°] < 63
DOY
Elevation [m]
Area [km^2]
≤ 1
≤ 1
≤ 2
≤ 2
≤ 3
2017: y = 0.01 x + 133.53 ; r = 0.11
2018: y = 0.01 x + 173.48 ; r = 0.12
2019: y = 0.03 x + 148.02 ; r = 0.78
2020: y = 0.03 x + 160.50 ; r = 0.25
2021: y = 0.02 x + 150.66 ; r = 0.37

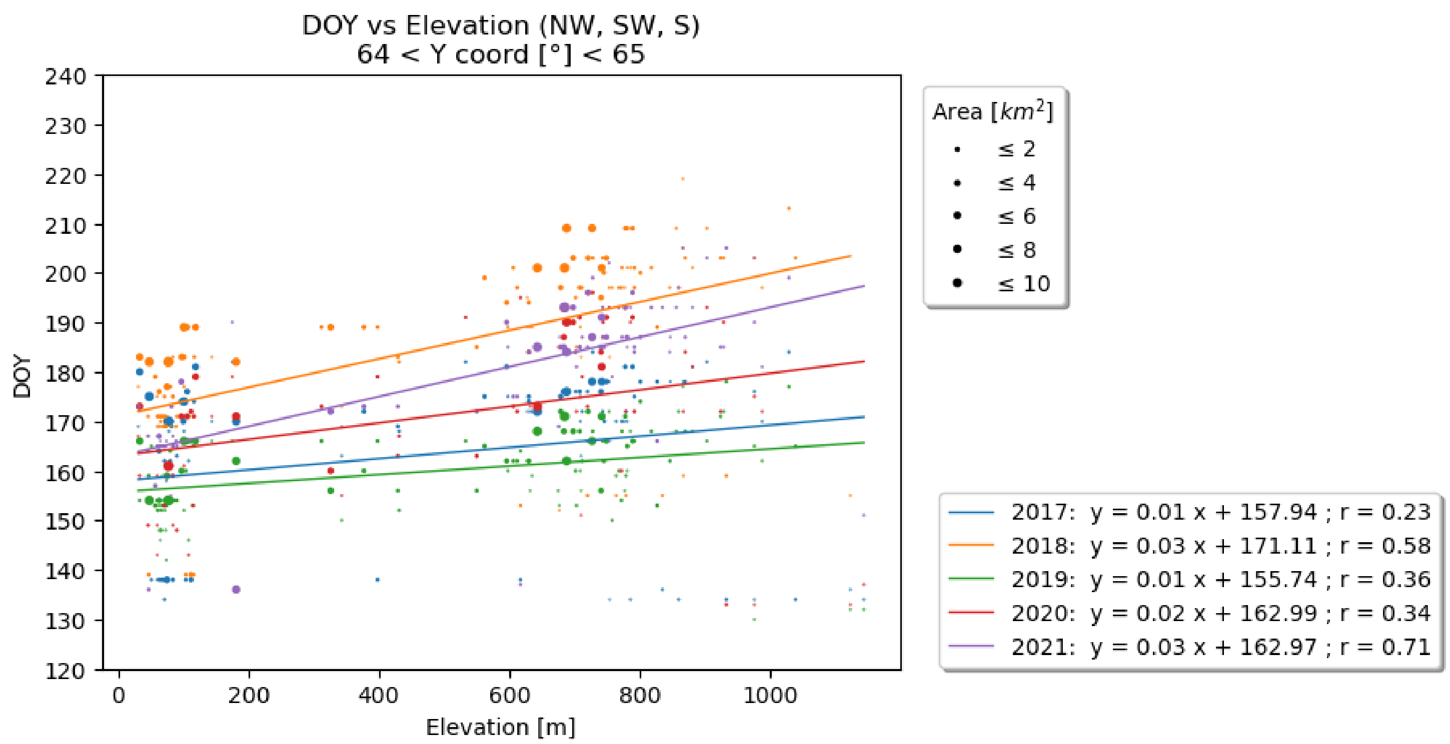
DOY vs Elevation (NW, SW, S)
64 < Y coord [°] < 65
DOY
Elevation [m]
Area [km^2]
≤ 2
≤ 4
≤ 6
≤ 8
≤ 10
2017: y = 0.01 x + 157.94 ; r = 0.23
2018: y = 0.03 x + 171.11 ; r = 0.58
2019: y = 0.01 x + 155.74 ; r = 0.36
2020: y = 0.02 x + 162.99 ; r = 0.34
2021: y = 0.03 x + 162.97 ; r = 0.71

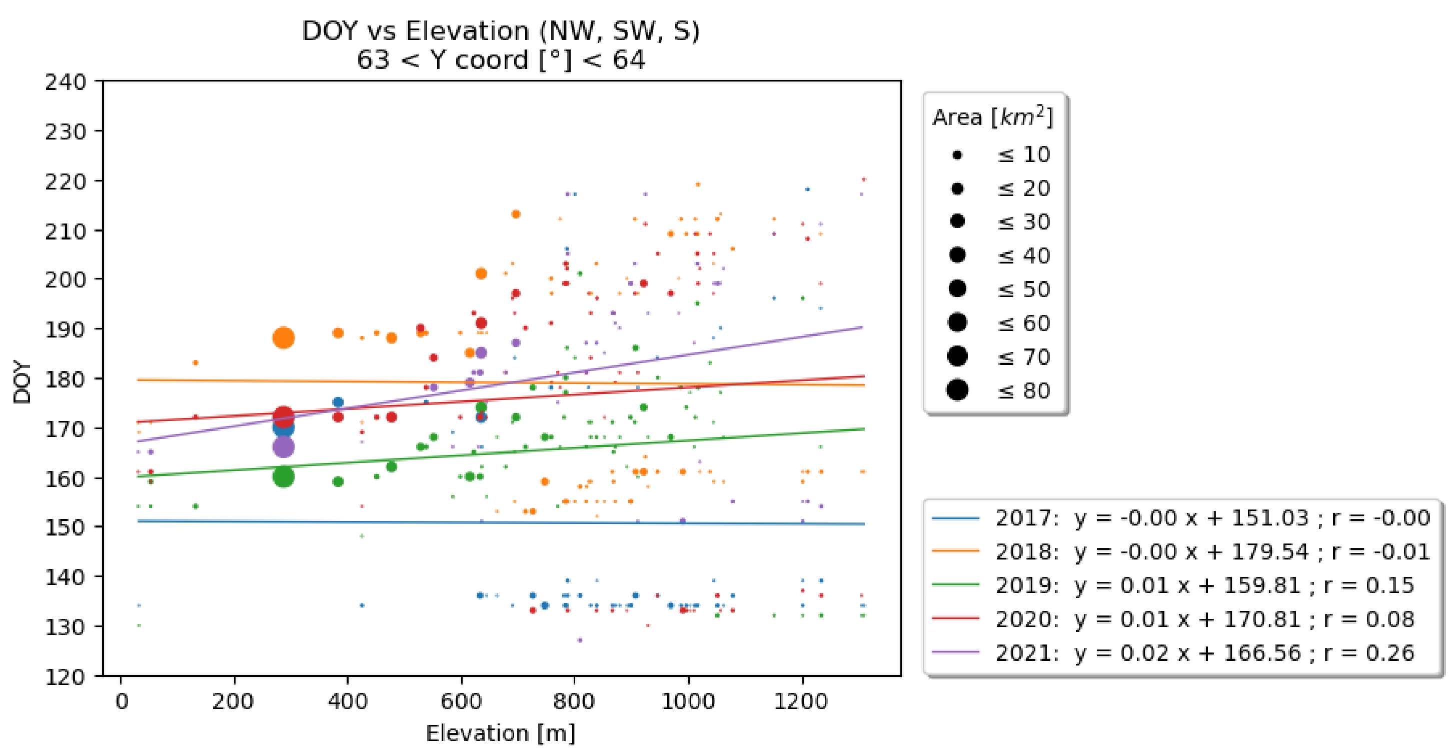
DOY vs Elevation (NW, SW, S)
63 < Y coord [°] < 64
DOY
Elevation [m]
Area [km^2]
≤ 10
≤ 20
≤ 30
≤ 40
≤ 50
≤ 60
≤ 70
≤ 80
2017: y = -0.00 x + 151.03 ; r = -0.00
2018: y = -0.00 x + 179.54 ; r = -0.01
2019: y = 0.01 x + 159.81 ; r = 0.15
2020: y = 0.01 x + 170.81 ; r = 0.08
2021: y = 0.02 x + 166.56 ; r = 0.26

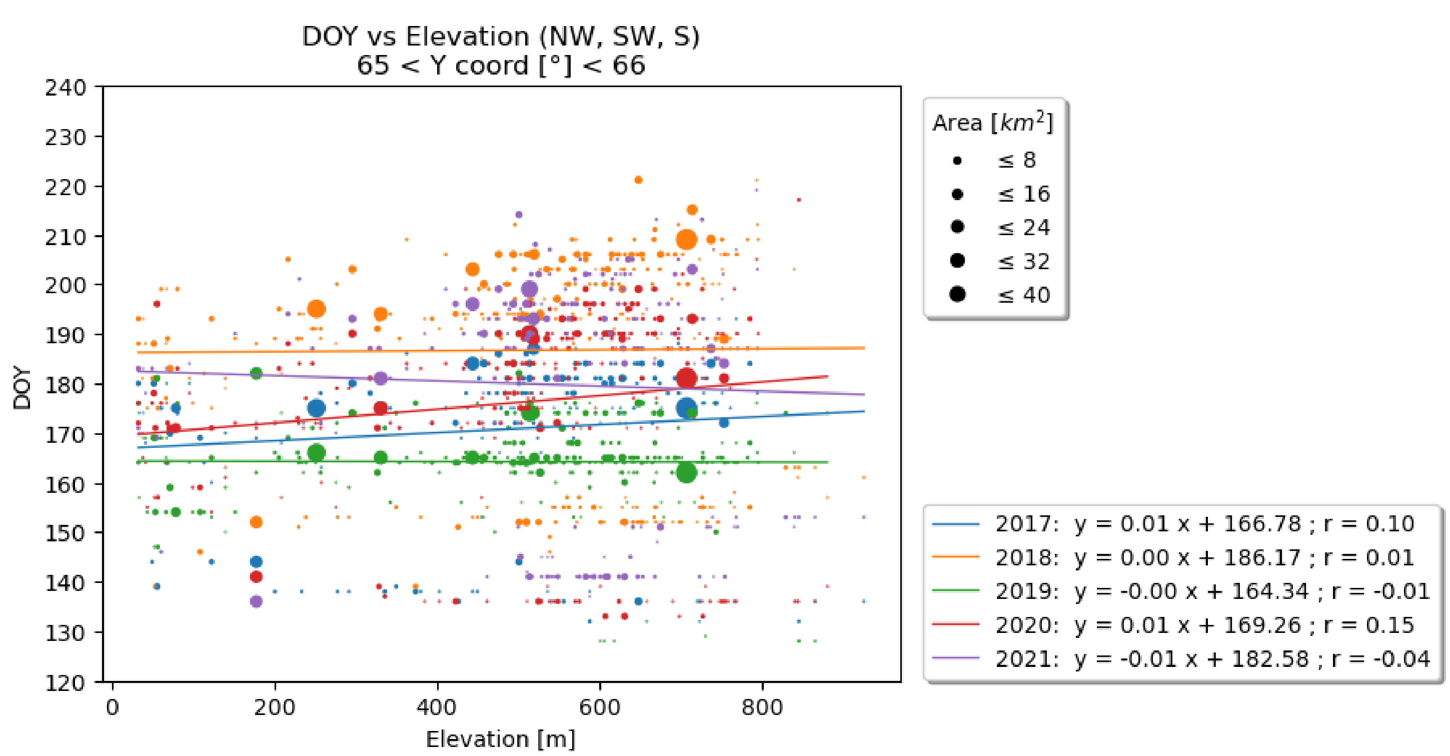
DOY vs Elevation (NW, SW, S)
65 < Y coord [°] < 66
DOY
Elevation [m]
Area [km^2]
≤ 8
≤ 16
≤ 24
≤ 32
≤ 40
2017: y = 0.01 x + 166.78 ; r = 0.10
2018: y = 0.00 x + 186.17 ; r = 0.01
2019: y = -0.00 x + 164.34 ; r = -0.01
2020: y = 0.01 x + 169.26 ; r = 0.15
2021: y = -0.01 x + 182.58 ; r = -0.04

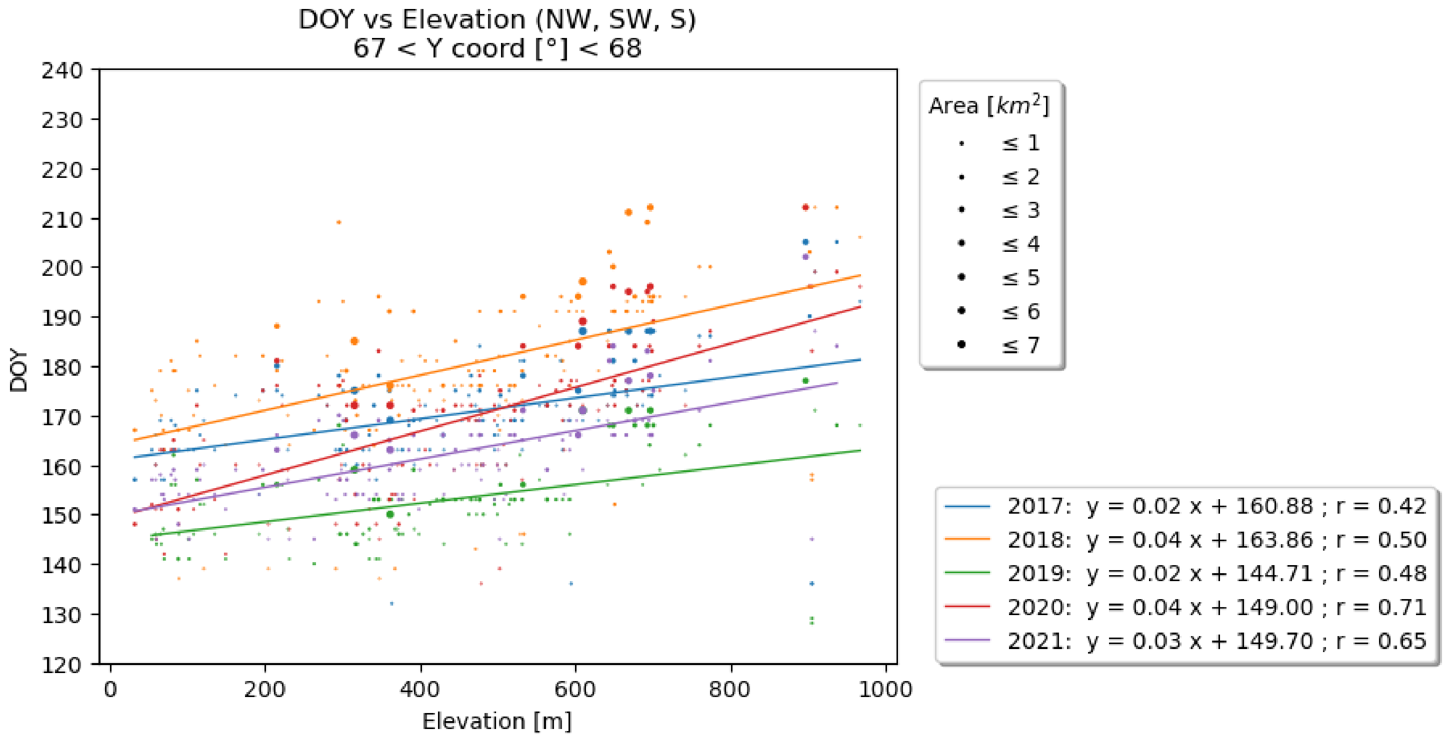
DOY vs Elevation (NW, SW, S)
67 < Y coord [°] < 68
DOY
Elevation [m]
Area [km^2]
≤ 1
≤ 2
≤ 3
≤ 4
≤ 5
≤ 6
≤ 7
2017: y = 0.02 x + 160.88 ; r = 0.42
2018: y = 0.04 x + 163.86 ; r = 0.50
2019: y = 0.02 x + 144.71 ; r = 0.48
2020: y = 0.04 x + 149.00 ; r = 0.71
2021: y = 0.03 x + 149.70 ; r = 0.65

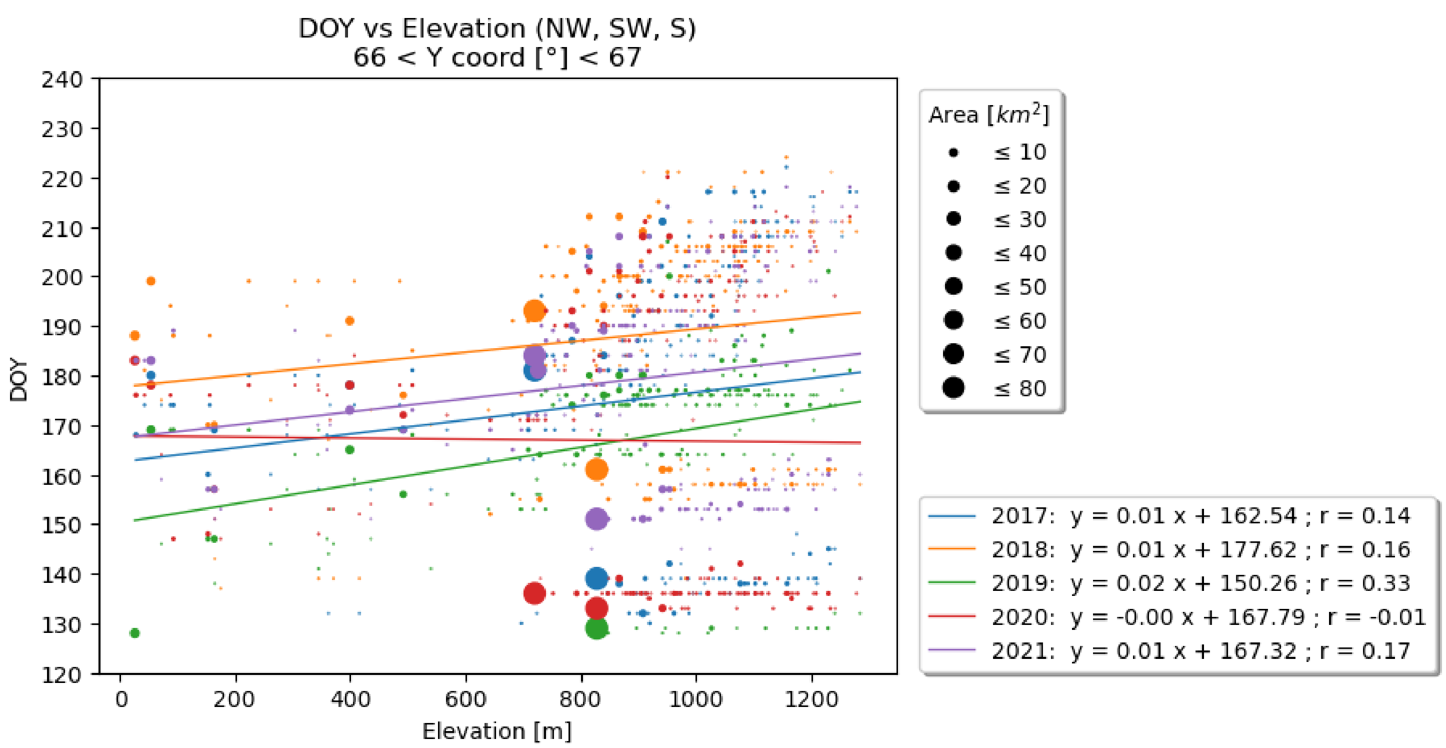
DOY vs Elevation (NW, SW, S)
66 < Y coord [°] < 67
DOY
Elevation [m]
Area [km^2]
≤ 10
≤ 20
≤ 30
≤ 40
≤ 50
≤ 60
≤ 70
≤ 80
2017: y = 0.01 x + 162.54 ; r = 0.14
2018: y = 0.01 x + 177.62 ; r = 0.16
2019: y = 0.02 x + 150.26 ; r = 0.33
2020: y = -0.00 x + 167.79 ; r = -0.01
2021: y = 0.01 x + 167.32 ; r = 0.17

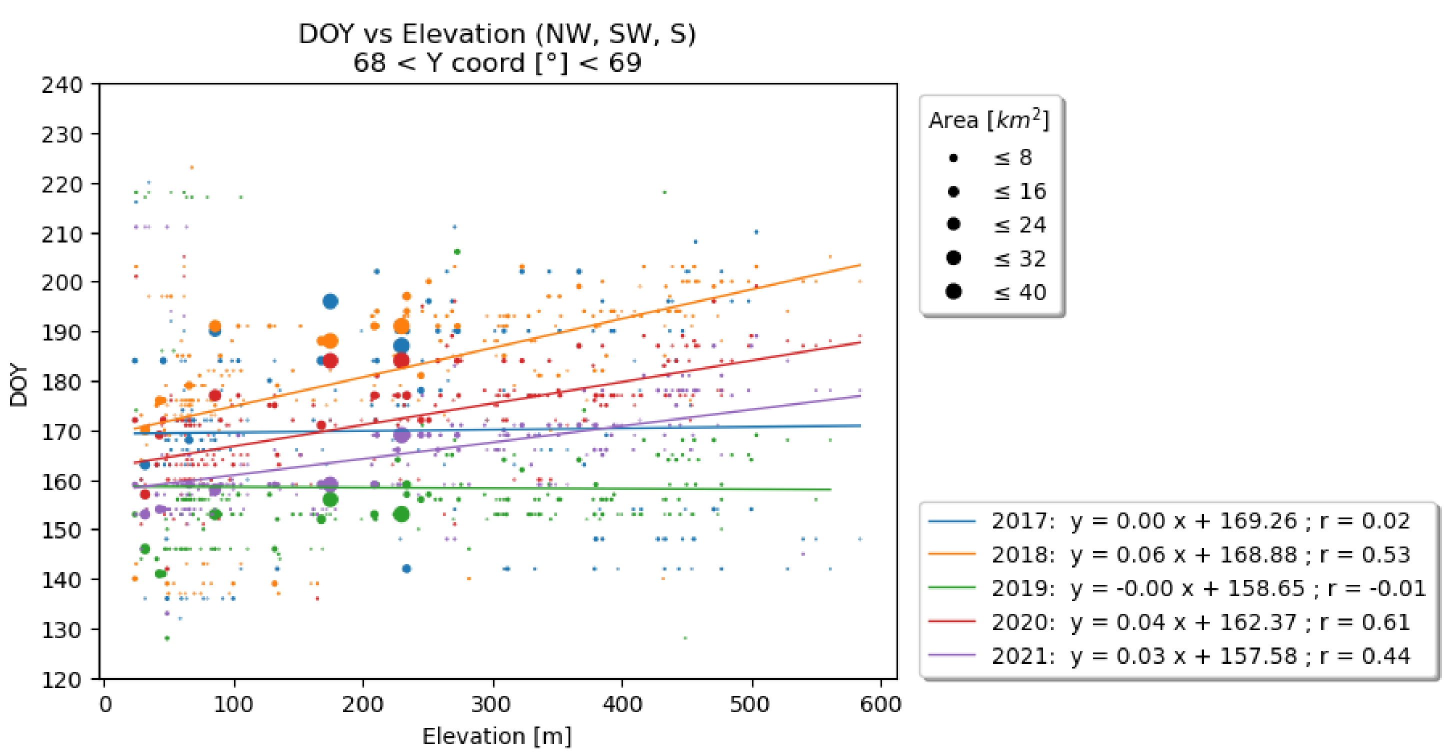
DOY vs Elevation (NW, SW, S)
68 < Y coord [°] < 69
DOY
Elevation [m]
Area [km^2]
≤ 8
≤ 16
≤ 24
≤ 32
≤ 40
2017: y = 0.00 x + 169.26 ; r = 0.02
2018: y = 0.06 x + 168.88 ; r = 0.53
2019: y = -0.00 x + 158.65 ; r = -0.01
2020: y = 0.04 x + 162.37 ; r = 0.61
2021: y = 0.03 x + 157.58 ; r = 0.44

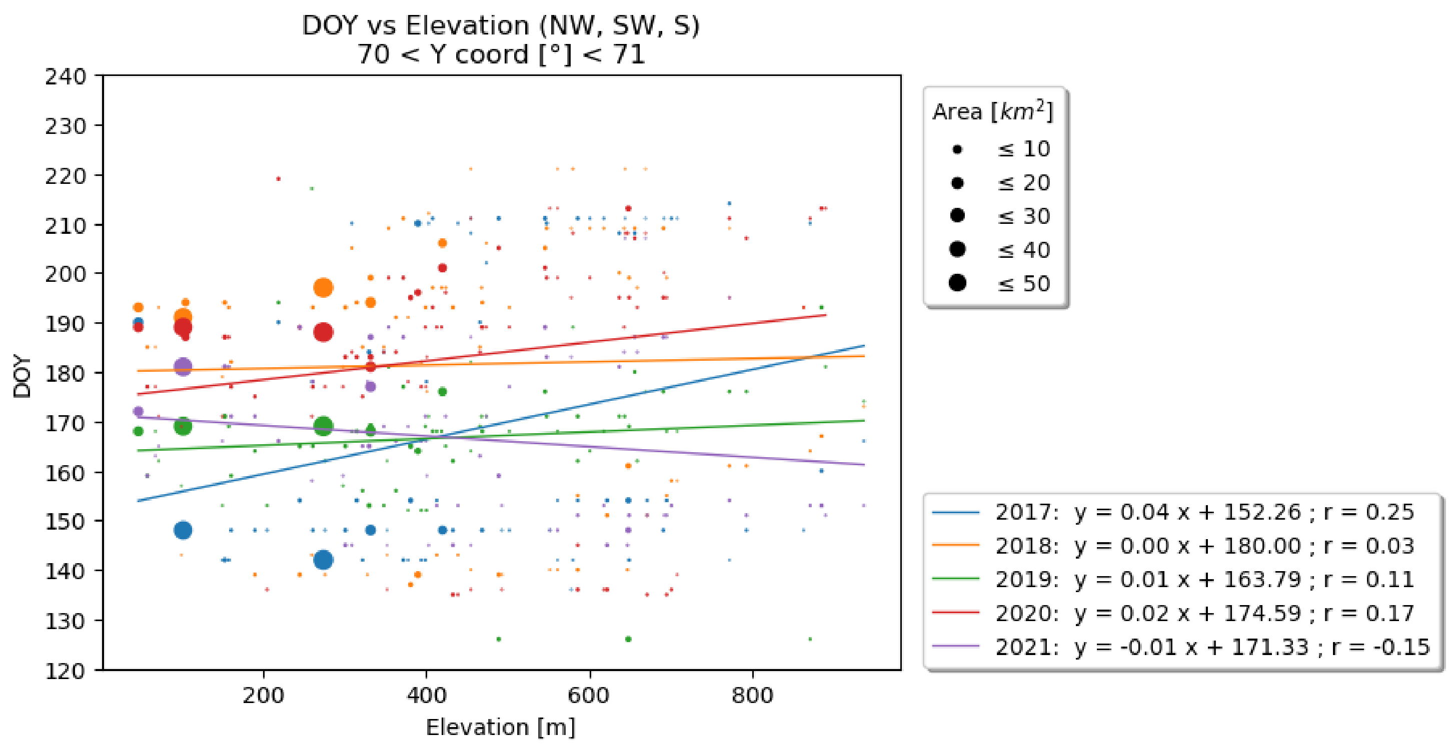
DOY vs Elevation (NW, SW, S)
70 < Y coord [°] < 71
DOY
Elevation [m]
Area [km^2]
≤ 10
≤ 20
≤ 30
≤ 40
≤ 50
2017: y = 0.04 x + 152.26 ; r = 0.25
2018: y = 0.00 x + 180.00 ; r = 0.03
2019: y = 0.01 x + 163.79 ; r = 0.11
2020: y = 0.02 x + 174.59 ; r = 0.17
2021: y = -0.01 x + 171.33 ; r = -0.15

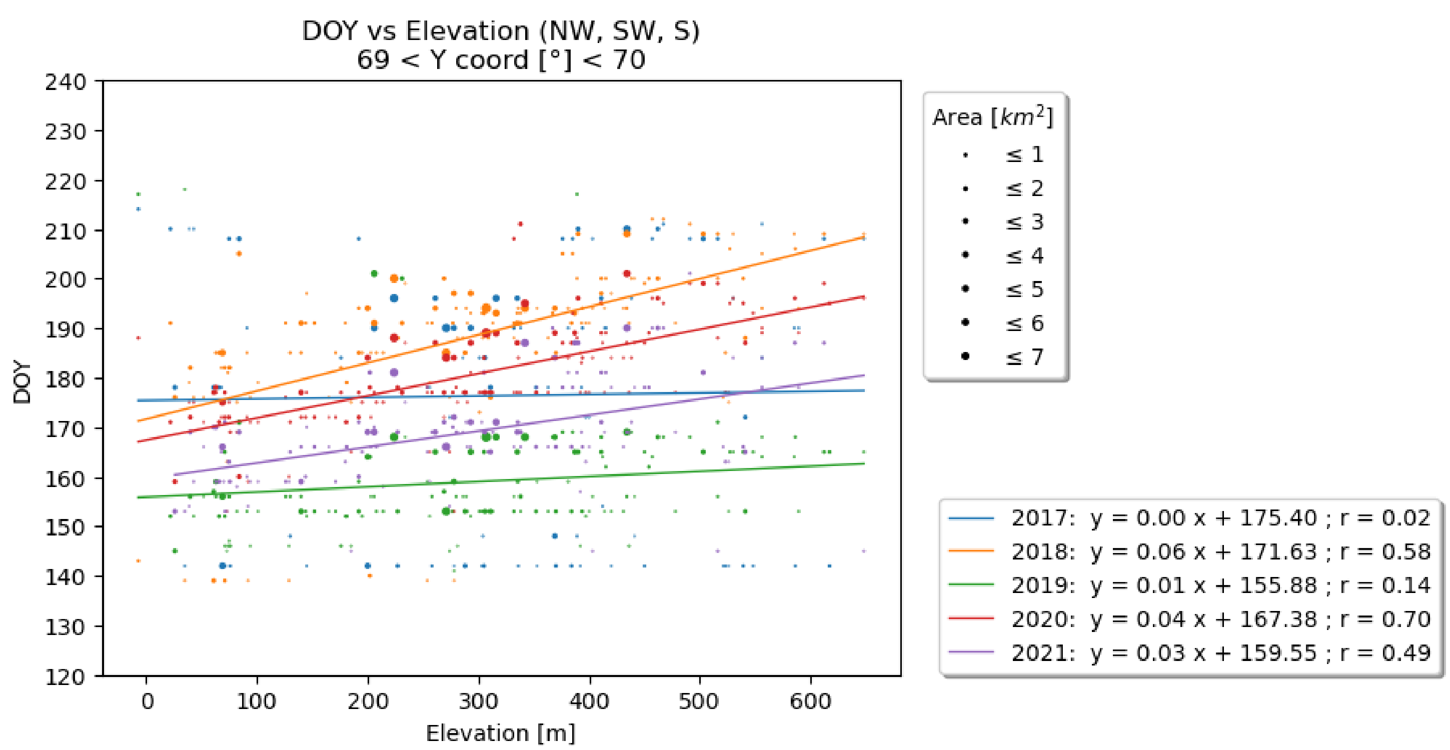
DOY vs Elevation (NW, SW, S)
69 < Y coord [°] < 70
DOY
Elevation [m]
Area [km^2]
≤ 1
≤ 2
≤ 3
≤ 4
≤ 5
≤ 6
≤ 7
2017: y = 0.00 x + 175.40 ; r = 0.02
2018: y = 0.06 x + 171.63 ; r = 0.58
2019: y = 0.01 x + 155.88 ; r = 0.14
2020: y = 0.04 x + 167.38 ; r = 0.70
2021: y = 0.03 x + 159.55 ; r = 0.49

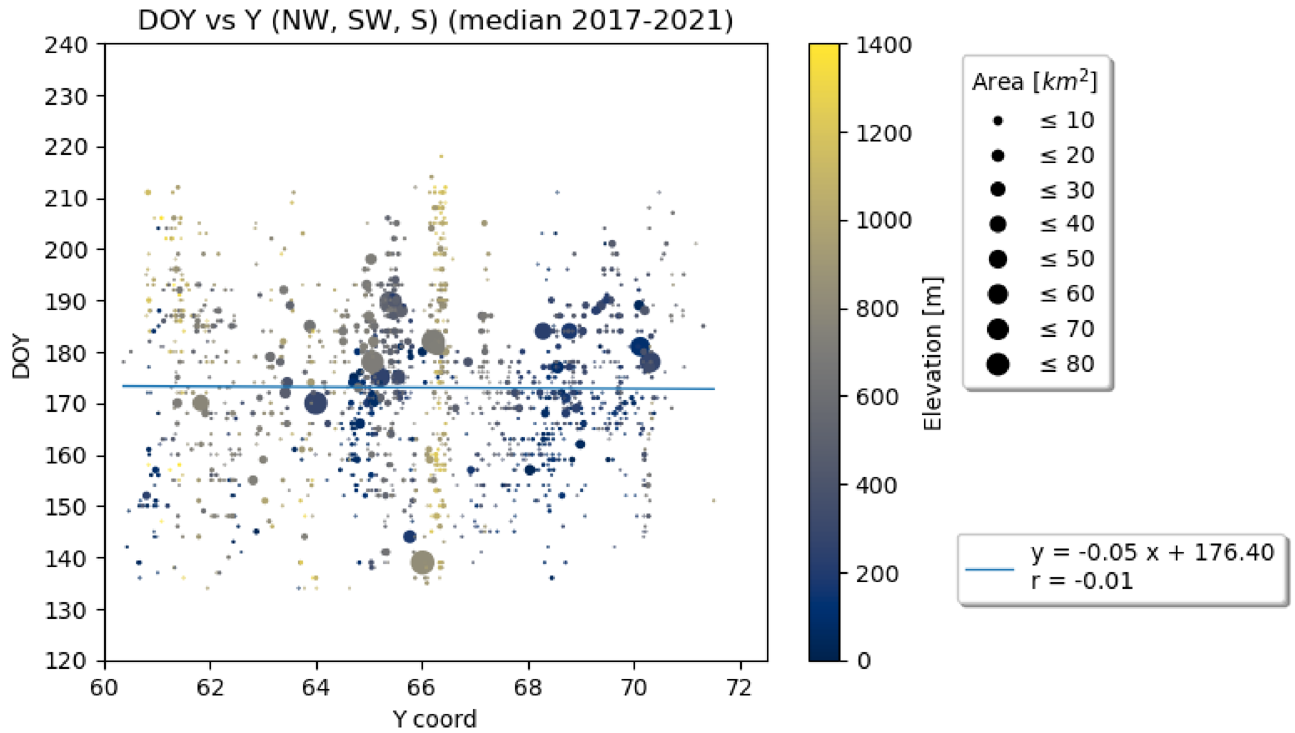
DOY vs Y (NW, SW, S) (median 2017-2021)
DOY
Y coord
Elevation [m]
Area [km^2]
≤ 10
≤ 20
≤ 30
≤ 40
≤ 50
≤ 60
≤ 70
≤ 80
y = -0.05 x + 176.40
r = -0.01

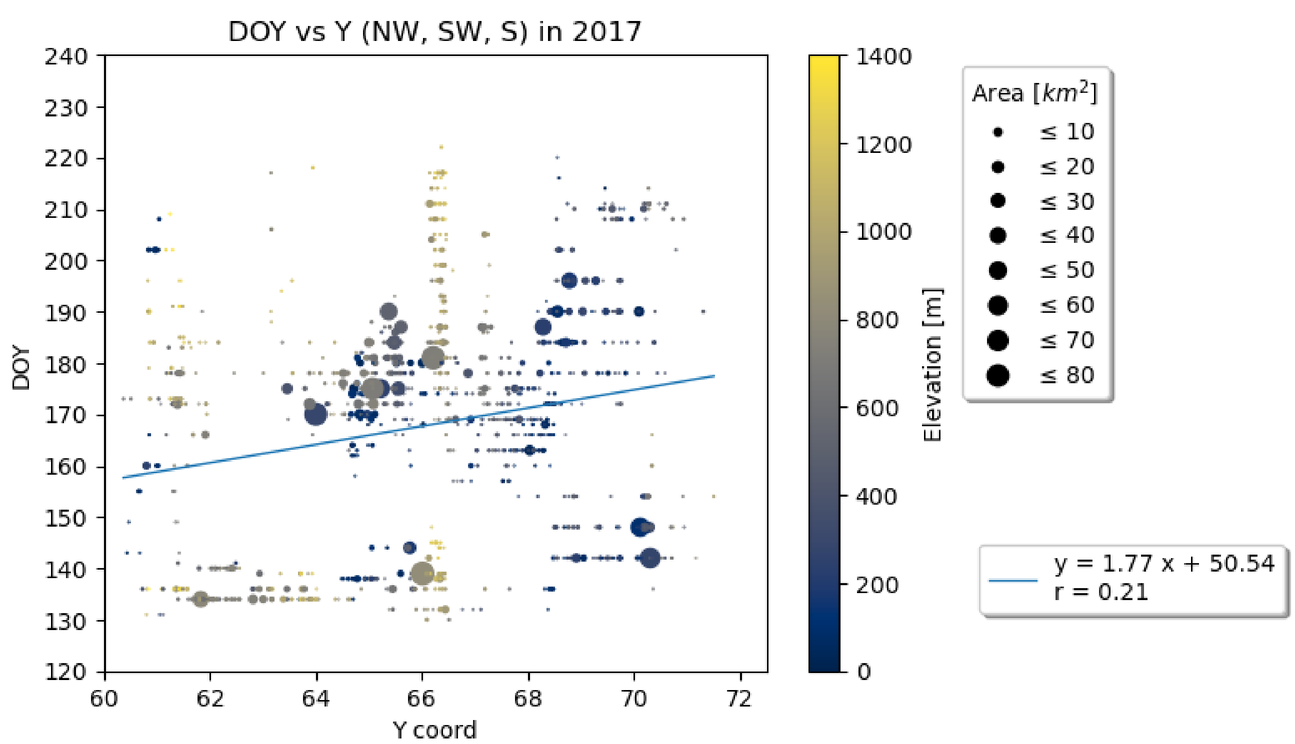
DOY vs Y (NW, SW, S) in 2017
DOY
Y coord
Elevation [m]
Area [km^2]
≤ 10
≤ 20
≤ 30
≤ 40
≤ 50
≤ 60
≤ 70
≤ 80
y = 1.77 x + 50.54
r = 0.21

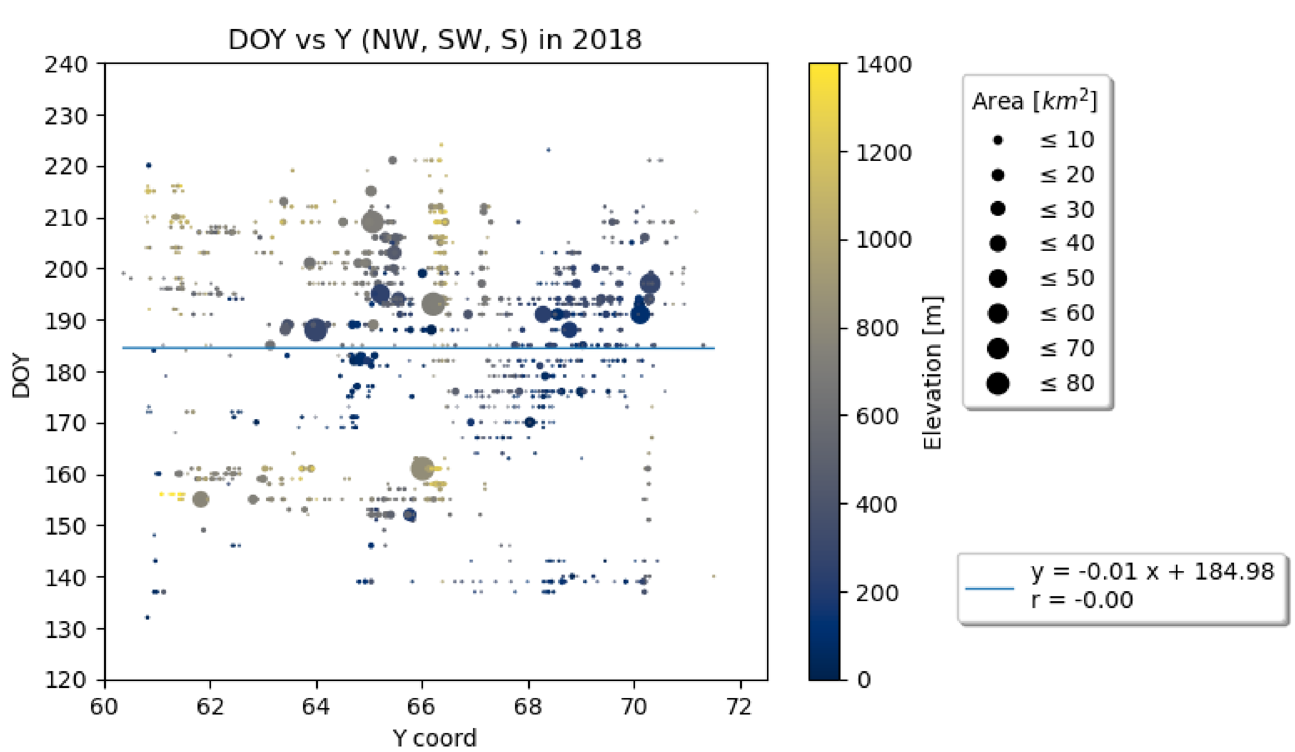
DOY vs Y (NW, SW, S) in 2018
DOY
Y coord
Elevation [m]
Area [km^2]
≤ 10
≤ 20
≤ 30
≤ 40
≤ 50
≤ 60
≤ 70
≤ 80
y = -0.01 x + 184.98
r = -0.00

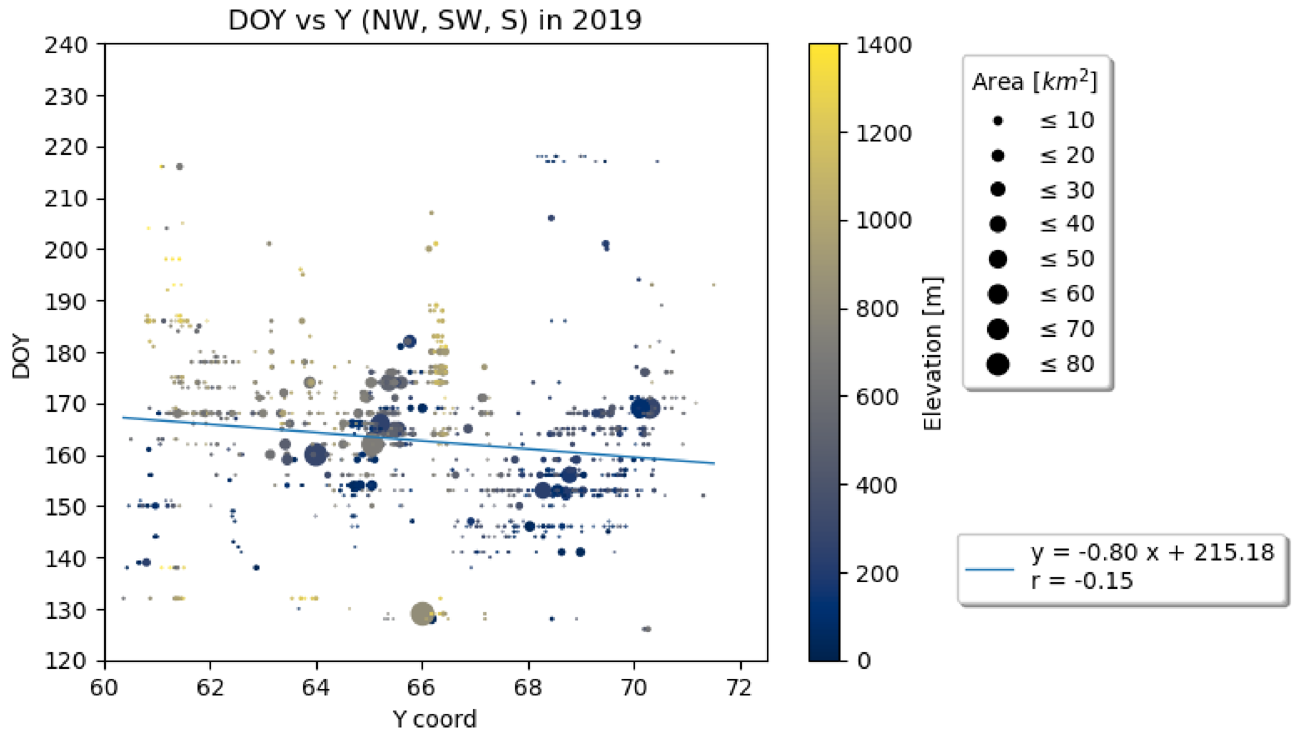
DOY vs Y (NW, SW, S) in 2019
DOY
Y coord
Elevation [m]
Area [km^2]
≤ 10
≤ 20
≤ 30
≤ 40
≤ 50
≤ 60
≤ 70
≤ 80
y = -0.80 x + 215.18
r = -0.15

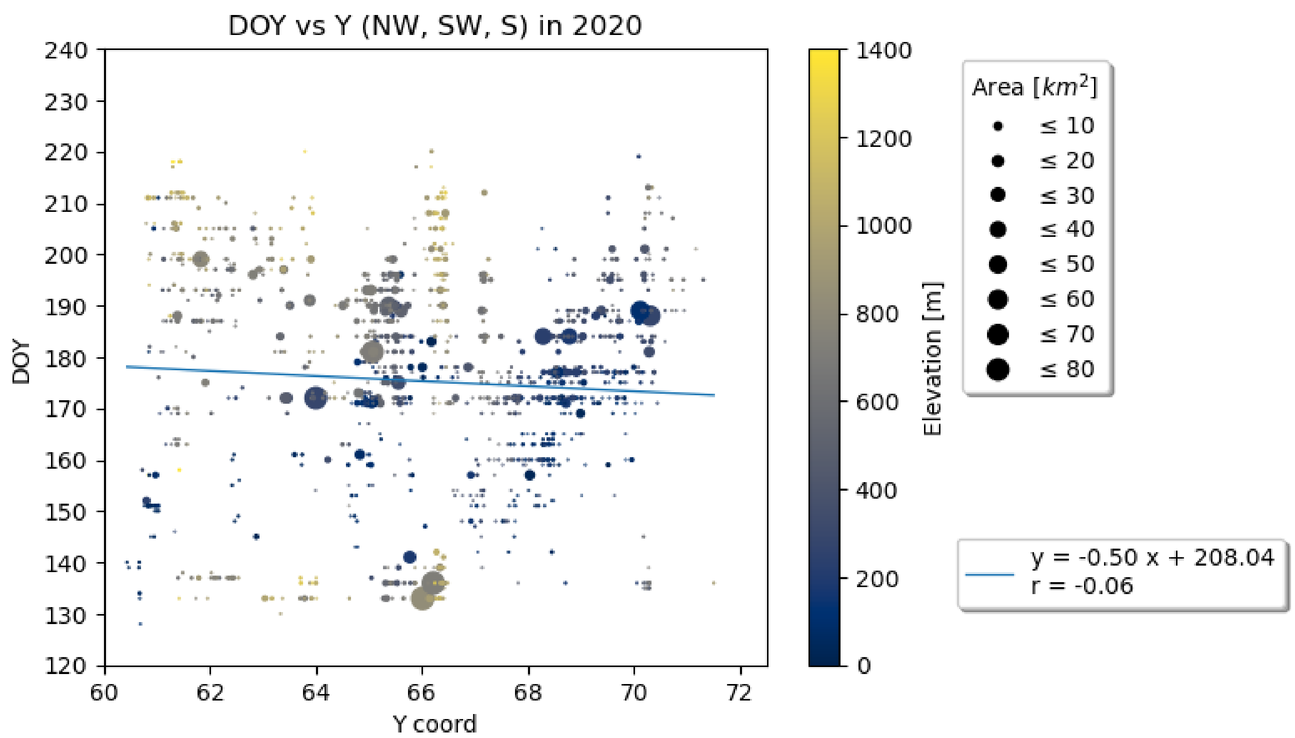
DOY vs Y (NW, SW, S) in 2020
DOY
Y coord
Elevation [m]
Area [km^2]
≤ 10
≤ 20
≤ 30
≤ 40
≤ 50
≤ 60
≤ 70
≤ 80
y = -0.50 x + 208.04
r = -0.06

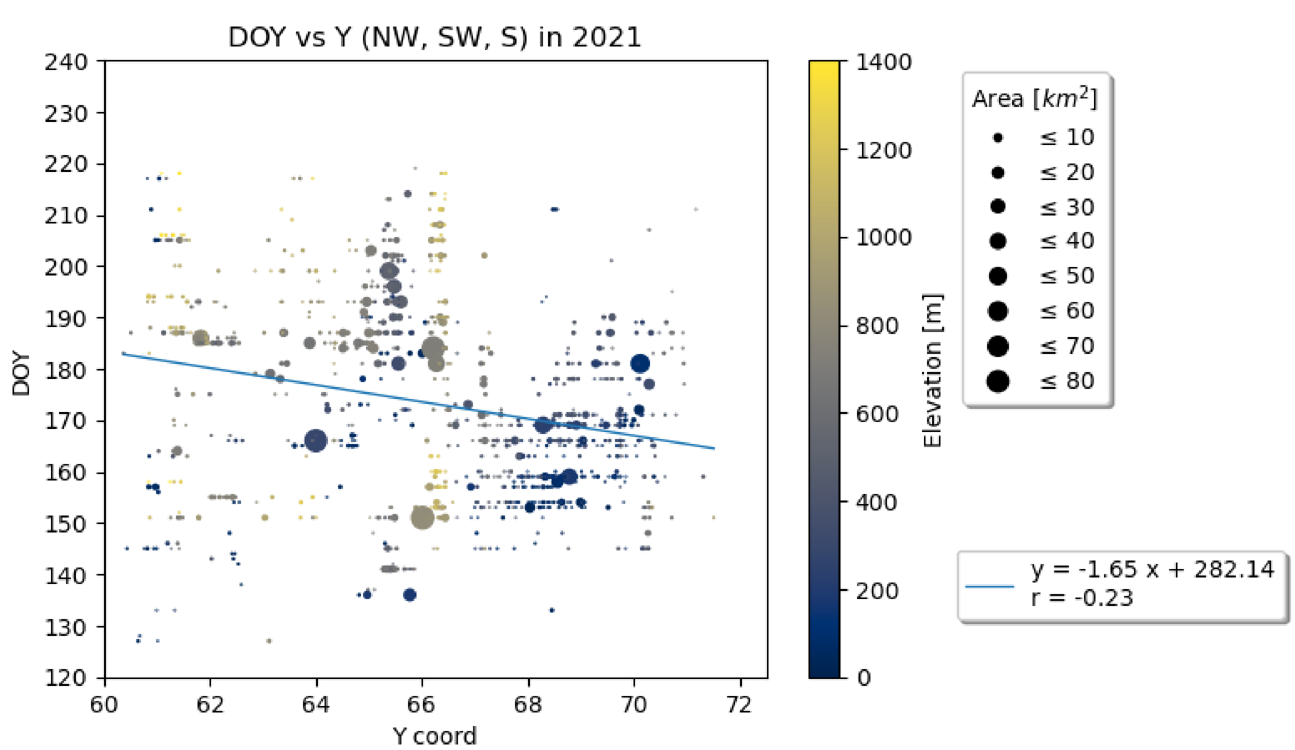
DOY vs Y (NW, SW, S) in 2021
DOY
Y coord
Elevation [m]
Area [km^2]
≤ 10
≤ 20
≤ 30
≤ 40
≤ 50
≤ 60
≤ 70
≤ 80
y = -1.65 x + 282.14
r = -0.23

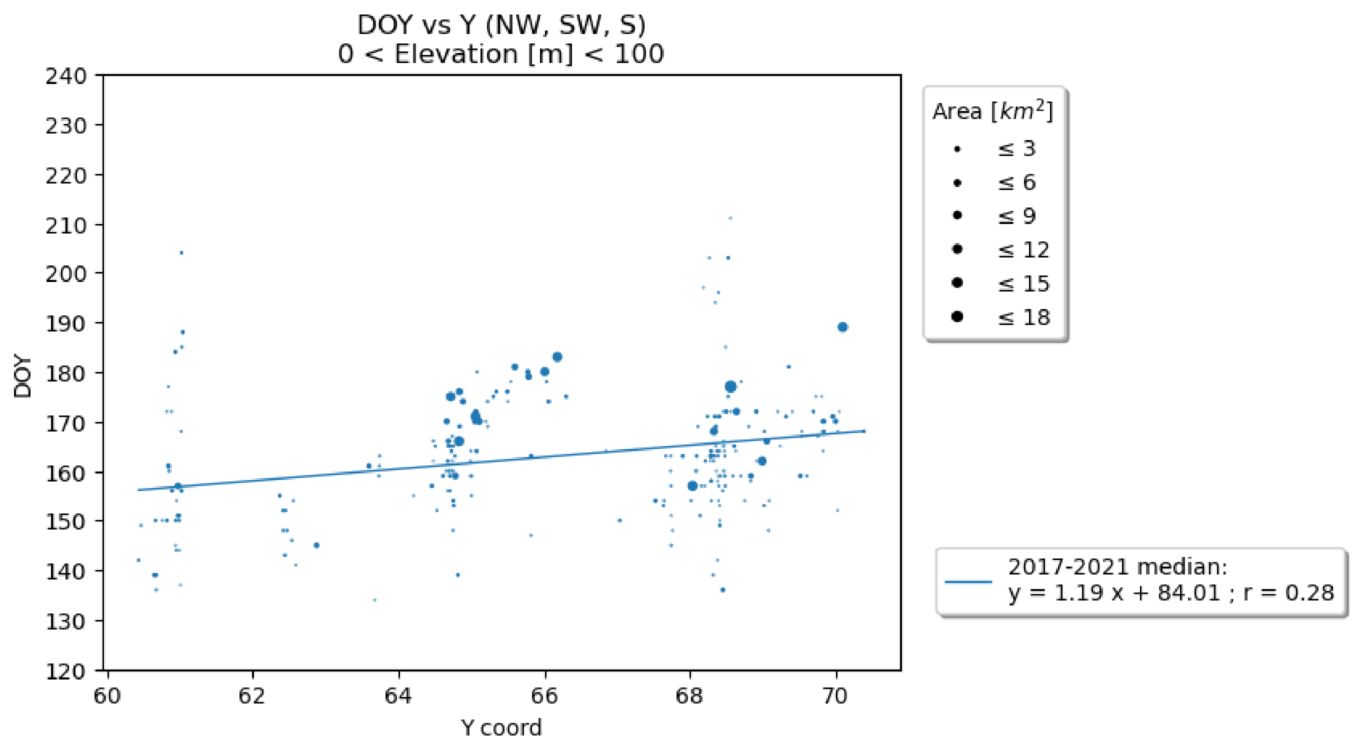
DOY vs Y (NW, SW, S)
0 < Elevation [m] < 100
DOY
Y coord
Area [km^2]
≤ 3
≤ 6
≤ 9
≤ 12
≤ 15
≤ 18
2017-2021 median:
y = 1.19 x + 84.01 ; r = 0.28

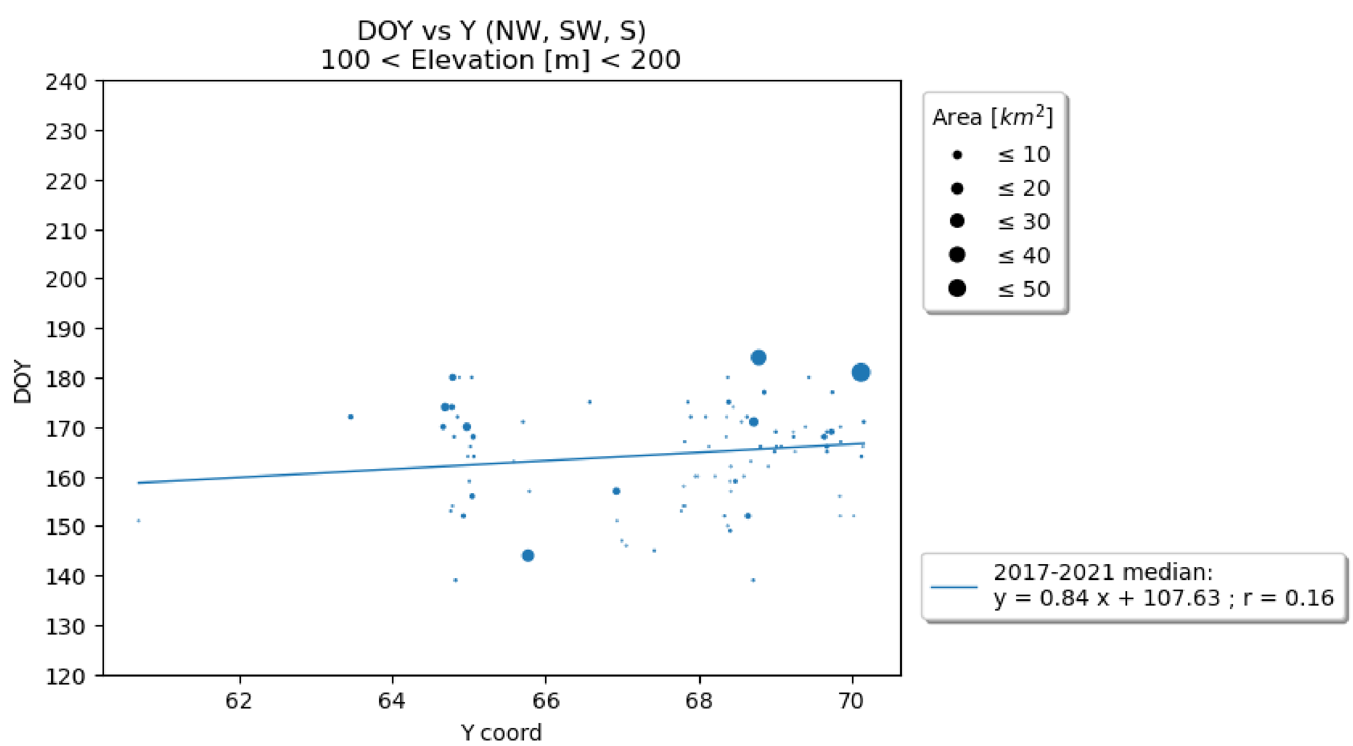
DOY vs Y (NW, SW, S)
100 < Elevation [m] < 200
DOY
Y coord
Area [km^2]
≤ 10
≤ 20
≤ 30
≤ 40
≤ 50
2017-2021 median:
y = 0.84 x + 107.63 ; r = 0.16

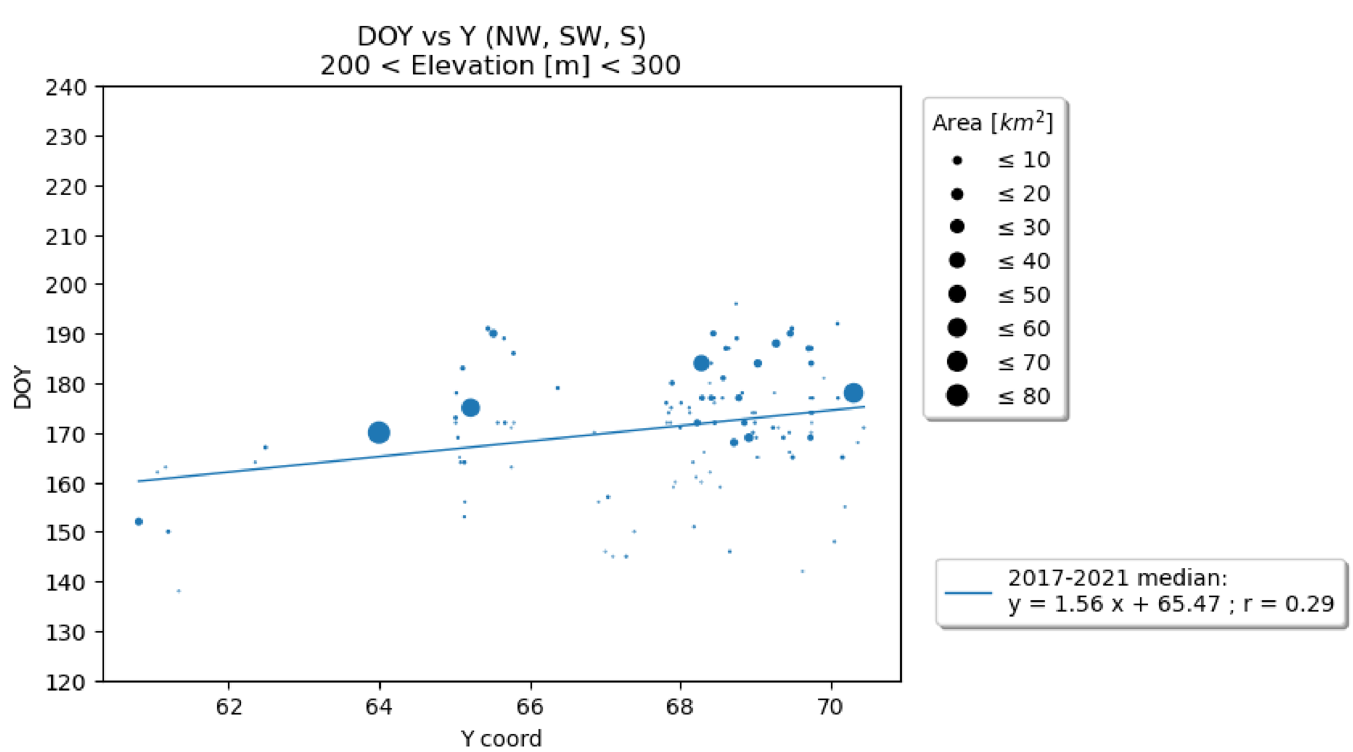
DOY vs Y (NW, SW, S)
200 < Elevation [m] < 300
DOY
Y coord
Area [km^2]
≤ 10
≤ 20
≤ 30
≤ 40
≤ 50
≤ 60
≤ 70
≤ 80
2017-2021 median:
y = 1.56 x + 65.47 ; r = 0.29

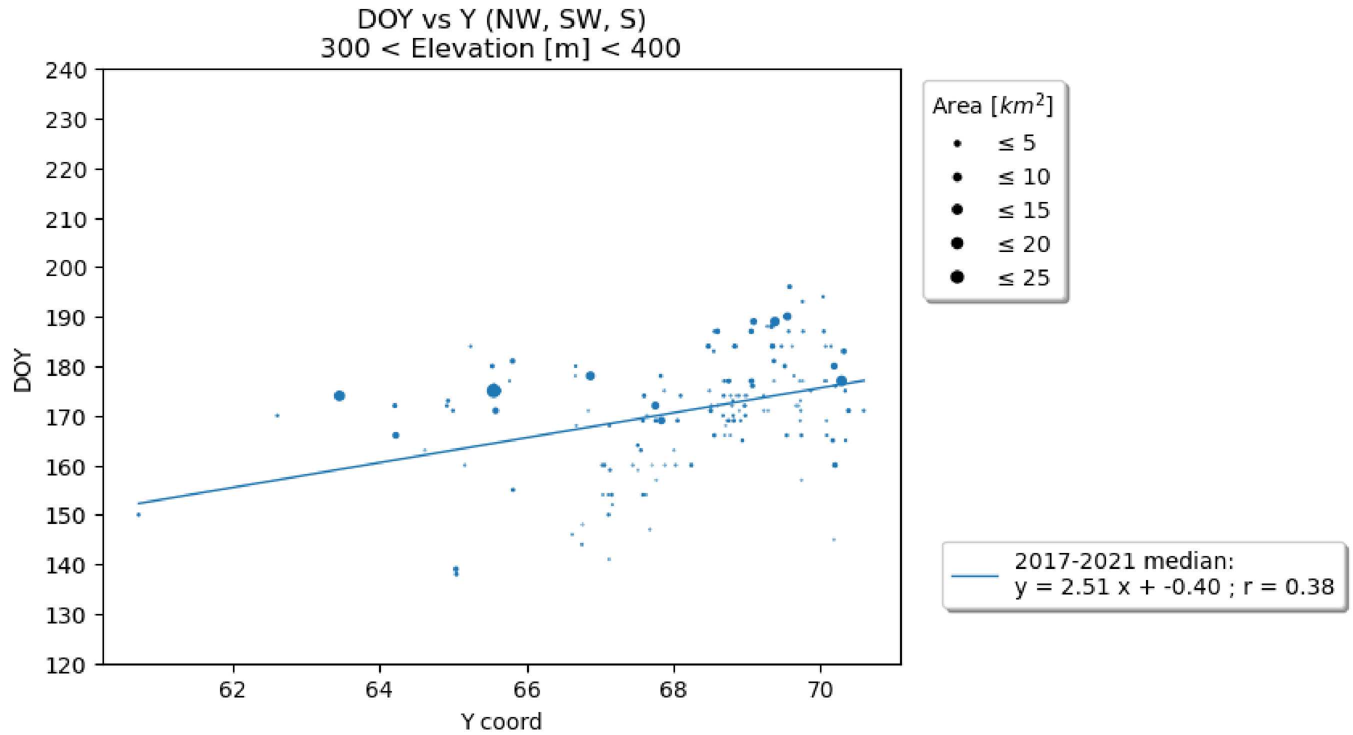
DOY vs Y (NW, SW, S)
300 < Elevation [m] < 400
DOY
Y coord
Area [km^2]
≤ 5
≤ 10
≤ 15
≤ 20
≤ 25
2017-2021 median:
y = 2.51 x + -0.40 ; r = 0.38

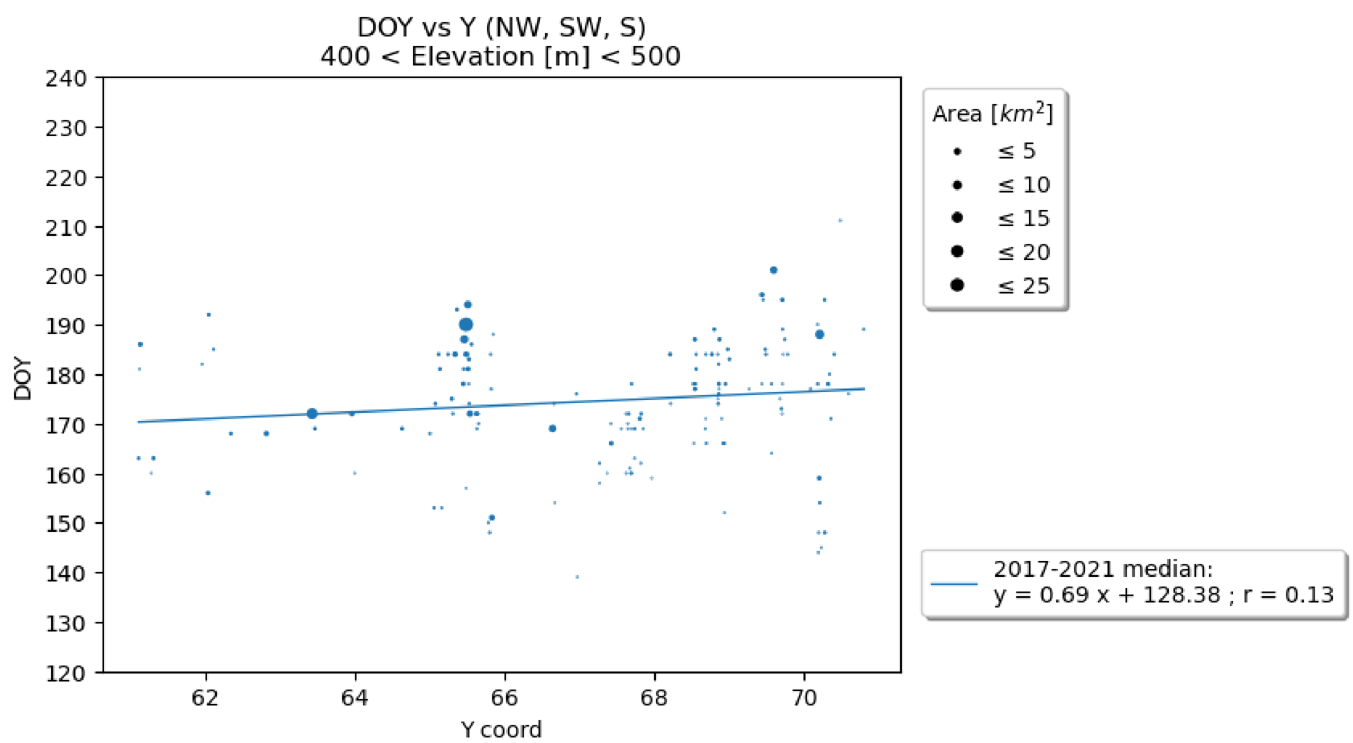
DOY vs Y (NW, SW, S)
400 < Elevation [m] < 500
DOY
Y coord
Area [km^2]
≤ 5
≤ 10
≤ 15
≤ 20
≤ 25
2017-2021 median:
y = 0.69 x + 128.38 ; r = 0.13

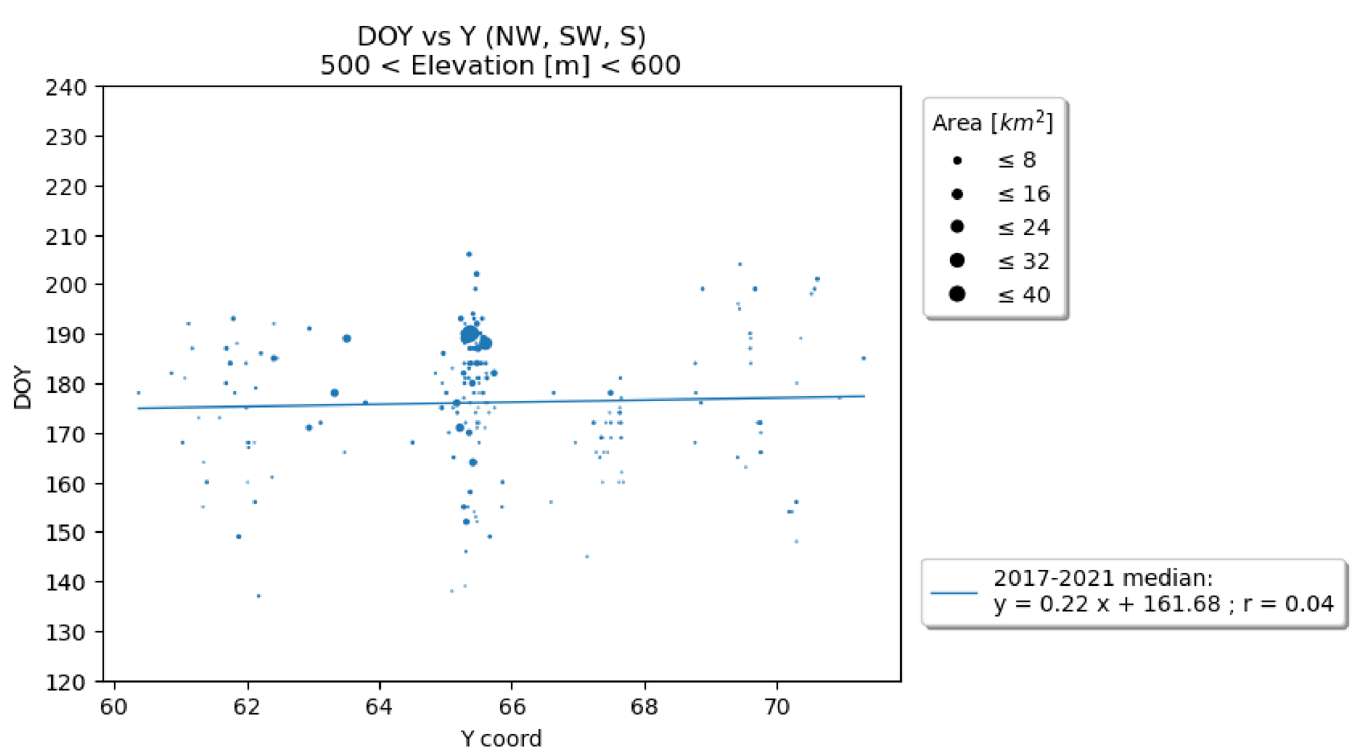
DOY vs Y (NW, SW, S)
500 < Elevation [m] < 600
DOY
Y coord
Area [km^2]
≤ 8
≤ 16
≤ 24
≤ 32
≤ 40
2017-2021 median:
y = 0.22 x + 161.68 ; r = 0.04

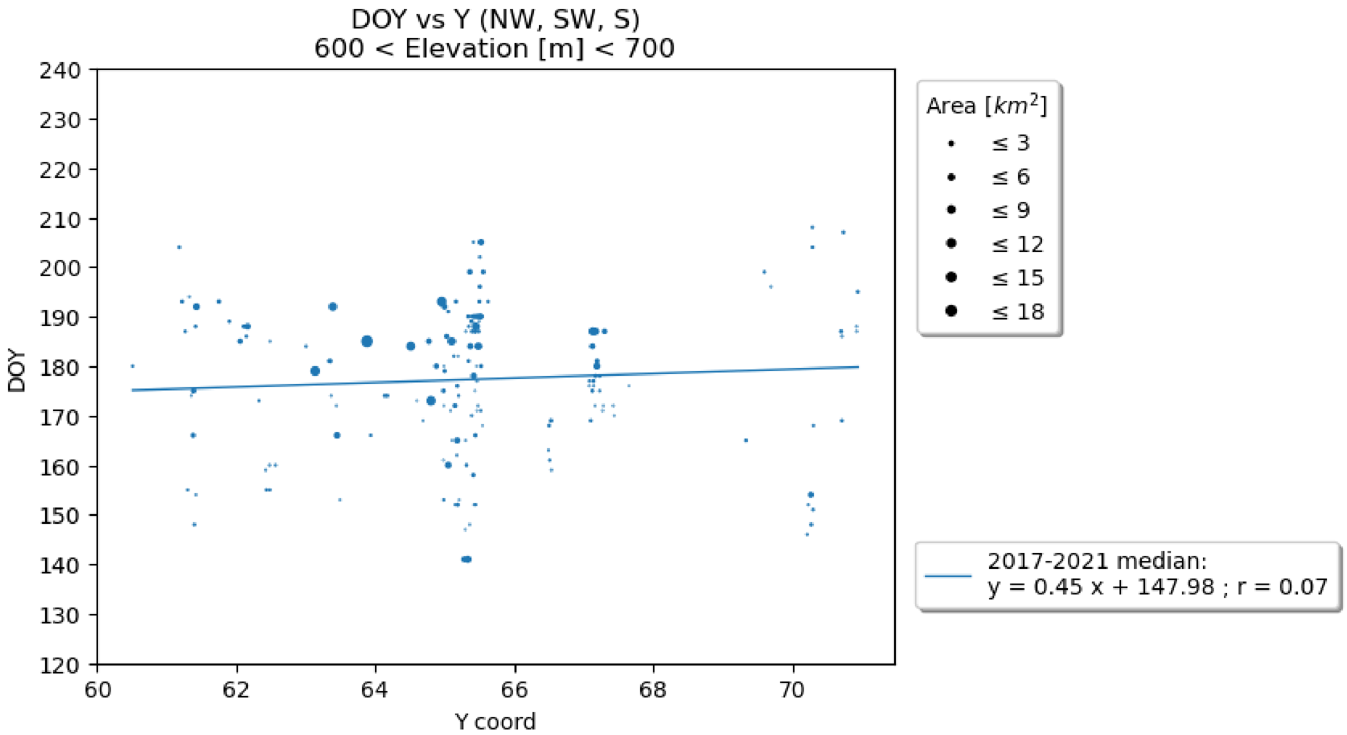
DOY vs Y (NW, SW, S)
600 < Elevation [m] < 700
DOY
Y coord
Area [km^2]
≤ 3
≤ 6
≤ 9
≤ 12
≤ 15
≤ 18
2017-2021 median:
y = 0.45 x + 147.98 ; r = 0.07

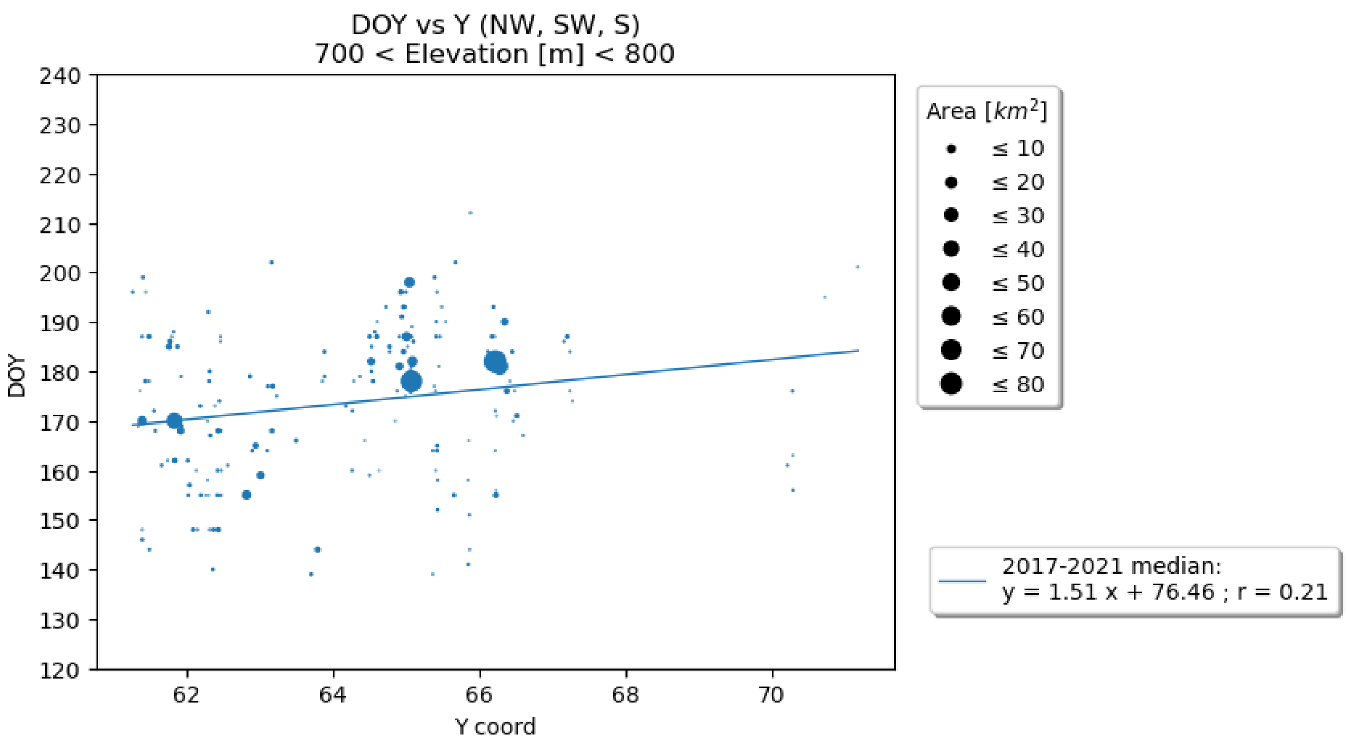
DOY vs Y (NW, SW, S)
700 < Elevation [m] < 800
DOY
Y coord
Area [km^2]
≤ 10
≤ 20
≤ 30
≤ 40
≤ 50
≤ 60
≤ 70
≤ 80
2017-2021 median:
y = 1.51 x + 76.46 ; r = 0.21

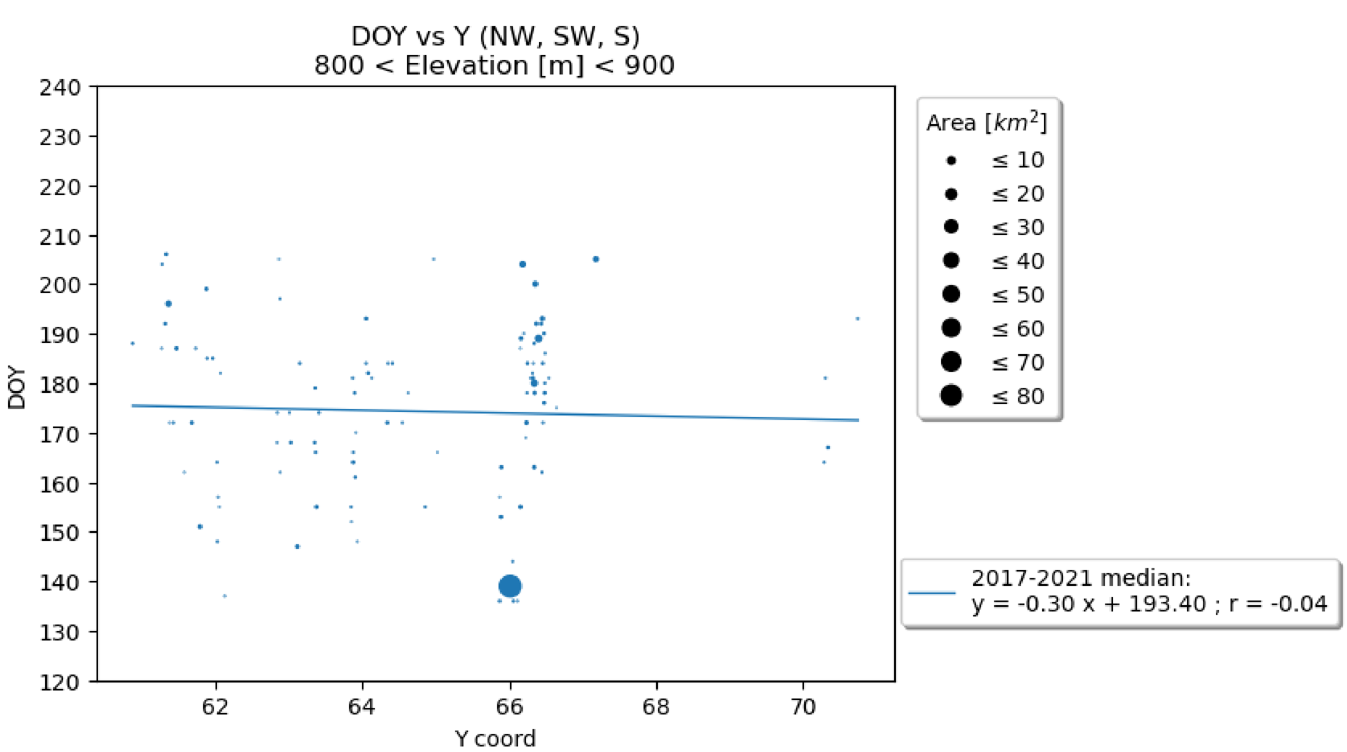
DOY vs Y (NW, SW, S)
800 < Elevation [m] < 900
DOY
Y coord
Area [km^2]
≤ 10
≤ 20
≤ 30
≤ 40
≤ 50
≤ 60
≤ 70
≤ 80
2017-2021 median:
y = -0.30 x + 193.40 ; r = -0.04

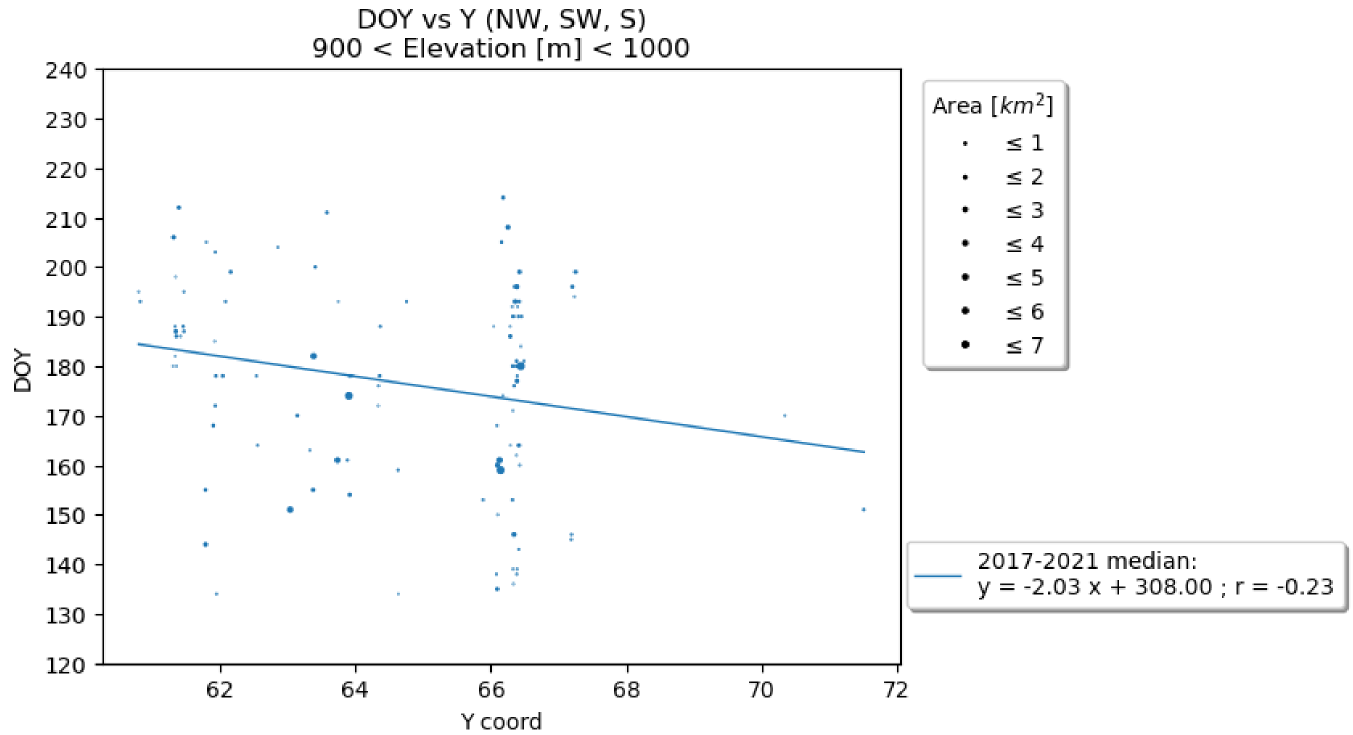
DOY vs Y (NW, SW, S)
900 < Elevation [m] < 1000
DOY
Y coord
Area [km^2]
≤ 1
≤ 2
≤ 3
≤ 4
≤ 5
≤ 6
≤ 7
2017-2021 median:
y = -2.03 x + 308.00 ; r = -0.23

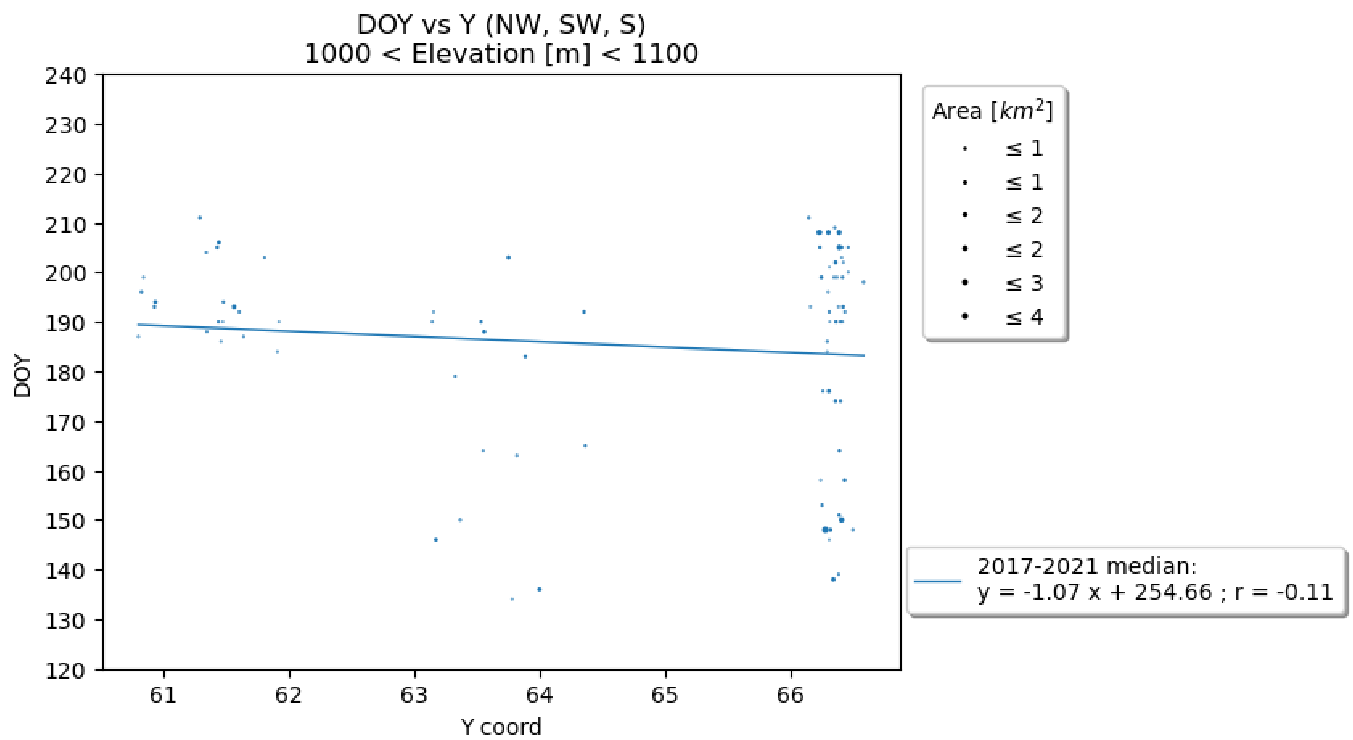
DOY vs Y (NW, SW, S)
1000 < Elevation [m] < 1100
DOY
Y coord
Area [km^2]
≤ 1
≤ 1
≤ 2
≤ 2
≤ 3
≤ 4
2017-2021 median:
y = -1.07 x + 254.66 ; r = -0.11

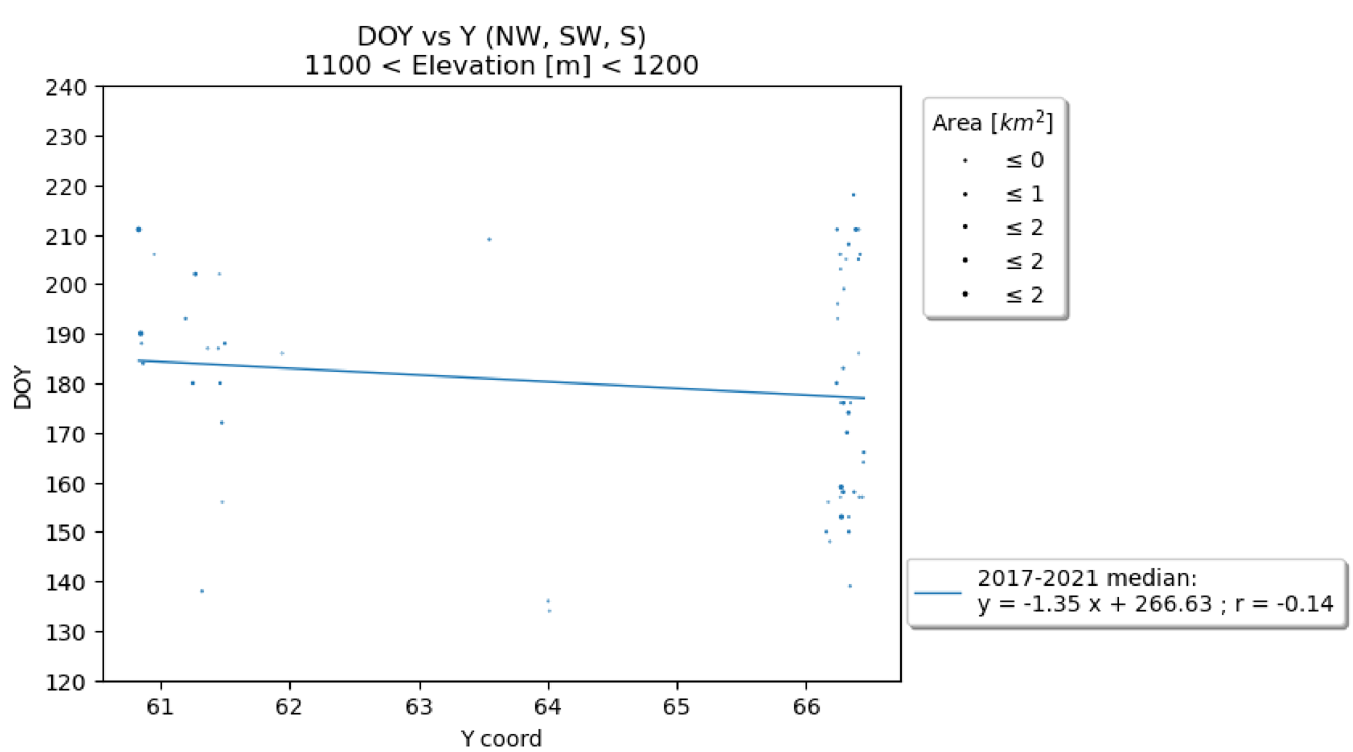
DOY vs Y (NW, SW, S)
1100 < Elevation [m] < 1200
DOY
Y coord
Area [km^2]
≤ 0
≤ 1
≤ 2
≤ 2
≤ 2
2017-2021 median:
y = -1.35 x + 266.63 ; r = -0.14

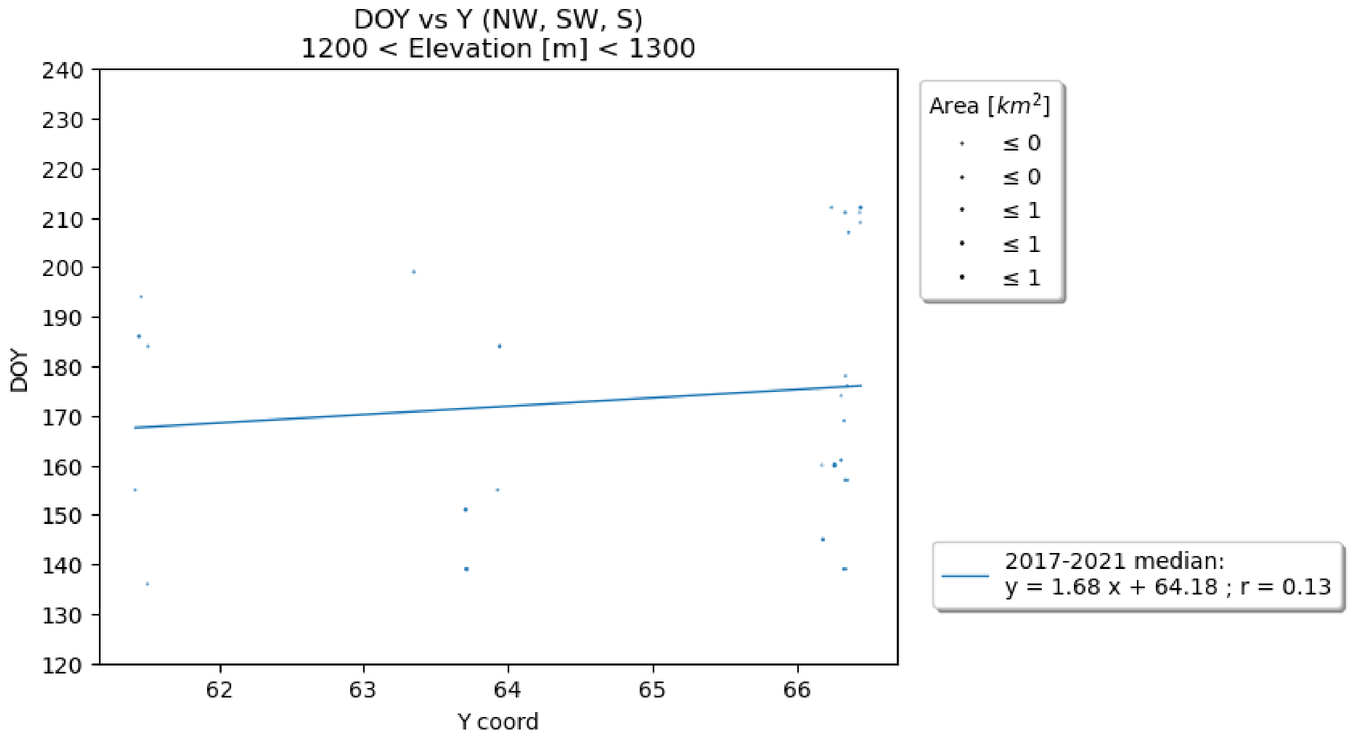

DOY vs Y (NW, SW, S)
1200 < Elevation [m] < 1300
DOY
Y coord
Area [km^2]
≤ 0
≤ 0
≤ 1
≤ 1
≤ 1
2017-2021 median:
y = 1.68 x + 64.18 ; r = 0.13

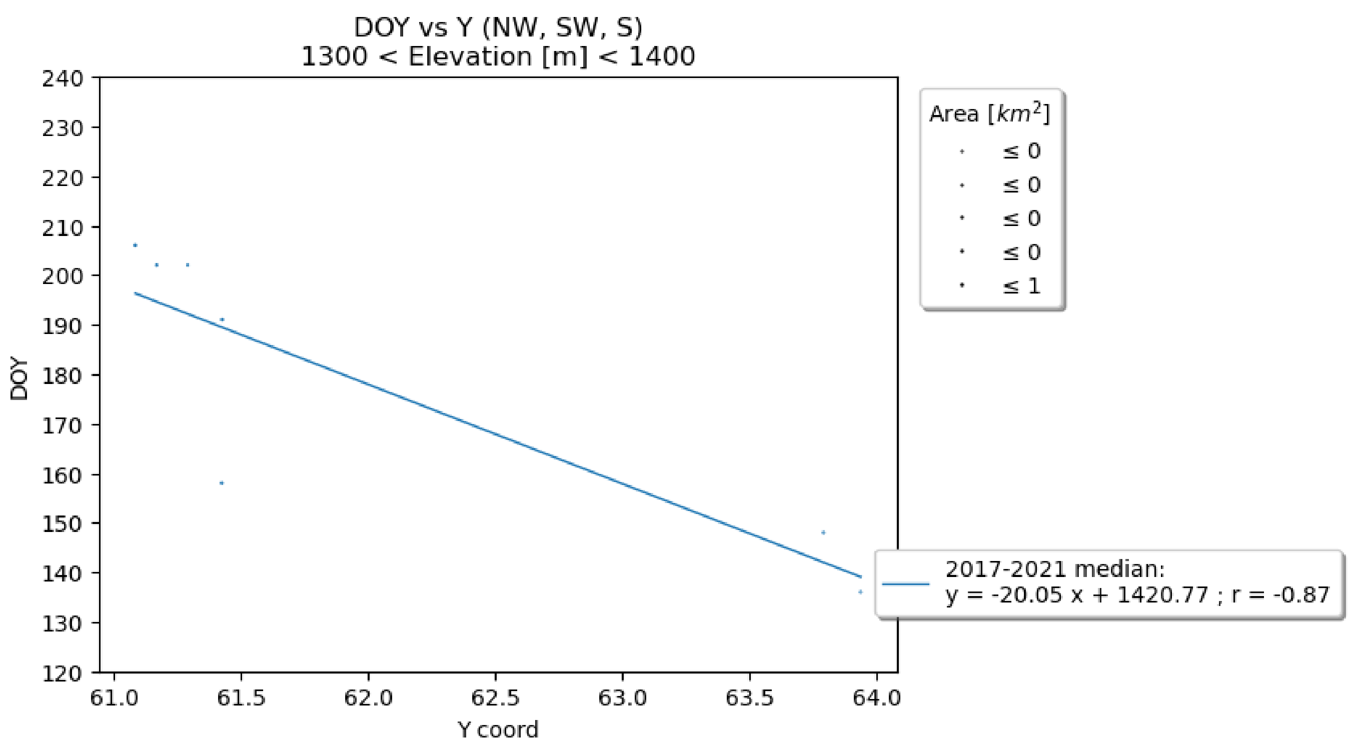

DOY vs Y (NW, SW, S)
1300 < Elevation [m] < 1400
DOY
Y coord
Area [km^2]
≤ 0
≤ 0
≤ 0
≤ 0
≤ 1
2017-2021 median:
y = -20.05 x + 1420.77 ; r = -0.87

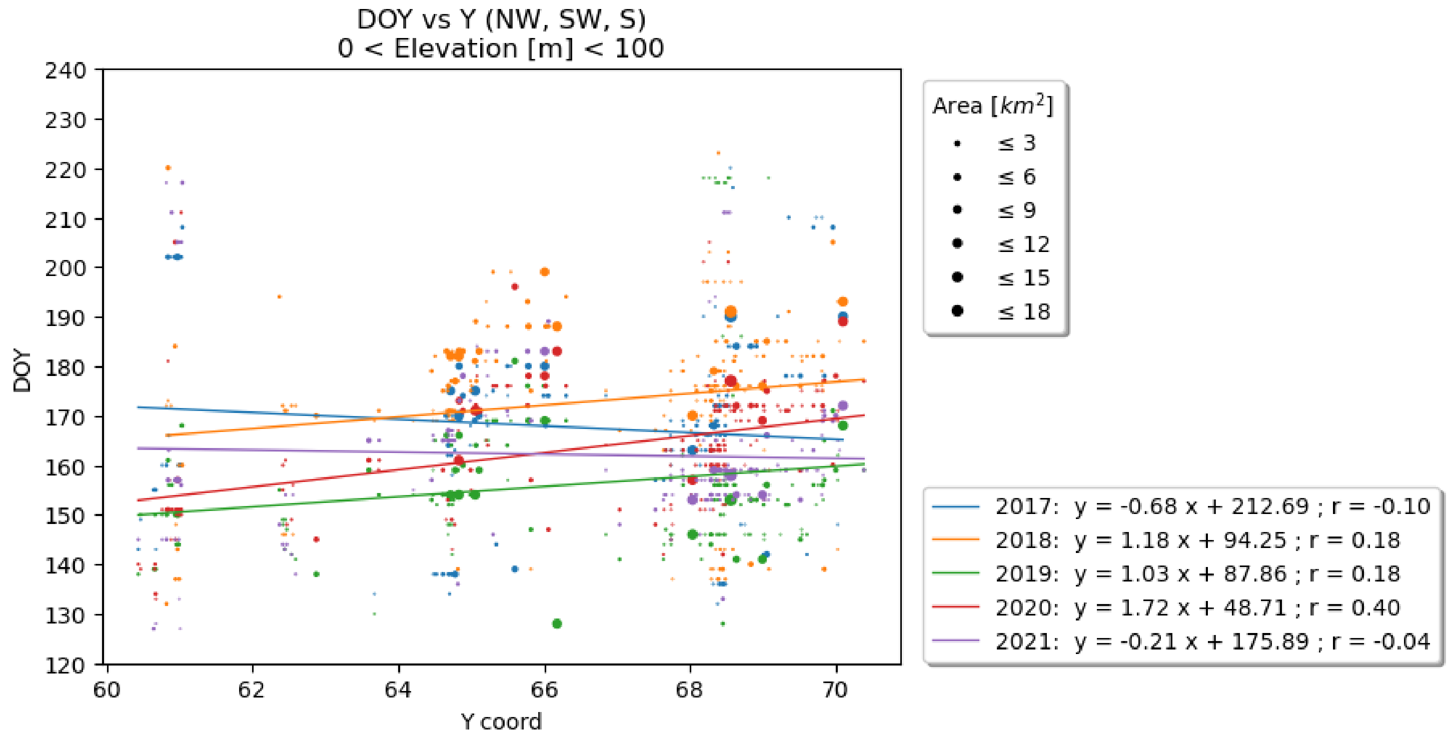

DOY vs Y (NW, SW, S)
0 < Elevation [m] < 100
DOY
Y coord
Area [km^2]
≤ 3
≤ 6
≤ 9
≤ 12
≤ 15
≤ 18
2017: y = -0.68 x + 212.69 ; r = -0.10
2018: y = 1.18 x + 94.25 ; r = 0.18
2019: y = 1.03 x + 87.86 ; r = 0.18
2020: y = 1.72 x + 48.71 ; r = 0.40
2021: y = -0.21 x + 175.89 ; r = -0.04

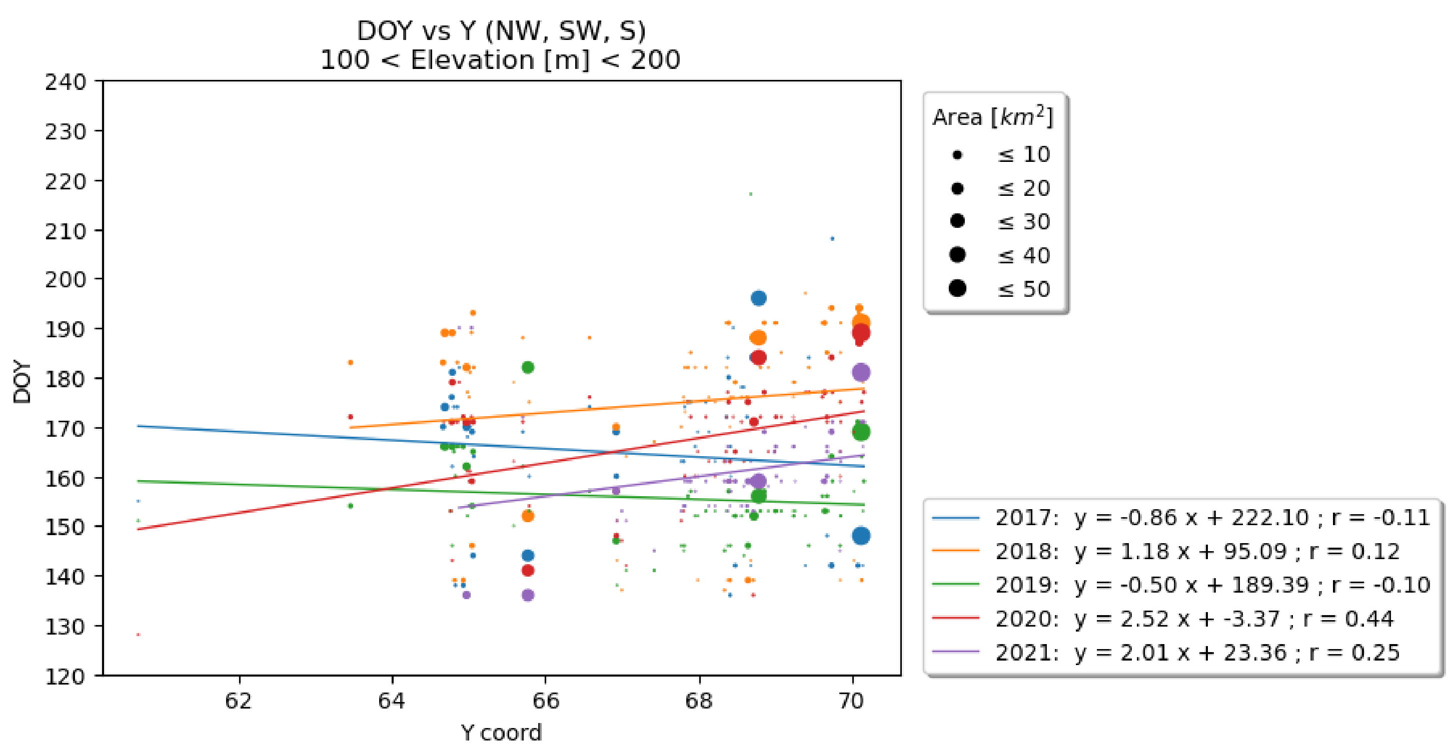

DOY vs Y (NW, SW, S)
100 < Elevation [m] < 200
DOY
Y coord
Area [km^2]
≤ 10
≤ 20
≤ 30
≤ 40
≤ 50
2017: y = -0.86 x + 222.10 ; r = -0.11
2018: y = 1.18 x + 95.09 ; r = 0.12
2019: y = -0.50 x + 189.39 ; r = -0.10
2020: y = 2.52 x + -3.37 ; r = 0.44
2021: y = 2.01 x + 23.36 ; r = 0.25

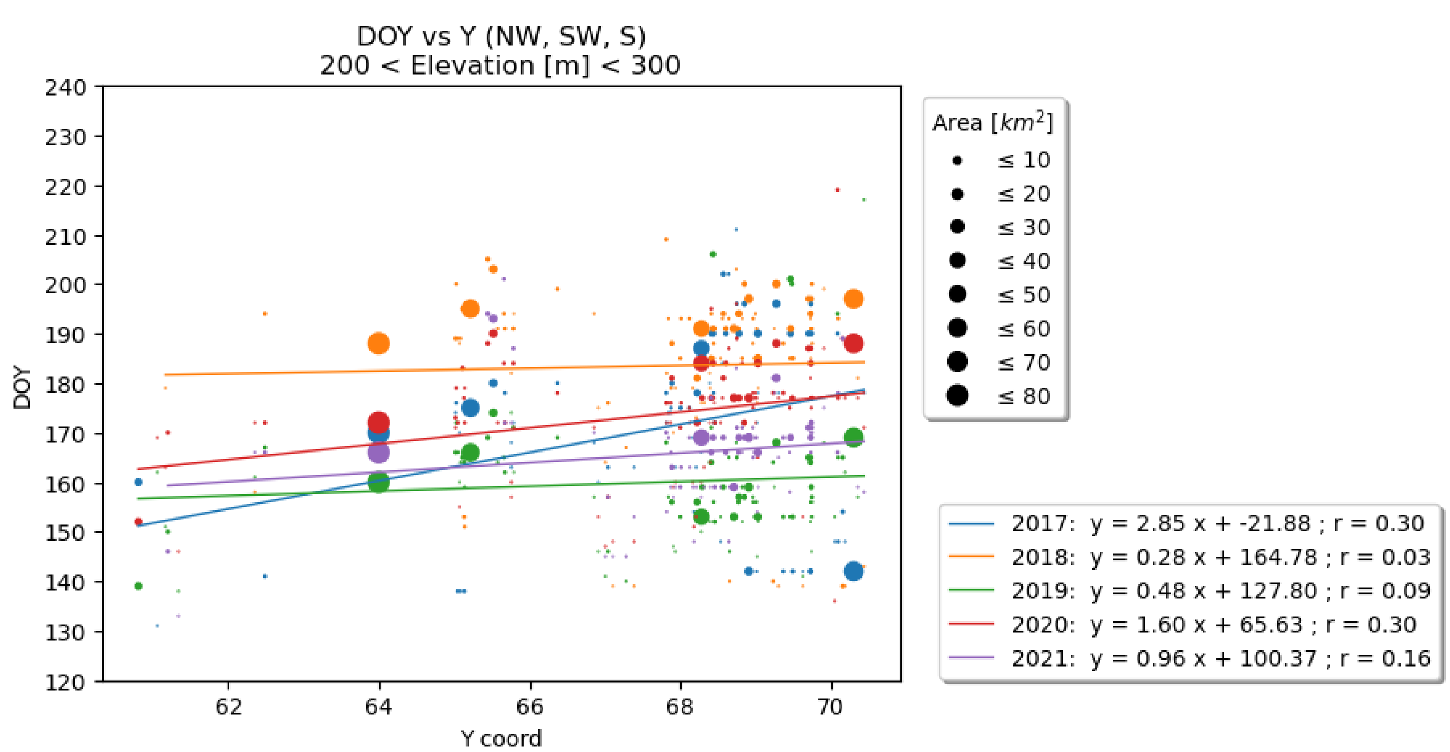

DOY vs Y (NW, SW, S)
200 < Elevation [m] < 300
DOY
Y coord
Area [km^2]
≤ 10
≤ 20
≤ 30
≤ 40
≤ 50
≤ 60
≤ 70
≤ 80
2017: y = 2.85 x + -21.88 ; r = 0.30
2018: y = 0.28 x + 164.78 ; r = 0.03
2019: y = 0.48 x + 127.80 ; r = 0.09
2020: y = 1.60 x + 65.63 ; r = 0.30
2021: y = 0.96 x + 100.37 ; r = 0.16

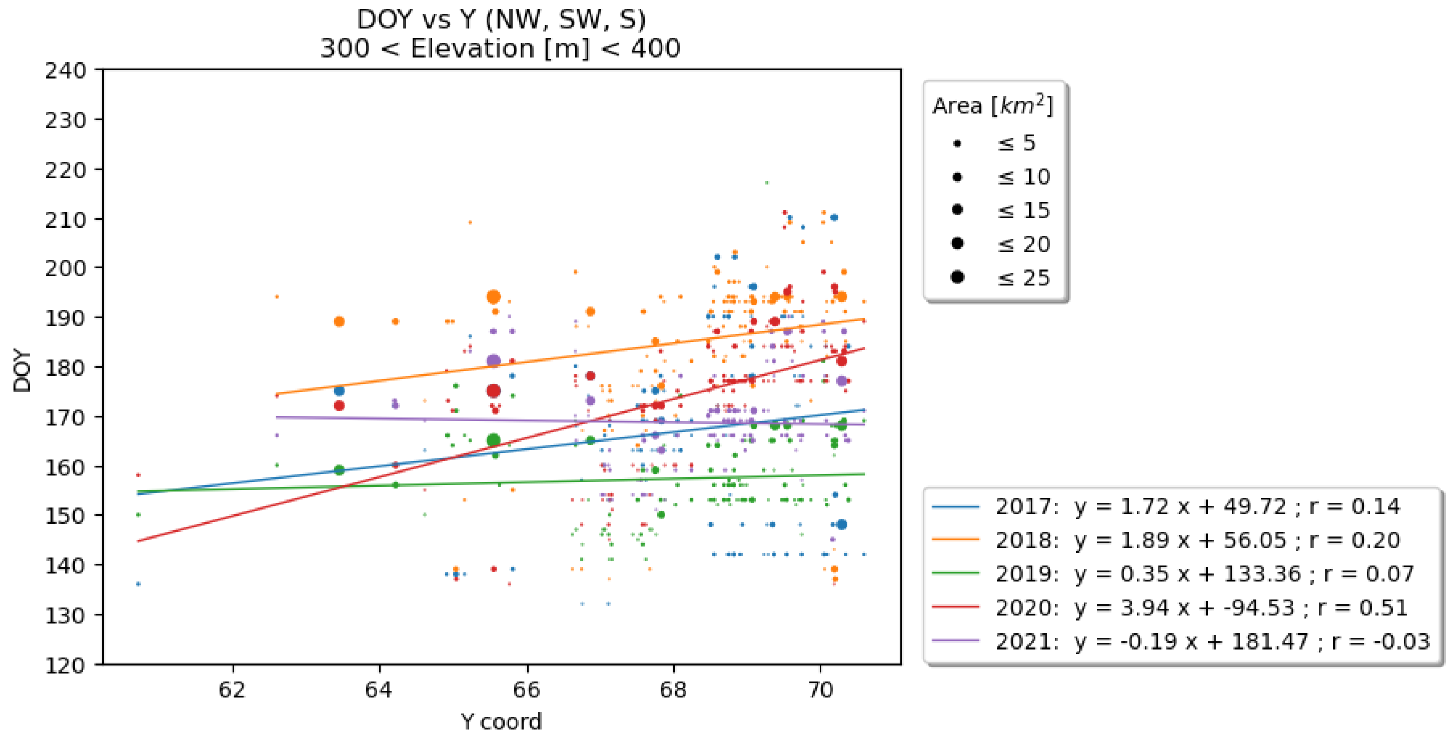

DOY vs Y (NW, SW, S)
300 < Elevation [m] < 400
DOY
Y coord
Area [km^2]
≤ 5
≤ 10
≤ 15
≤ 20
≤ 25
2017: y = 1.72 x + 49.72 ; r = 0.14
2018: y = 1.89 x + 56.05 ; r = 0.20
2019: y = 0.35 x + 133.36 ; r = 0.07
2020: y = 3.94 x + -94.53 ; r = 0.51
2021: y = -0.19 x + 181.47 ; r = -0.03

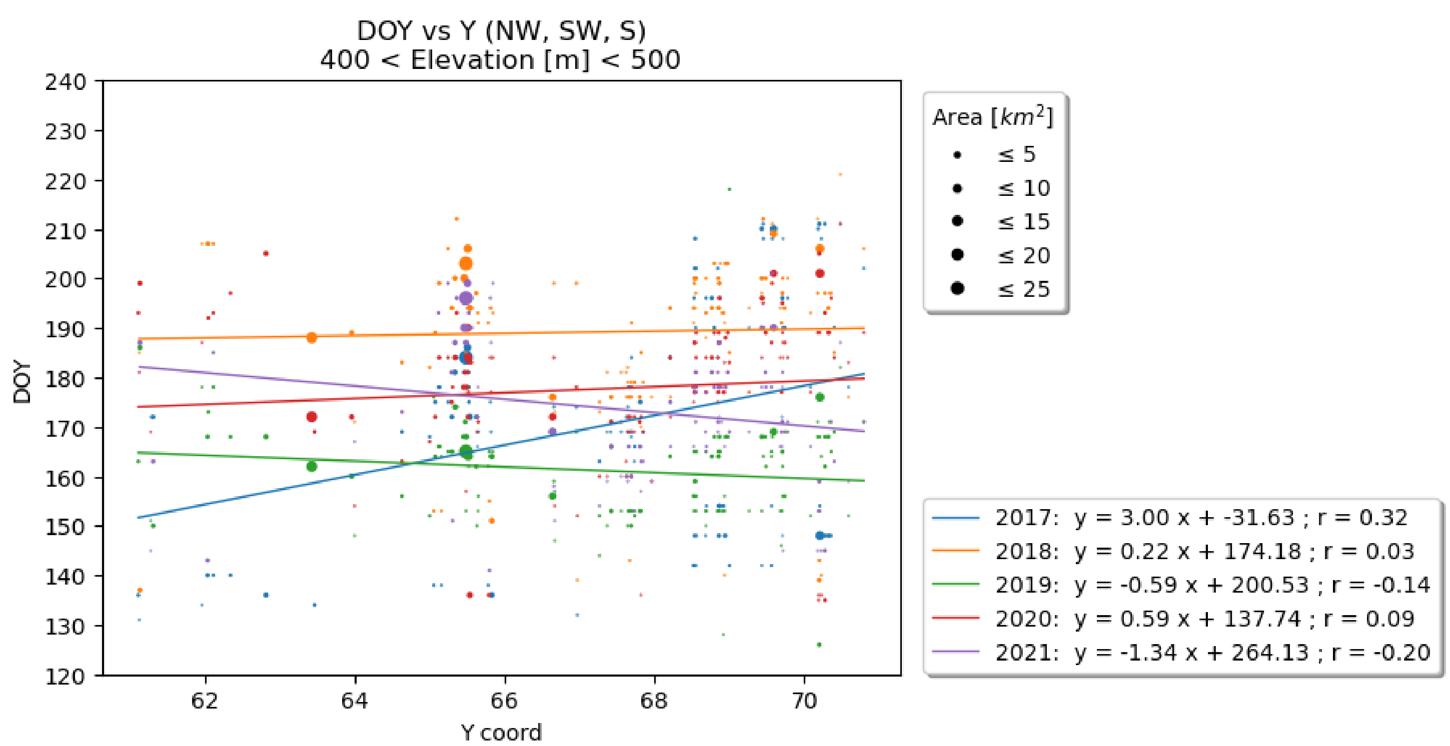

DOY vs Y (NW, SW, S)
400 < Elevation [m] < 500
DOY
Y coord
Area [km^2]
≤ 5
≤ 10
≤ 15
≤ 20
≤ 25
2017: y = 3.00 x + -31.63 ; r = 0.32
2018: y = 0.22 x + 174.18 ; r = 0.03
2019: y = -0.59 x + 200.53 ; r = -0.14
2020: y = 0.59 x + 137.74 ; r = 0.09
2021: y = -1.34 x + 264.13 ; r = -0.20

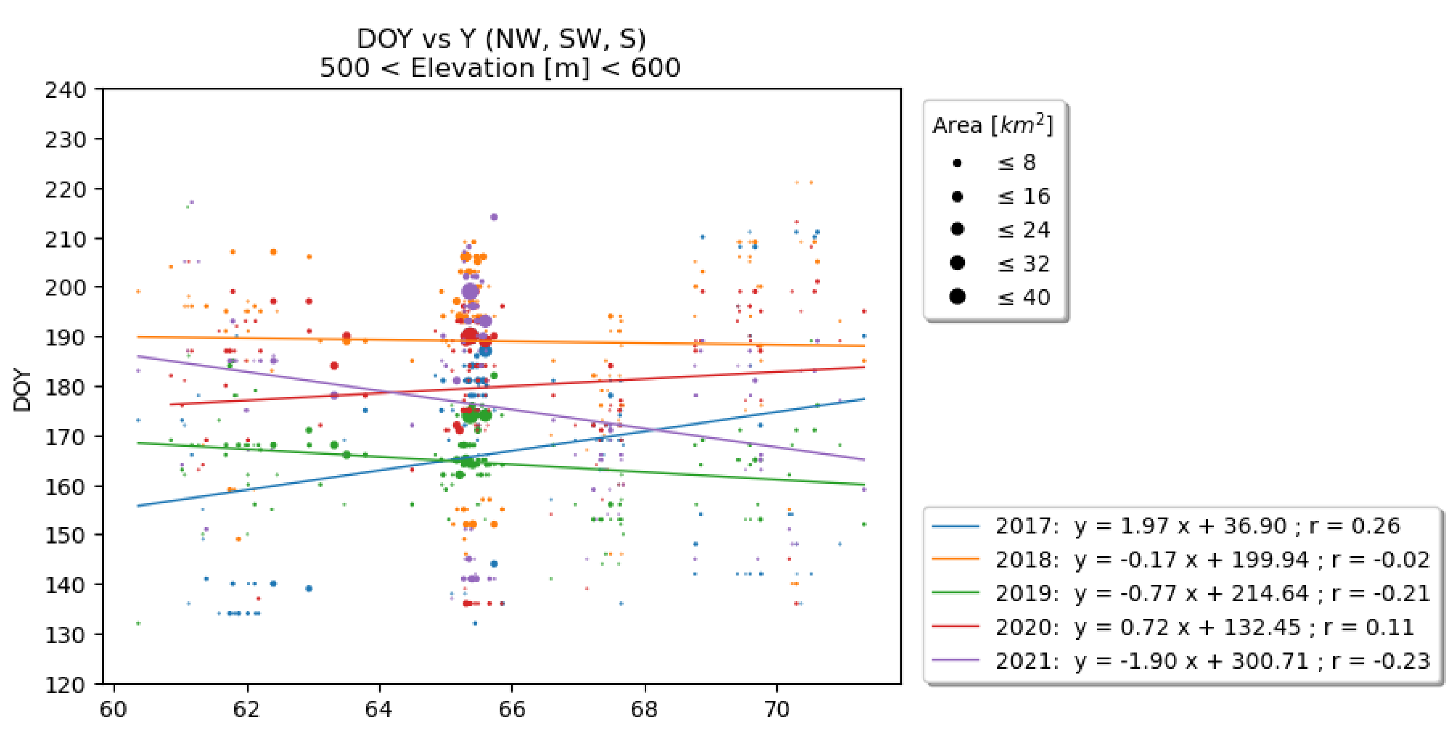

DOY vs Y (NW, SW, S)
500 < Elevation [m] < 600
DOY
Y coord
Area [km^2]
≤ 8
≤ 16
≤ 24
≤ 32
≤ 40
2017: y = 1.97 x + 36.90 ; r = 0.26
2018: y = -0.17 x + 199.94 ; r = -0.02
2019: y = -0.77 x + 214.64 ; r = -0.21
2020: y = 0.72 x + 132.45 ; r = 0.11
2021: y = -1.90 x + 300.71 ; r = -0.23

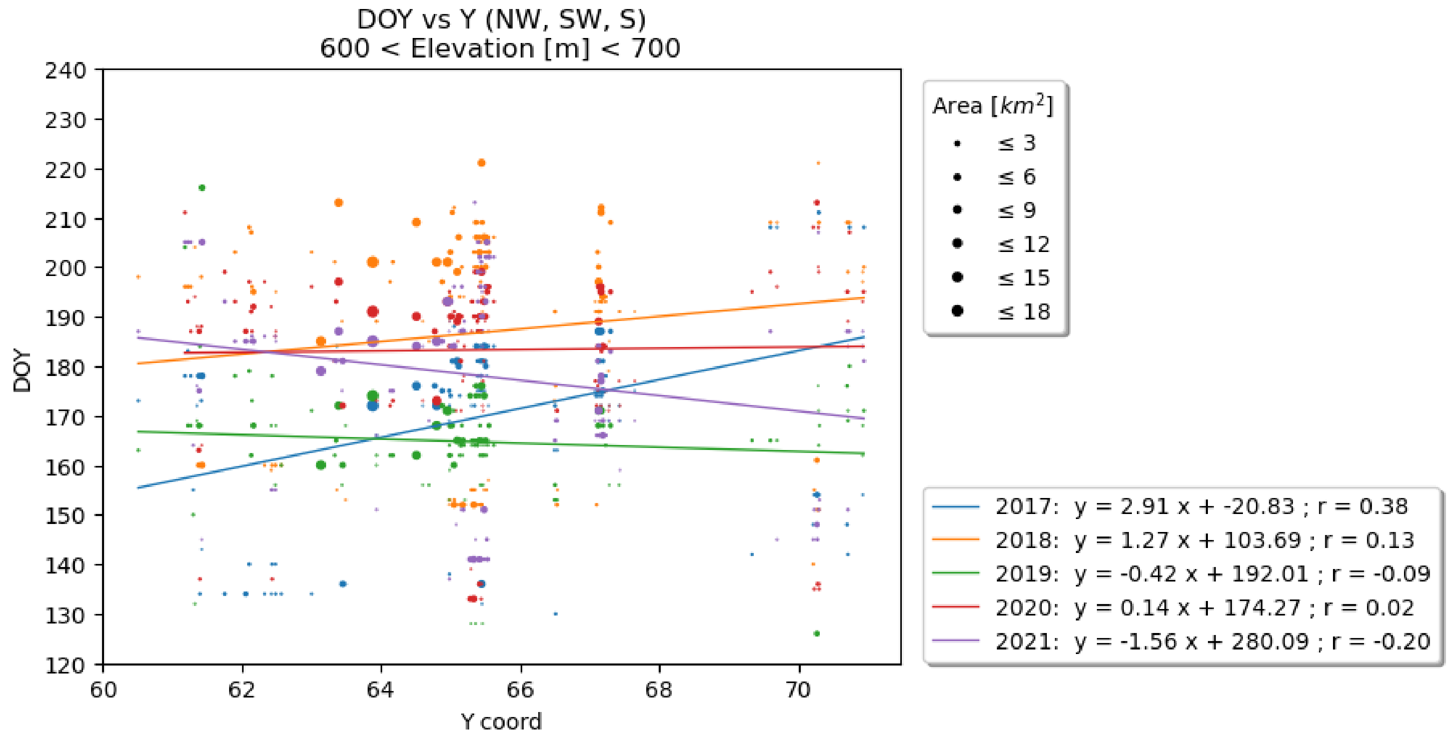
DOY vs Y (NW, SW, S)
600 < Elevation [m] < 700
DOY
Y coord
Area [km^2]
≤ 3
≤ 6
≤ 9
≤ 12
≤ 15
≤ 18
2017: y = 2.91 x + -20.83 ; r = 0.38
2018: y = 1.27 x + 103.69 ; r = 0.13
2019: y = -0.42 x + 192.01 ; r = -0.09
2020: y = 0.14 x + 174.27 ; r = 0.02
2021: y = -1.56 x + 280.09 ; r = -0.20

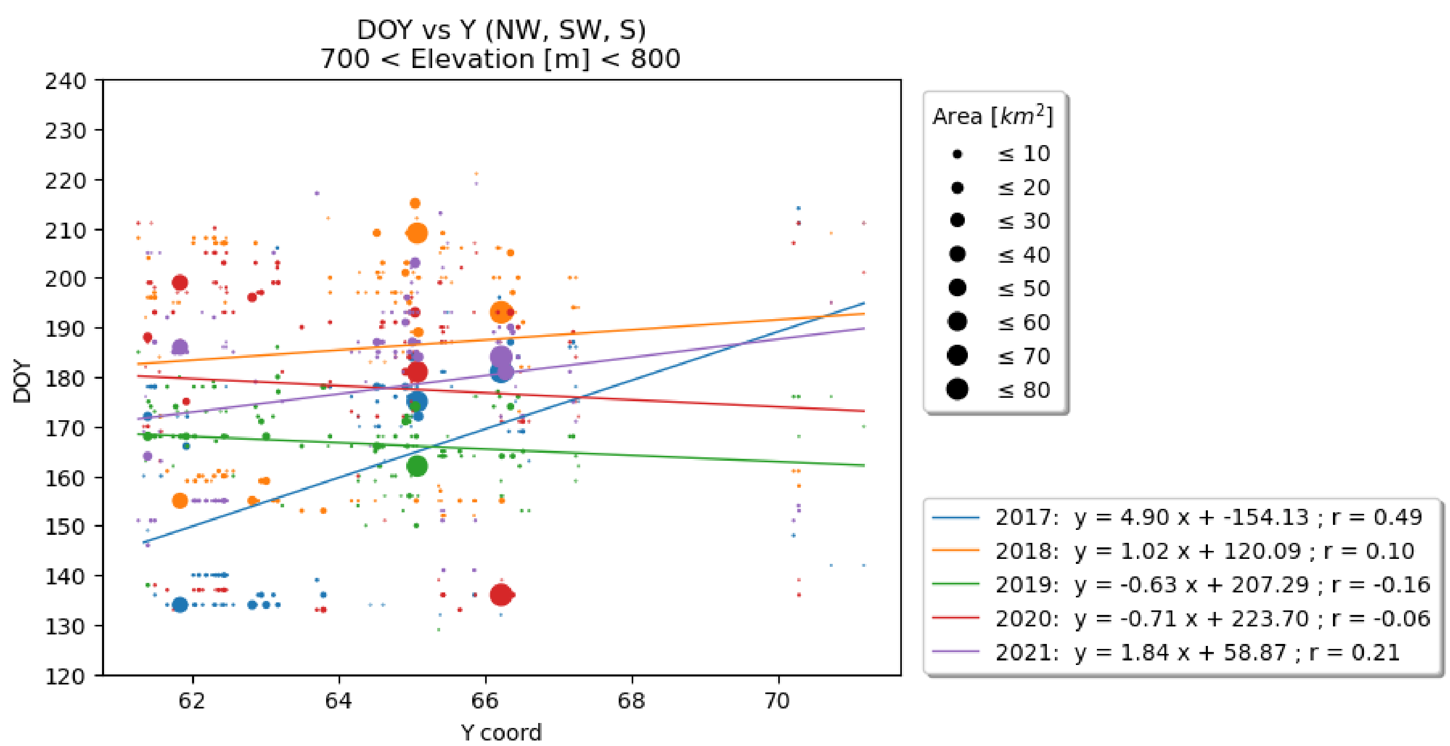
DOY vs Y (NW, SW, S)
700 < Elevation [m] < 800
DOY
Y coord
Area [km^2]
≤ 10
≤ 20
≤ 30
≤ 40
≤ 50
≤ 60
≤ 70
≤ 80
2017: y = 4.90 x + -154.13 ; r = 0.49
2018: y = 1.02 x + 120.09 ; r = 0.10
2019: y = -0.63 x + 207.29 ; r = -0.16
2020: y = -0.71 x + 223.70 ; r = -0.06
2021: y = 1.84 x + 58.87 ; r = 0.21

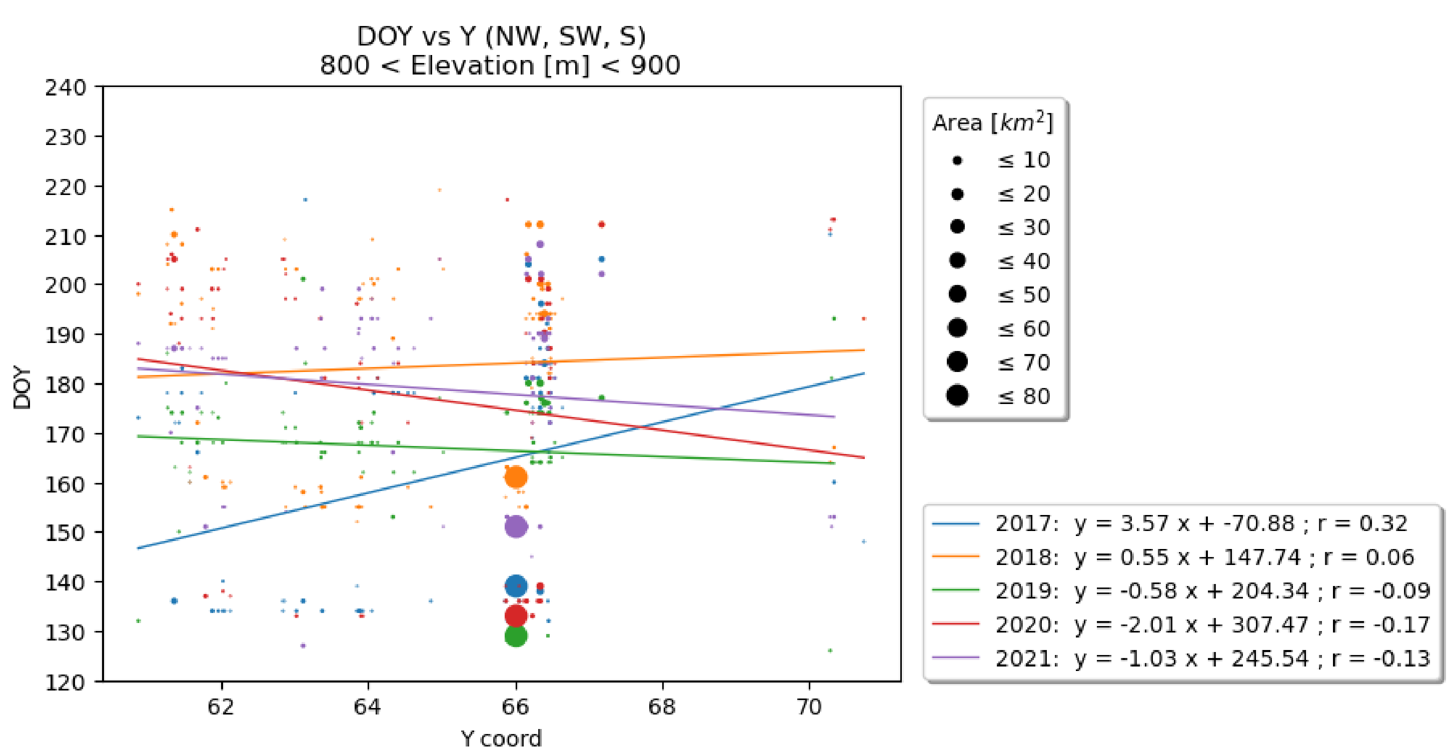
DOY vs Y (NW, SW, S)
800 < Elevation [m] < 900
DOY
Y coord
Area [km^2]
≤ 10
≤ 20
≤ 30
≤ 40
≤ 50
≤ 60
≤ 70
≤ 80
2017: y = 3.57 x + -70.88 ; r = 0.32
2018: y = 0.55 x + 147.74 ; r = 0.06
2019: y = -0.58 x + 204.34 ; r = -0.09
2020: y = -2.01 x + 307.47 ; r = -0.17
2021: y = -1.03 x + 245.54 ; r = -0.13

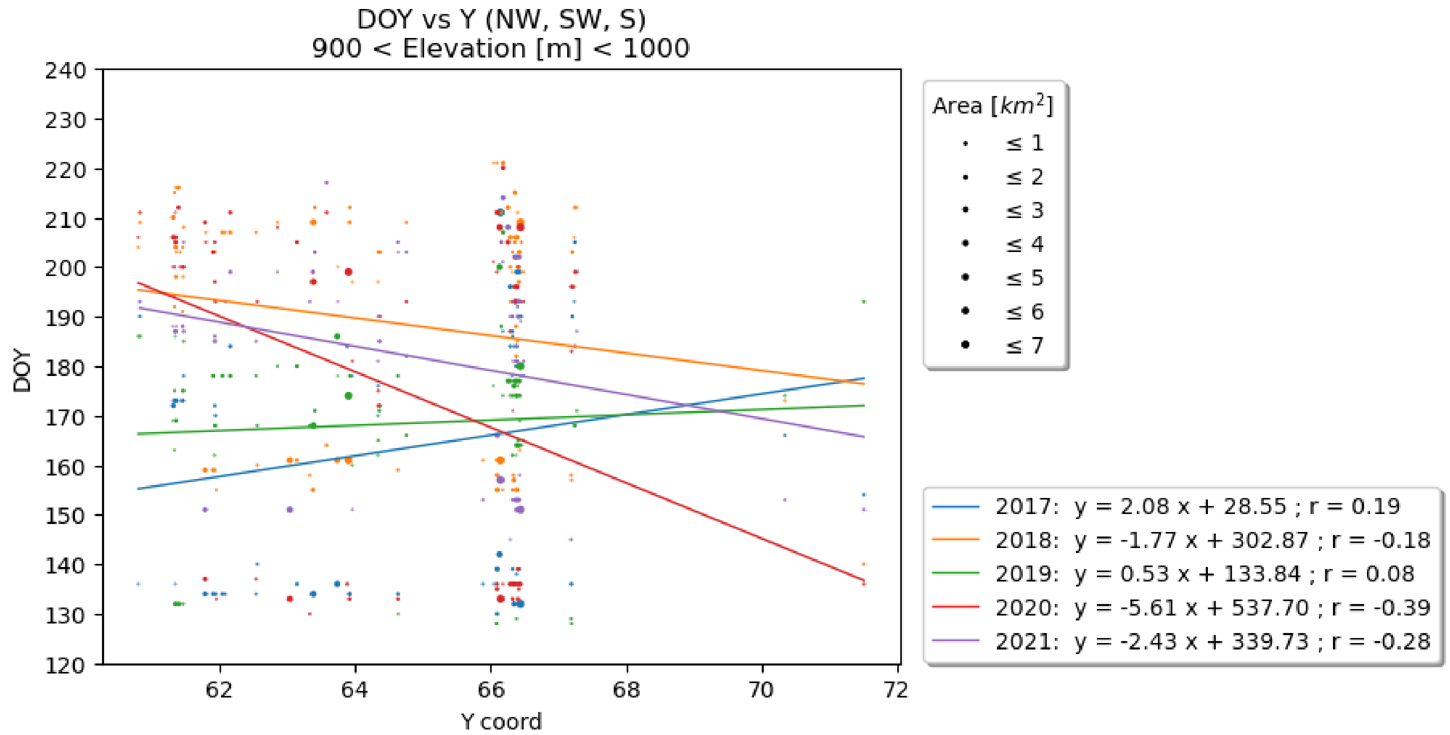
DOY vs Y (NW, SW, S)
900 < Elevation [m] < 1000
DOY
Y coord
Area [km^2]
≤ 1
≤ 2
≤ 3
≤ 4
≤ 5
≤ 6
≤ 7
2017: y = 2.08 x + 28.55 ; r = 0.19
2018: y = -1.77 x + 302.87 ; r = -0.18
2019: y = 0.53 x + 133.84 ; r = 0.08
2020: y = -5.61 x + 537.70 ; r = -0.39
2021: y = -2.43 x + 339.73 ; r = -0.28

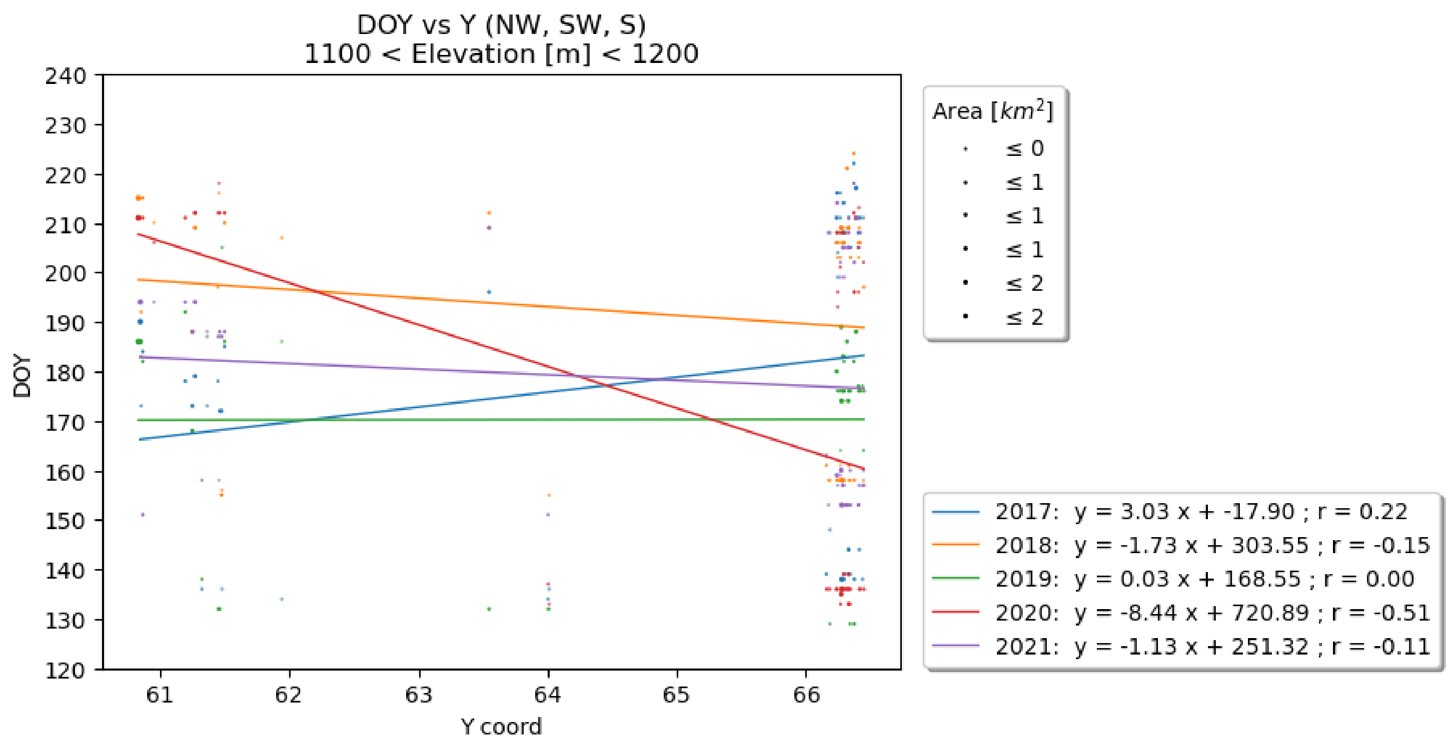
DOY vs Y (NW, SW, S)
1100 < Elevation [m] < 1200
DOY
Y coord
Area [km^2]
≤ 0
≤ 1
≤ 1
≤ 1
≤ 2
≤ 2
2017: y = 3.03 x + -17.90 ; r = 0.22
2018: y = -1.73 x + 303.55 ; r = -0.15
2019: y = 0.03 x + 168.55 ; r = 0.00
2020: y = -8.44 x + 720.89 ; r = -0.51
2021: y = -1.13 x + 251.32 ; r = -0.11

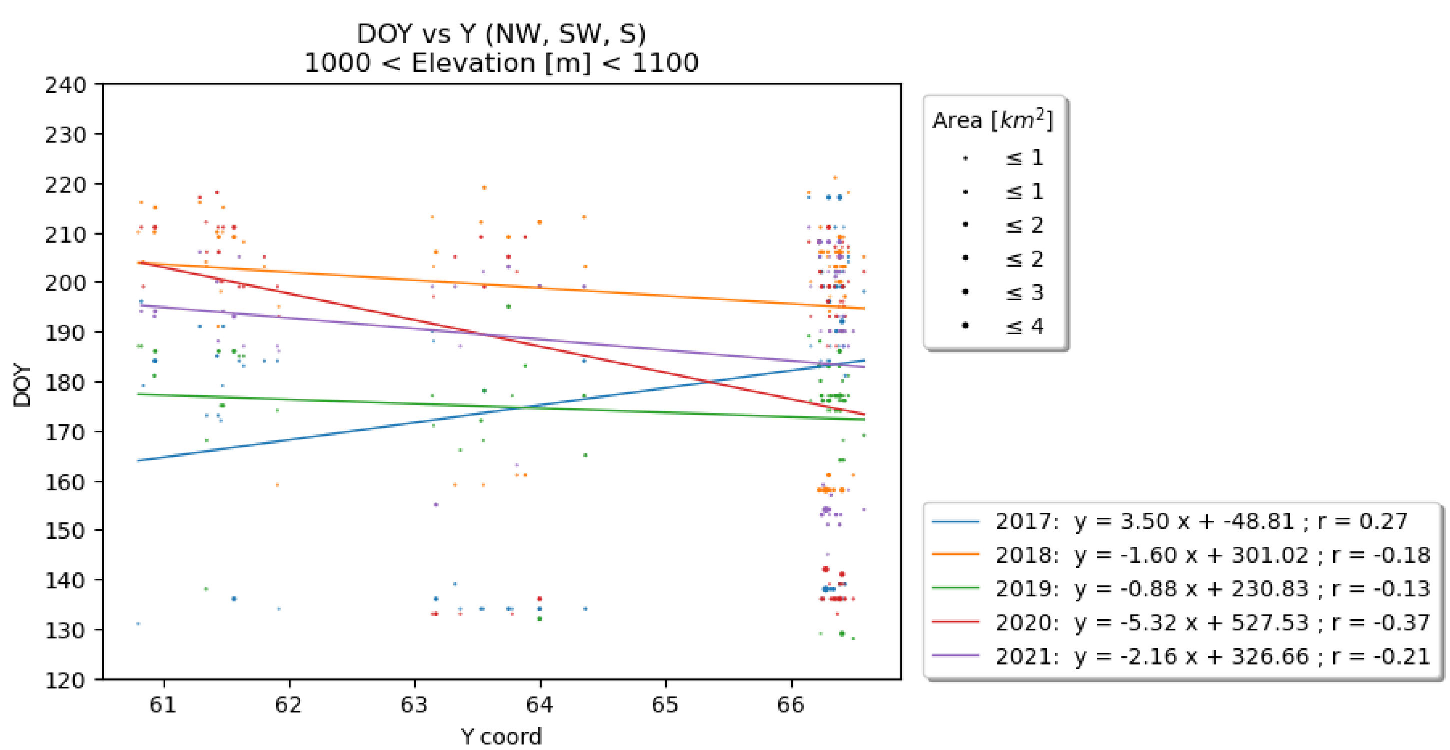
DOY vs Y (NW, SW, S)
1000 < Elevation [m] < 1100
DOY
Y coord
Area [km^2]
≤ 1
≤ 1
≤ 2
≤ 2
≤ 3
≤ 4
2017: y = 3.50 x + -48.81 ; r = 0.27
2018: y = -1.60 x + 301.02 ; r = -0.18
2019: y = -0.88 x + 230.83 ; r = -0.13
2020: y = -5.32 x + 527.53 ; r = -0.37
2021: y = -2.16 x + 326.66 ; r = -0.21

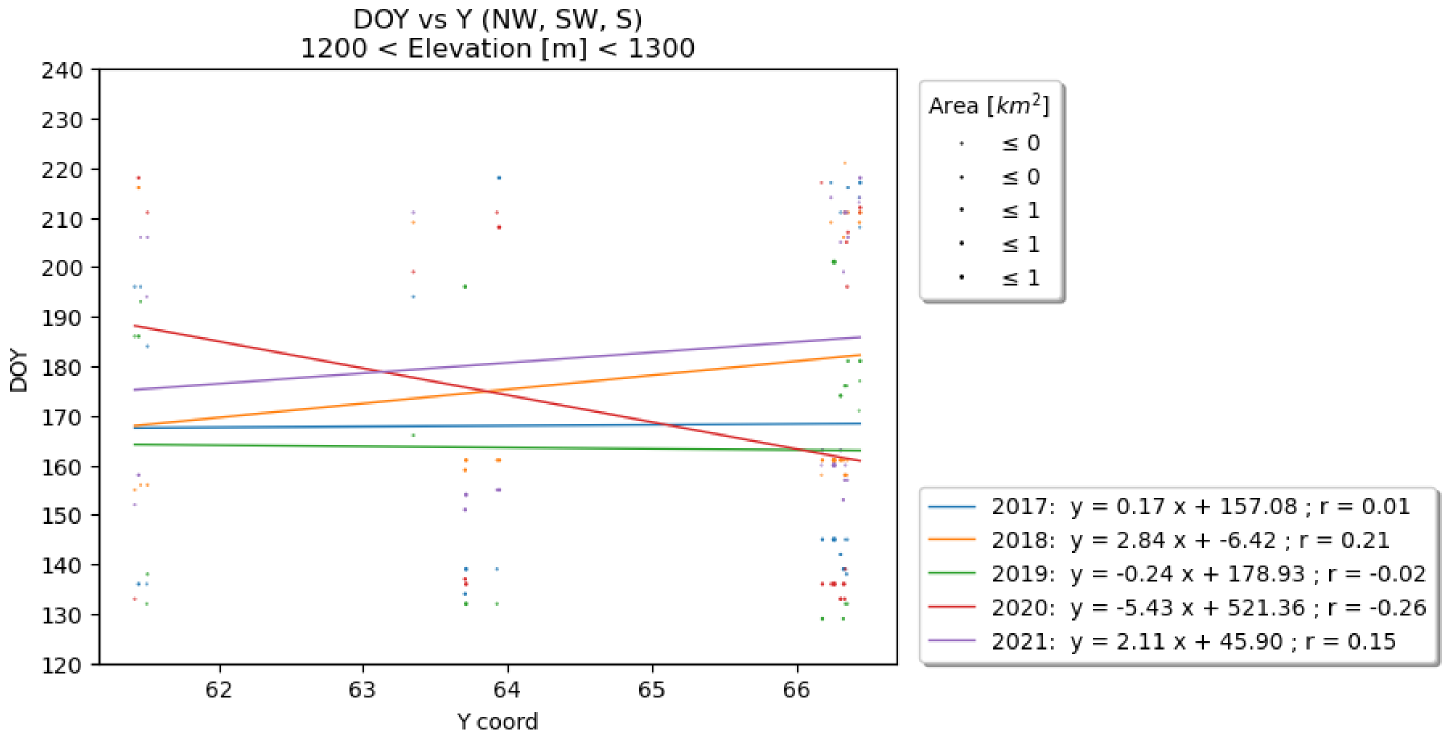
DOY vs Y (NW, SW, S)
1200 < Elevation [m] < 1300
DOY
Y coord
Area [km^2]
≤ 0
≤ 0
≤ 1
≤ 1
≤ 1
2017: y = 0.17 x + 157.08 ; r = 0.01
2018: y = 2.84 x + -6.42 ; r = 0.21
2019: y = -0.24 x + 178.93 ; r = -0.02
2020: y = -5.43 x + 521.36 ; r = -0.26
2021: y = 2.11 x + 45.90 ; r = 0.15

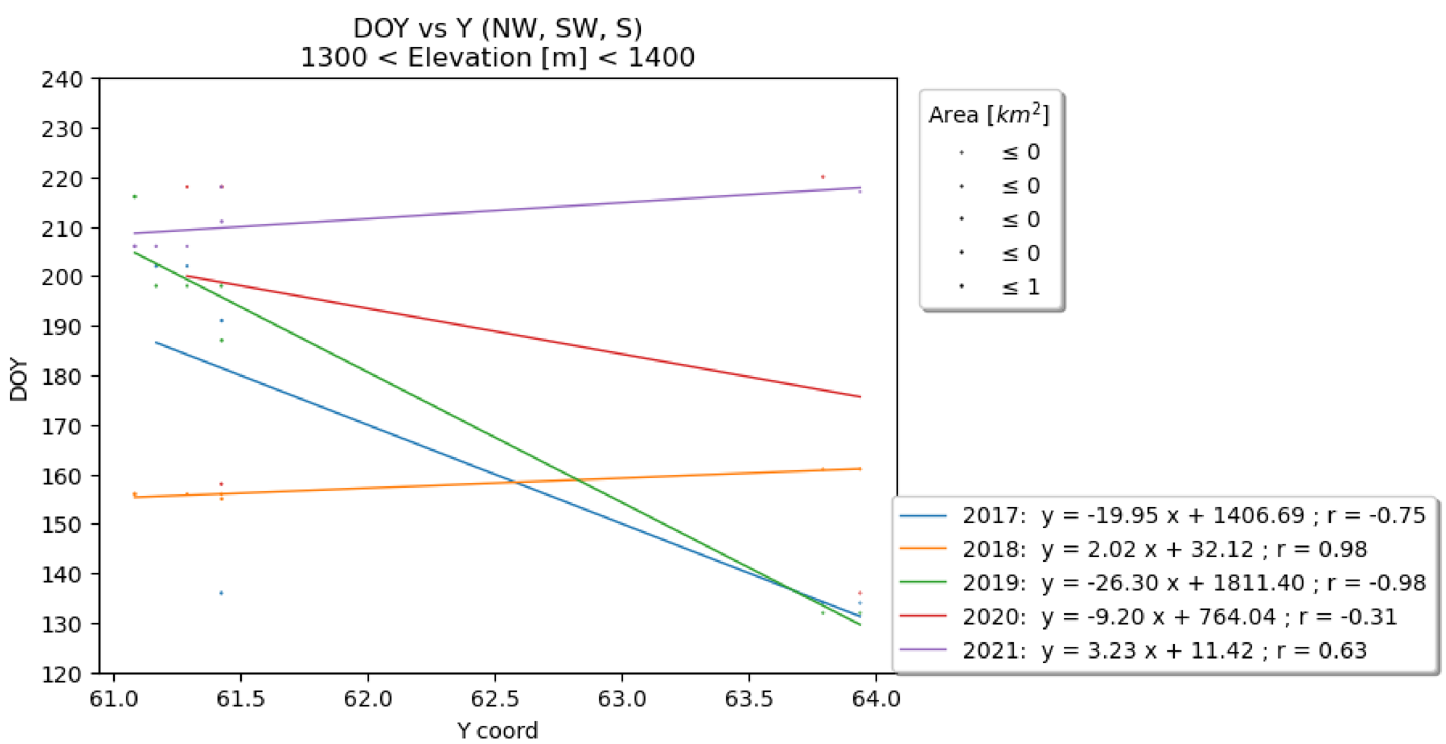
DOY vs Y (NW, SW, S)
1300 < Elevation [m] < 1400
DOY
Y coord
Area [km^2]
≤ 0
≤ 0
≤ 0
≤ 0
≤ 1
2017: y = -19.95 x + 1406.69 ; r = -0.75
2018: y = 2.02 x + 32.12 ; r = 0.98
2019: y = -26.30 x + 1811.40 ; r = -0.98
2020: y = -9.20 x + 764.04 ; r = -0.31
2021: y = 3.23 x + 11.42 ; r = 0.63

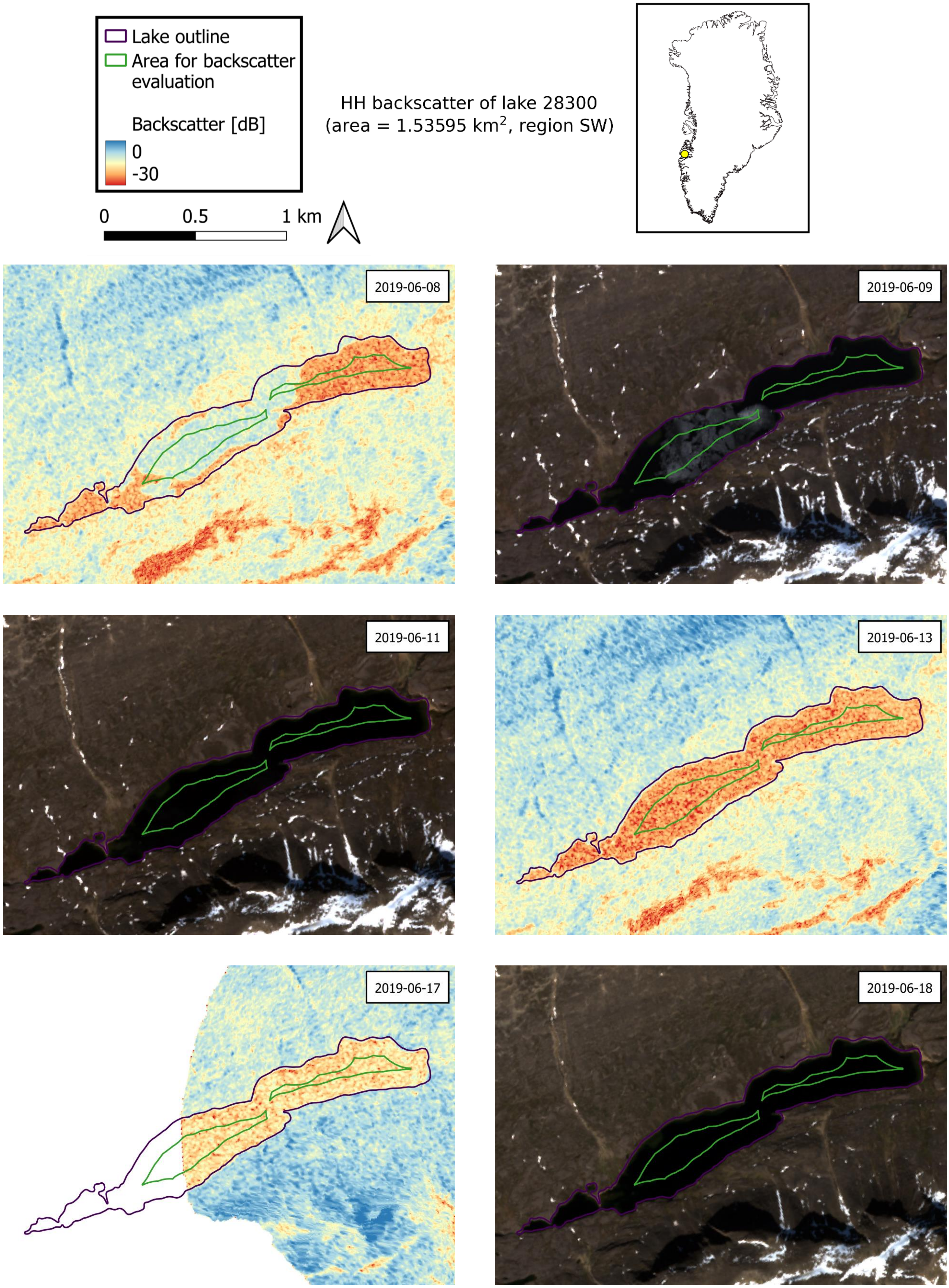
Lake outline
Area for backscatter evaluation
Backscatter [dB]
0
-30
0
0.5
1 km
HH backscatter of lake 28300
(area = 1.53595 km², region SW)
2019-06-08
2019-06-09
2019-06-11
2019-06-13
2019-06-17
2019-06-18

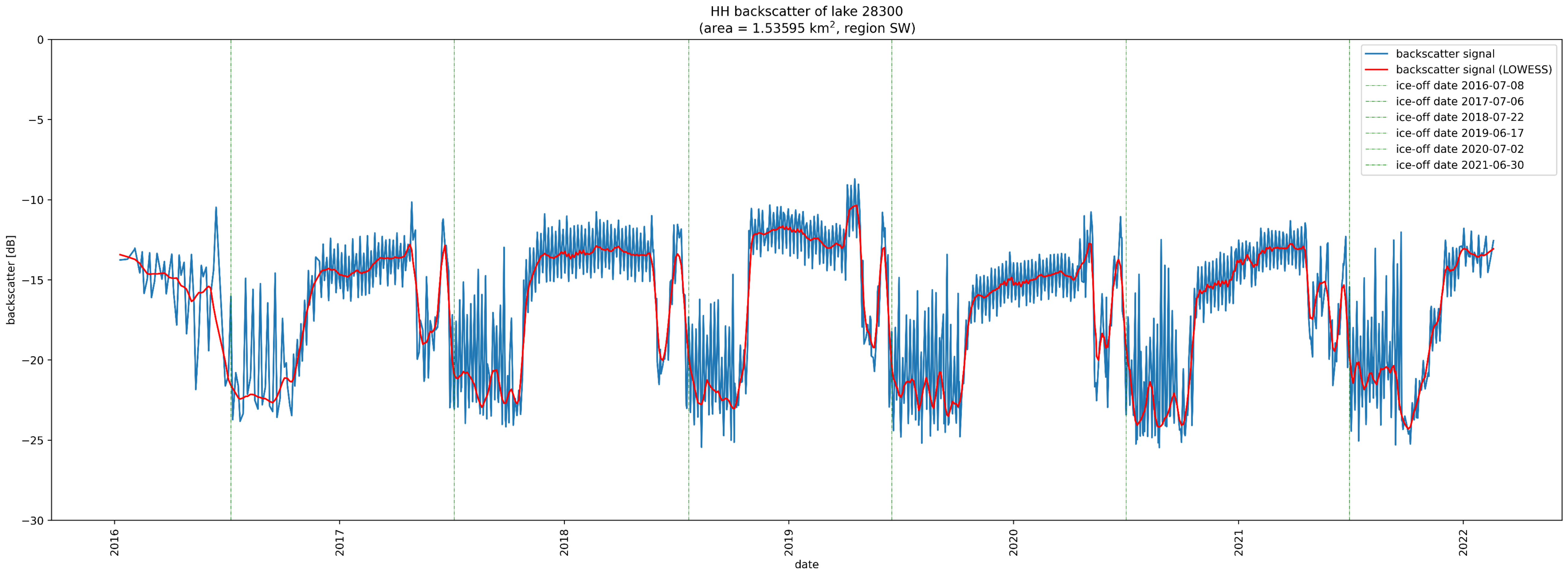

HH backscatter of lake 28300
(area = 1.53595 km², region SW)
backscatter signal
backscatter signal (LOWESS)
ice-off date 2016-07-08
ice-off date 2017-07-06
ice-off date 2018-07-22
ice-off date 2019-06-17
ice-off date 2020-07-02
ice-off date 2021-06-30
backscatter [dB]
0
−5
−10
−15
−20
−25
−30
2016
2017
2018
2019
2020
2021
2022
date